

UCLA

UCLA Electronic Theses and Dissertations

Title

Mechanisms of Transcription Elongation on Chromatin and Gene Silencing

Permalink

<https://escholarship.org/uc/item/64s755nn>

Author

Kuryan, Benjamin George

Publication Date

2013

Peer reviewed|Thesis/dissertation

UNIVERSITY OF CALIFORNIA
Los Angeles

Mechanisms of Transcription Elongation on Chromatin and Gene Silencing

A dissertation submitted in partial satisfaction of the requirements for the degree Doctor of
Philosophy in Molecular Biology

by

Benjamin George Kuryan

2013

ABSTRACT OF THE DISSERTATION

Mechanisms of Transcription Elongation on Chromatin and Gene Silencing

By

Benjamin George Kuryan

Doctor of Philosophy in Molecular Biology

University of California, Los Angeles, 2013

Professor Michael F. Carey, Chair

In the nucleus, the genomes of eukaryotes are packaged with histone proteins to form nucleosomes. Nucleosomes are the biological substrate for all of the processes that require access to the genomic DNA sequence. The first half of my research sought to address questions related to how one of these processes, transcription by RNA pol II, occurs on chromatin and how this process affects chromatin structure. The second half of my research focused on yeast silent chromatin and how it is affected by histone modifications and other chromatin factors. Chapter 1 of this dissertation is a general introduction to transcription and chromatin biology. This chapter should give the reader a general introduction to the importance of these topics, how the two intersect, and the key concepts required to understand the fields today. Chapter 2 of the dissertation describes published work demonstrating the cooperation between the histone chaperone NAP1 and the chromatin remodeling complex RSC. The data shows, in a reconstituted biochemical system, that these enzymes coordinate to evict one H2A-H2B dimer from the nucleosome and allow elongation through a nucleosome template. Chapter

3 of the dissertation describes work involving the function of a core module of the Rpd3 histone deacetylase complex in stabilizing chromatin structure independent of histone deacetylase activity. This core complex has both chromatin assembly activity and the capability to block nucleosome eviction by the RSC complex. Chapter 4 is a study of telomere position effect variegation and heterochromatin in yeast. A key result from the study is that methylation of H3K79 blocks the ability of the Sir complex to silence chromatin in vivo and in vitro without disrupting the ability of the complex to bind to nucleosomes. Chapter 5, the final chapter, is a study that started with a proteomic screen to identify proteins that interact with yeast heterochromatin. This screen identified the Ino80 complex as an interactor with heterochromatin. This interaction was confirmed in a reconstituted system and subsequent in vivo analysis showed that key subunits of the complex are important for silencing the hidden mating locus HML.

The dissertation of Benjamin George Kuryan is approved.

Steven G. Clarke

Reid C. Johnson

Siavash K. Kurdistani

Michael F. Carey, Committee Chair

University of California, Los Angeles

2013

To Mom and Dad

TABLE OF CONTENTS

Title Page	i
Abstract of the Dissertation	ii
Committee Page	iv
Dedication	v
Table of Contents	vi
List of Figures and Tables	viii
Acknowledgements	xi
Vita	xiii
Chapter 1: Introduction to Transcription and Chromatin	1
Figures	22
References	25
Chapter 2: Histone density is maintained during transcription mediated by the chromatin remodeler RSC and histone chaperone NAP1 in vitro	36
References	42
Contribution	49
Chapter 3: The Rpd3 core complex is a chromatin stabilization module	50
References	57
Contribution	69
Chapter 4: Mechanism for epigenetic variegation of gene expression at yeast telomeric heterochromatin	70
References	81
Contribution	102
Chapter 5: Identification of the Ino80 Complex as a regulator of the silent mating loci	103

Figures	112
Contribution	119
References	120

LIST OF FIGURES AND TABLES

Chapter 1	
Figure 1	22
Figure 2	23
Figure 3	24
Chapter 2	
Figure 1	38
Figure 2	39
Figure 3	40
Figure 4	41
Figure 5	42
Supplemental Figure 1	44
Supplemental Figure 2	44
Supplemental Figure 3	45
Supplemental Figure 4	45
Supplemental Figure 5	46
Supplemental Figure 6	46
Supplemental Figure 7	47
Supplemental Figure 8	47
Supplemental Figure 9	48
Chapter 3	
Figure 1	52
Figure 2	54
Figure 3	55
Figure 4	56
Supplemental Figure 1	60

Supplemental Figure 2	62
Supplemental Figure 3	63
Chapter 4	
Figure 1	73
Figure 2	74
Figure 3	75
Figure 4	76
Figure 5	77
Figure 6	79
Figure 7	80
Supplemental Table 1	90
Supplemental Table 2	91
Supplemental Table 3	92
Supplemental Figure 1	96
Supplemental Figure 2	97
Supplemental Figure 3	98
Supplemental Figure 4	99
Supplemental Figure 5	100
Supplemental Figure 6	101
Chapter 5	
Figure 1	112
Figure 2	113
Figure 3	114
Figure 4	115
Figure 5	116
Figure 6	117

Table 1

118

Table 2

119

ACKNOWLEDGEMENTS

First, I need to thank my mentor, Dr. Michael Carey. He let me join his lab and do research, so none of this work could have been possible without him. Mike helped learn how to think like a scientist, to present scientific data, write grants, and even do experiments. Mike is one of the few PIs that know how to get their lab coat dirty doing bench work. He also brings a level of excitement and involvement into the lab not seen by many other PIs. I am thankful to have been able to work for him. Next I must thank my thesis committee: Drs. Siavash Kurdistani, Reid Johnson, and Steven Clarke. They have all giving me much support during my time here. Siavash and Reid I am lucky to have been able to share lab space next to yours. I enjoyed the collaboration and interaction that we shared. Steve, you did a great as director of the MBI institute and running the CMB training program, which I was lucky to participate in.

I need to thank the fellow members of the Carey lab that I worked along side, you guys are great and the experience would not have been the same without you. Specifically Josh Black, Justin Lin, Xiao-Fen Chen, Lynn Lehmann, Jessica Kim, Nancy Tran, Jason Gehrke, and Tasuku Kitada (honorary member). I appreciate the members of the Biological Chemistry, Molecular Biology, and the Gene Regulation program for helping to foster a great intellectual environment to do research.

Finally, I need to acknowledge my family and friends for your support. Mom I am glad I got to come home every once in a while to get fed and do some laundry. Dad, I enjoyed the trips to Hawaii to come visit you. It was definitely a fun time. My sister, Rachel, I would like to thank you for hanging out and eating food with me and helping me keep perspective on everything. I would also like to thank my good friend, and former freshman roommate, Louie Cruz. I've learned a lot

from you about friendship, being cool, and how to enjoy life. Once again, thanks to everyone for making this time of my life what it was!

Chapter 2 of this dissertation is a version of Kuryan BG, Kim J, Tran NN, Lombardo SR, Venkatesh S, Workman JL, Carey M. Proc Natl Acad Sci U S A. 2012 Feb 7;109(6):1931-6

Chapter 3 of this dissertation is a version of Chen XF, Kuryan B, Kitada T, Tran N, Li JY, Kurdistani S, Grunstein M, Li B, Carey M. Curr Biol. 2012 Jan 10;22(1):56-63

Chapter 4 of this dissertation is a version of Kitada T, Kuryan BG, Tran NN, Song C, Xue Y, Carey M, Grunstein M. Genes Dev. 2012 Nov 1;26(21):2443-55

Chapter 5 is based on work with I performed with collaborators Tasuku Kitada, Jason Gehrke, and Nancy Tran.

VITA

2007

Bachelors of Science in Biochemistry
University of California, Los Angeles
Los Angeles, California

PUBLICATIONS

Chen XF, Kuryan B, Kitada T, Tran N, Li JY, Kurdistani S, Grunstein M, Li B, Carey M. (2012) *The Rpd3 core complex is a chromatin stabilization module. Curr Biol.* 22(1):56-63

Kuryan BG, Kim J, Tran NN, Lombardo SR, Venkatesh S, Workman JL, Carey M. (2012). *Histone density is maintained during transcription mediated by the chromatin remodeler RSC and histone chaperone NAP1 in vitro. Proc Natl Acad Sci U S A.* 109(6):1931-6

Kitada T, Kuryan BG, Tran NN, Song C, Xue Y, Carey M, Grunstein M. (2012). *Mechanism for epigenetic variegation of gene expression at yeast telomeric heterochromatin. Genes Dev.* 26(21):2443-55

PRESENTATIONS

Kuryan BG*, Kim J, Venkatesh S, Workman JL, Carey M. 2011. Cooperation between a histone chaperone and chromatin remodeling complex allows transcription through the nucleosome. *Cold Spring Harbor Laboratory: Mechanisms of Eukaryotic Transcription*, Cold Spring Harbor, NY (Poster) [*Presenter]

Chen XF*, Kuryan B, Li B, Carey M. 2011. The Rpd3 histone deacetylases stabilize yeast chromatin structure. *Cold Spring Harbor Laboratory: Mechanisms of Eukaryotic Transcription*, Cold Spring Harbor, NY (Poster) [*Presenter]

Kuryan BG*, Kim J, Carey M. 2010. Cooperation between a histone chaperone and chromatin remodeling complex allows transcription through the nucleosome. *ASBMB Special Symposia: Transcriptional Regulation by Chromatin and RNA polymerase II*, Tahoe City, CA (Poster) [*Presenter]

Chen XF*, Kuryan B, Li B, Carey M. 2010. Yeast Rpd3S exhibits nucleosome assembly activity. *Cold Spring Harbor Asia conference: Epigenetics, Chromatin & Transcription*, Suzhou, Jiangsu Province, China (Poster) [*Presenter]

Kuryan BG* and Carey M. 2010. Mechanisms of Histone Chaperones and Chromatin Remodelers in Transcription Elongation. *Experimental Biology and ASBMB Annual Meeting*, Anaheim, CA (Poster) [*Presenter]

Chapter 1

Introduction to Transcription and Chromatin

Transcription in Eukaryotes

Transcription is the biochemical process by which RNA is synthesized from precursor nucleotides using DNA as a template. This activity is the first step of gene expression and is central to all living organisms. The fundamental importance of regulating transcription is highlighted by sophisticated mechanisms that have evolved in the simplest of living systems such as the bacteriophage [1]. As organisms become more complex many more layers of regulation are observed. For instance, bacteria contain one copy of RNA polymerase, the enzyme that catalyzes transcription. In eukaryotes, however, there are three: RNA pol I, II and III [2]. Each of which is responsible for the transcription of different classes of genes [3-5].

Beyond the division of labor among RNA polymerases, transcription in eukaryotes is heavily influenced by genomic structure. Eukaryotic genomes are organized into a compact protein-DNA structure termed chromatin. This structure not only serves to compact and protect eukaryotic genomes, but it also regulates the nuclear processes that require access to the underlying DNA sequence. This includes DNA replication, DNA repair, and transcription [6-8]. Chromatin has many orders of organization [9], but the most basic repeating unit is the nucleosome. The nucleosome is comprised of 145-147 bp of DNA wrapped around a globular histone octamer (containing two copies of each of the histones H3, H4, H2A, and H2B) [10]. Sticking out from the nucleosome core are the unstructured N-terminal tails of the histones which are subject to numerous posttranslational modifications [11].

RNA pol II transcribes all of the protein coding genes in eukaryotes. Transcription by pol II is regulated by the coordinated actions of activators, coactivators, and transcription factors. These proteins control many key events required for the transcription of a gene. Steps controlled by these factors includes assembly of the preinitiation complex (PIC), phosphorylation of the pol II C-terminal domain (CTD), promoter escape, and the transition to productive elongation [12].

In chromatin, nucleosomes act as general repressors to transcription by pol II. They inhibit both the steps of initiation and elongation [13]. Because of this repressive function, additional proteins are required for transcription in the context chromatin [8]. Interestingly, during elongation, not only must these factors permit pol II to elongate the full length of the transcribed gene, but they must also maintain the chromatin structure within gene bodies. Failure to properly coordinate this process can cause aberrant transcription initiation to occur inside open reading frames [14].

The research in this dissertation utilized a biochemical approach to study the processes that occur during transcription on chromatin. Expanding on earlier research [15], an in vitro system was developed. This system consists of purified *S. cerevisiae* protein complexes and defined chromatin templates. It was designed to test the functions of specific enzymes and chromatin modifications thought to function during transcription elongation by pol II. Of particular interest in these projects were two questions: 1) what enzymes facilitate nucleosomal elongation by pol II and 2) how is chromatin structure maintained during the process? This research resulted in the discovery of a novel synergy between two chromatin proteins in simultaneously facilitating elongation by pol II and maintaining histone density [16]. Results also revealed a previously unknown activity for another protein complex in stabilizing the nucleosomes of transcribed genes [17].

Chromatin and Genome Organization

Chromatin within the cell exists in two general states: euchromatin and heterochromatin. Emil Heitz coined the terms in 1928 [18]. By staining cells with carmine acetic acid, he observed that most chromatin transitioned through states of condensation and decondensation with the cell cycle. Other regions, however, remained condensed and stained throughout the cell cycle. He

called these deeply staining regions ‘heterochromatin’ as opposed to the euchromatin or ‘true chromatin.’ The distinction remains to this day and many of the mechanisms that regulate these states have been determined. Euchromatin is an open and accessible chromatin state associated with active regions of the genome. Heterochromatin is a dense and compact structure associated with silent regions of the genome [19].

The idea that chromatin is a repeating unit of histones and DNA was proposed by Rodger Kornberg in 1974 [20], based on biochemical and x-ray diffraction studies. Independently, electron micrographs of chromatin revealed chain-like structures of 10 nm particles along DNA [21-23]. This is the most basic conformation of chromatin, termed the 10 nm fiber or “beads-on-a-string.” The 10 nm fiber can fold onto itself and compact to form a higher order structure called the 30 nm fiber [24]. 30 nm fibers can further fold and interact to form even higher levels of order, but little is known about those levels of organization.

Cytological studies have shown that, at the chromosomal level, individual chromosomes occupy nonrandom regions of the nucleus, forming discrete “chromosome territories” [25]. The function of chromosome territories and the mechanisms that regulate them are areas of active research. Recent studies utilizing high throughput methods based on the chromosome conformation capture technique have confirmed chromosome territories and revealed further levels of genome organization [26].

Nucleosome Structure

A high resolution crystal structure of the nucleosome core particle was published in 1997 [27]. This structure revealed the protein-protein interactions present within the histone octamer and the histone-DNA interactions between the octamer and nucleosomal DNA (Figure 1). The histone tails were mostly not present in the crystal structure. They are thought to be

unstructured and extend away from the nucleosomal DNA. The structure does show that the tail of histone H4 can interact with a neighboring nucleosome, possibly stabilizing higher order structures. In general, the tails are believed to serve mostly regulatory functions because they contain the sites of the majority of posttranslational histone modifications.

Histone Modifications

The posttranslational modification (PTM) of proteins is a mechanism that allows cell to regulate protein activity after synthesis. Histone proteins are remarkable in that they are subject to a multitude of modifications at many different sites. These include the acetylation of lysines, the methylation of lysines and arginines, the phosphorylation of serines and threonines, and much more. Methylation of lysines can occur in three states: mono-, di- and tri-methyl. Arginine methylation can occur in up to four different states. A recent study utilizing advanced proteomic technology identified 130 different PTM sites on histones, 67 of which were previously undiscovered [28].

Histone modifications regulate chromatin function through two distinct mechanisms. First, they may alter the binding affinity of non-histone proteins to chromatin. Domains within non-histone proteins such as chromo-, bromo-, and PHD domains have been shown recognize specific modified histones and influence the function of the proteins that contain them [29-32]. The second mechanism is that histone modifications can influence the higher order structure of chromatin. This can be mediated by a change the charge of the histones or by altering nucleosome-to-nucleosome interaction surfaces. Both of these mechanisms are utilized by the cell to regulate gene expression (reviewed in [11]).

The first paper linking histone methylation and acetylation to gene regulation was published in 1964 [33], but it took 40 years to discover the enzymes responsible for adding and removing

these marks. The laboratory of C. David Allis discovered the first histone acetyl transferase (HAT) in 1996 [34]. This was followed by the discovery of the first histone deacetylase (HDAC) [35], histone methyltransferase (HMT) [36], and, finally, the first histone demethylase in 2004 [37]. The advent of genome wide chromatin immunoprecipitation technologies has enabled the distributions of many histone modifications to be determined. This has allowed their presence or absence to be correlated with the transcriptional state of all the genes [8].

Numerous modifications of have shown to affect other modifications in a phenomenon known as histone crosstalk [38-41]. For instance, the presence of one modification may be required prior to the deposition of another. It has been observed that specific patterns of histone modifications tend to co-occur in specific contexts. Some modifications are found in active genes while other modifications are found in repressed genes. This led to the proposal of the “histone code” hypothesis which states that specific combinations of modifications lead to distinct transcriptional outcomes [42]. The hypothesis has remained controversial and as new layers of regulation in chromatin biology have been discovered, the complexity of histone crosstalk has even been described as a “language” [43].

Interestingly, histone modifications exist outside of chromatin. In fact, they start in the cytosol either during or shortly after translation by the ribosome [44, 45]. Histone acetylation of H4K5 (H4K5Ac) and H4K12 (H4K12Ac) in newly synthesized H4 are conserved modifications throughout the eukaryotic domain [46]. These two marks appear to be involved in a set of sequential steps required for import of H3-H4 dimers into the nucleus [45]. After import into the nucleus, H3K56 is acetylated prior to histone deposition [47, 48]. In *S. cerevisiae*, the nuclear HAT RTT109 makes this modification before the H3-H4 dimers are assembled into chromatin [49]. Without this modification, or the assembly factors that recognize it, genomic instability is observed [50]. The presence of these marks prior the deposition of histones means they will be

present in chromatin at areas of DNA replication and histone exchange, unless they are actively removed.

H3K4 methylation is a modification associated with actively transcribed genes. *S. cerevisiae* contain one complex, Set1/COMPASS, that produces this mark, while humans contain 6 COMPASS complexes [51]. Methylation of H3K4 is enriched at the promoters and coding regions of actively transcribed genes [8]. In mammalian systems, it has been shown to enhance transcription. This occurs via the recruitment of positive effector proteins such as chromodomain-containing remodeling complexes, MYST family HATs, and the TFIID initiation complex to the promoters of genes [11, 52-55]. Set1/COMPASS complex is thought leave the promoter and associate with the elongating Pol II leading to some methylation within the gene body [56, 57].

In contrast to more complex eukaryotes, H3K4 methylation in *S. cerevisiae* is not essential [58] and the chromodomain-containing enzyme CHD1 does not recognize methylated H3K4 [54]. However, there is still a growth phenotype in its absence, indicating that it is required for optimal fitness. The modification appears to be important for regulating histone acetylation levels and promoting efficient termination of unstable transcripts [59, 60].

The general acetylation of lysines on histones positively correlates with transcription. In *S. cerevisiae*, SAGA and NuA4 are the most abundant HAT complexes involved in transcription. SAGA primarily acetylates H3 and H2B while NuA4 acetylates H4 and H2A. These enzymes are recruited to promoters by activators and co-activators [60]. They are also believed to function within the coding regions of genes facilitating pol II elongation. The acetylation marks lower the positive charge on histone tails and recruit the bromodomain-containing remodeling complexes RSC and SWI/SNF [8, 61, 62].

H3K79 methylation by Dot1 is another modification associated with active transcription. This mark is found in the coding regions of transcribed genes and the level of enrichment correlates with transcriptional activity. The Dot1 enzyme associates with the elongating pol II through interaction with the Paf1 complex [56]. H3K79 methylation blocks the repressive activity of the heterochromatic Sir proteins [63] and is also speculated to serve as a transcriptional memory [64].

H3K36 methylation is also associated with the coding regions of transcribed genes. This mark is a product of the Set2 enzyme [65]. Set2 is recruited to coding regions directly by elongating RNA pol II via an interaction with the phosphorylated CTD [66]. This mark recruits the Rpd3S HDAC complex to deacetylate the nucleosomes in the coding regions of genes after pol II passage [67].

In *S. cerevisiae* silent regions of the genome are typically void of the activating marks, but other eukaryotes possess specific modifications associated with silent chromatin. These include the methylation of H3K9 and H3K27, which recruit the heterochromatic HP1 and PRC1 complexes [11, 68]

Histone Variants

In addition to the canonical histones described above, there are variant histones that further add to the complexity of chromatin biology. These alternative histones are incorporated into chromatin and have the potential to create nucleosomes with altered structures and functions. Variants are involved in numerous biological processes including DNA repair, chromosome segregation, and transcription. Some variants are lineage specific while others are nearly universal among eukaryotes (reviewed in [69]).

All eukaryotes possess an alternative H3 histone present at centromeres termed CenH3. CenH3 is divergent from canonical H3, lacking the N-terminal tail and only sharing about 50-60% sequence homology in the histone fold domain [69]. The nucleosomes it forms have a very different structure than canonical nucleosomes [70]. The function of CenH3 is to epigenetically define the centromere and it is required for kinetochore assembly [71]. The composition of CenH3 nucleosomes has been a subject of controversy, with proposals of mutually exclusive models. One model suggests that CenH3 forms right-handed hemisomes with one copy each of CenH3, H4, H2A, and H2B [70].

A second conserved H3 variant is H3.3. Phylogenetic analysis shows that H3.3 is the ancestor to H3 [72]. In mammals H3.3 only differs from canonical H3 by four amino acids. It functions as part of the replication-independent chromatin assembly pathway [72, 73], which means that outside of DNA replication it is the H3 variant that is incorporated into chromatin. *S. cerevisiae* only encodes H3.3 and therefore it is utilized in both replication-independent and replication-dependent pathways. The exact function of H3.3 is unclear, but studies in metazoan systems indicate it is important in germ line development [74].

The histone variant H2AZ is found in eukaryotes from yeast to mammals. Genome wide it is found near transcription start sites where it can positively influence transcription [75]. The crystal structure of nucleosomes containing this variant reveal there are no substantial changes in structure when compared to canonical nucleosomes [76]. Some evidence indicates that nucleosomes containing H2AZ may be less stable than canonical nucleosomes in vivo [77, 78]. However, an in vitro study did not detect significant differences in stability [79]. These conflicting results may be explained by other factors in the nuclear environment. Indeed, H2AZ contains

unique modification sites [80], which may result in decreased stability and an open chromatin structure.

Histone Chaperones in Transcription

Histone chaperones are a large class of proteins that are defined by their ability to bind to histones. These proteins are required for the assembly of nucleosomes under physiological conditions, shuttle histones into the nucleus, facilitate modifications, and promote transcription [81-83].

Facilitates Chromatin Transcription (FACT) is a heterodimeric complex that was discovered based on its ability to stimulate transcription on chromatin in vitro [84]. Human FACT (hFACT) consists of the Spt16 and SSRP1 subunits, while yeast FACT (yFACT) contains Spt16, Pob3, and possibly Nhp6 [85]. In *S. cerevisiae* both Spt16 and Pob3 are essential for viability. It has been shown by ChIP to enrich in the coding regions of genes and associate with the elongating RNA pol II [86, 87]. Mutations in the complex hinder elongation and cause defects in the chromatin structure of gene bodies [88]. It is believed to promote transcription by destabilizing H2A-H2B dimers during elongation and then to reassemble nucleosomes behind pol II [89-91].

Spt6 is another essential histone chaperone complex. Like FACT, Spt6 associates with the elongating Pol II during transcription and has chromatin assembly activity in vitro [87, 92, 93]. A tandem SH2 domain is believed to mediate the interaction with the elongating pol II by recognizing phosphorylated serines on the CTD [94]. Again, like FACT, mutations in Spt6 result in defects in the chromatin structure of open reading frames [88].

Asf1 is a histone chaperone that specifically interacts with H3-H4 dimers. It is involved in the H3-H4 nuclear import pathway and facilitates the acetylation of H3K56 on newly synthesized

histones [45, 95]. The crystal structure of Asf1 in complex with H3-H4 was solved and shows that its interaction with the dimer blocks formation of the H3-H4 tetramer [96]. This supports the model that Asf1 can function as a nucleosome disassembly protein, which has been suggested in numerous *in vivo* studies [97-99]. However, Asf1 has also been shown to be important in chromatin assembly [97, 100], indicating that its role in chromatin dynamics may be complex.

NAP1 is a homodimeric chaperone that is involved in many biological activities. These include the shuttling histones into the nucleus and the promotion of nucleosome reassembly during transcription elongation [101, 102]. *In vitro*, it is a very potent nucleosome assembly factor [103] and has been shown to interact with both H3-H4 tetramers and H2A-H2B dimers [104]. The *in vitro* properties of this enzyme in histone binding and chromatin assembly have been well studied. Thermodynamic models suggest that NAP1 preferentially binds to H3-H4 tetramers and assembles them on to DNA, forming tetrasomes. It then binds to H2A-H2B dimers and deposits them onto tetrasomes to form nucleosomes [105]. Additionally, it removes H2A-H2B dimers that are associated non-specifically with DNA, which further promotes nucleosome assembly [106]. Some biochemical studies have linked it with transcription [107, 108] and in Chapter 2 of this dissertation I will show that it can cooperate with a chromatin remodeling complex to facilitate elongation on chromatin *in vitro*.

ATP-dependent Chromatin Remodeling Enzymes

ATP-dependent chromatin remodeling enzymes (ATPases) are enzymes that utilize the hydrolysis of ATP to disrupt histone-DNA contacts. ATPases have several activities including nucleosomes spacing, eviction, and the exchange of histone variants. They can be categorized into four main families: the SWI/SNF family, the Ino80 family, the CHD family, and the ISWI family [109].

The *S. cerevisiae* SWI/SNF complex was the first ATPase to be discovered. Subunits of the complex were identified in genetic screens designed to identify regulators of the HO and SUC2 genes (for review see [110]). Later, it was shown that the isolated complex could alter nucleosomes in vitro and promote transcription factor binding [111]. The second SWI/SNF family member in yeast is the RSC complex. This essential ATPase was discovered based on homology to the SWI/SNF complex [112]. Both SWI/SNF and RSC contain bromodomains that selectively recognize acetylated histones [113].

The Ino80 family of ATPases includes the Ino80 complex (Ino80C) and the SWR1 complex (SWR1-C). This family is characterized by a split ATPase domain and the presence of the Rvb proteins [114]. In yeast, both ATPases have been shown to exchange histone variants of H2A. SWR1-C incorporates H2AZ into chromatin and Ino80C removes it [115, 116]. Both complexes are involved in DNA repair and transcription [114].

Heterochromatin in *S. cerevisiae*

Heterochromatin in *S. cerevisiae* is characterized by the presence of the Silent Information Regulator (Sir) complex, which consists of the proteins Sir2, Sir3, and Sir4, and the lack of histone acetyl- and methylation. The Sir proteins bind to silencer elements encoded in the genome and spread along chromosomes to form a silent chromatin structure (for review see [117]). Silencing elements are present in the telomeres and flanking the silent mating loci. The Sir proteins were originally identified with a genetic screen that identified genes required for repression of a gene cassette inserted into the silent mating type loci [118].

The silent mating loci, HML and HMR, contain unexpressed copies of the MAT locus alleles α and **a** respectively. These alleles encode regulators of the two haploid mating types and the diploid formed after mating. In haploid cells, the presence of either α or **a** alleles at the MAT

locus (MAT α or MATa) determines the mating type of the strain. Haploid cells are only able to mate with other haploid cells of the opposite mating type. When the cells mate to form a diploid, both a copy of MAT α and MATa will be present which expresses the diploid program and prevents further mating. Through a tightly controlled and site-specific homologous recombination event, the MAT locus alleles can be replaced with copies from the silent mating loci. This process allows yeast to switch their mating type up to once per generation [119]. The proper silencing of HML and HMR is essential to ensure that haploid strains express only one mating type allele and are able to mate. In fact, the silent mating type loci are two of the least transcribed regions in the genome [120].

The Sir complex has served as a very important model system to study the properties of heterochromatin and gene silencing. The complex consists of the proteins Sir2, Sir3, and Sir4. Sir2 is the most well known protein of the three because it was the first member of the sirtuin family of proteins to be discovered. Sir2 is an NAD-dependent HDAC that forms a dimer with Sir4. It is known to deacetylate H3K9, H3K14, and H4K16. When the deacetylation reaction occurs one molecule of an NAD metabolite called O-acetyl-ADP ribose (AAR) is produced. AAR has been shown to promote Sir3 binding to Sir2 and Sir4 and cause a conformation change in the Sir complex [121]. Both Sir3 and Sir4 are non-enzymatic proteins, but they perform important structural roles in yeast heterochromatin [117].

Sir3 contains a conserved bromo-adjacent homology (BAH) domain that has been the subject of many studies. Mutations within the domain have been shown to disrupt silencing [122]. Protein-protein interaction studies revealed that the BAH regulates the binding of Sir3 to nucleosomes through interactions with the H4 tail and the H3 globular domain [123]. A crystal structure of the BAH domain in complex with the nucleosome provided a molecular understanding of how these interactions occur [124]. When Sir3 is in contact with the

nucleosome it has interactions with the H4 tail near residues H4K16 and with the H3 globular domain near H3K79. As noted, H4K16 is subject to acetylation and H3K79 to methylation. Mutations in either of these residues have been shown to disrupt silent chromatin function [64, 125]. Additionally, in vitro results have shown that the Sir complex is inhibited from silencing transcription on H4K16 acetylated and H3K79 methylated templates [63, 126].

As mentioned, the Sir complex assembles on silencer elements and spreads outward to create silent regions. At the telomere, the Rap1 transcription factor binds to TG₁₋₃ repeats and directly interacts with Sir4. Recruitment of Sir4 brings in Sir2, which then facilitates the binding of Sir3 [117]. At the HM loci, a similar mechanism occurs. These regions are flanked by silencing elements termed E and I (for Essential and Important). E and I serve as binding sites for the transcription factors Rap1, Abf1 and Orc1. These proteins interact with Sir1 which cooperates with the transcription factors to bring in Sir4, Sir2 and Sir3 [117].

One of the interesting aspects of heterochromatin is the ability for it to spread from initiation sites along chromosomes to create silent domains independent of the underlying DNA sequence. The Sir proteins achieve this via the enzymatic activity of Sir2 and the interactions of the complex with histones H3 and H4 and each other. The current model suggests that Sir2 deacetylates its target substrates in adjacent nucleosomes. The deacetylation of H4K16 creates high affinity binding site for Sir3, which in turn recruits more Sir4 and Sir2. This process continues in iterative cycles as the proteins spread outward from the silencing element and create a silent region (see Figure 2) [117]. The spreading thought to be stopped when the heterochromatin reaches a barrier (or insulator) element. Barrier elements surrounding the HM loci have been identified as nearby genes and upstream activator sequences. In the subtelomeric regions elements called STARs, which recruit Reb1 and Tbf1 transcription factors, have been associated with barrier function [127, 128]. These barriers likely exert their effect

by the recruitment of chromatin modifying enzymes that block spreading. The acetylation of H4K16 by Sas2 and methylation of H3K79 by Dot1 have been shown to be important for preventing the spreading. Additionally, some screens have identified a function for TFIID, mediator, SWI/SNF, and other chromatin proteins in blocking the spreading of heterochromatin [128]. This indicates the potential for multiple and overlapping functions utilized to restrict Sir complex spreading.

The precise mechanism by which the Sir proteins block transcription remains unknown. Different *in vivo* studies have been published suggesting that the Sirs block either PIC assembly or initiation [129, 130]. The conflict between these studies was partially resolved by recent *in vitro* work that suggested that the Sirs function to block both steps [131]. Thus, it is possible that the Sirs function at both steps and gene-to-gene variability may influence which one the Sirs function at.

Multiple studies have shown that merely the presence of the Sir proteins is not sufficient for gene silencing *in vivo*. The deletions of Spt10 and Spt21, mutations in H3K56, and the presence of H3K79 methylation have all been shown to disrupt silencing without significantly altering the Sir protein binding to genes [63, 132, 133]. It is possible that this phenotype may be due to changes in higher order structure of the silent regions. This is supported by the increased *dam* methylase accessibility observed in some of these studies [132, 133]. Further support for a role of higher order structure or nuclear organization comes from cellular imaging studies show that Rap1, the Sir proteins, and silent regions form clusters at the nuclear periphery [134-136]. Furthermore, 3C techniques have shown that HML and HMR associate with each other in a manner that is dependent on the Sir proteins [137].

Transcription Elongation on Chromatin

Transcription of a gene starts with the assembly of the PIC at the gene promoter. After initiation begins, RNA pol II is phosphorylated on the CTD and initiation factors are exchanged for elongation factors [138-140]. At the 5' end of the gene the CTD repeats are phosphorylated on serines 5 and 7. As the polymerase moves away from the transcription start site and towards the 3' end of the gene, phosphorylation at serines 5 and 7 decreases and phosphorylation at serine 2 increases [87, 141]. A primary function of serine 5 phosphorylation is the recruitment of the 5' capping enzymes. In fact, inviable strains of fission yeast lacking all copies of serine 5 can be rescued by fusion of the capping enzymes to RNA pol II [142]. Ser2 phosphorylation appears to have functions beyond RNA processing. While it is involved in 3' processing [143], it also is recognized by histone chaperone Spt6 and histone methyltransferase Set2 [94, 144]. Spt6, however, is recruited to the pol II elongation complex very early during transcription, along with the Paf complex, FACT, and Spt4/5 [87]. Based on the proteins associated with the elongating pol II, it can be inferred that two very important activities that must be coupled with RNA synthesis are RNA processing and chromatin regulation.

Several studies from the late 1980's demonstrated that nucleosomes are repressive to transcription both in vivo and in vitro [145-148]. How this barrier is overcome, and what happens to histones in coding regions during transcription, has been the subject of much research and a lot of emphasis has been focused on the proteins associated with elongating pol II (for reviews [8, 13, 149]). ChIP studies show that some histones remain in the coding regions of transcribed genes and undergo constant exchange [150]. As mentioned in the section on histone chaperones, mutations in FACT, Spt6, and Asf1 lead to defects in the chromatin structure of open reading frames. Their loss leads to reduction in the histone density within coding regions. This, in turn, results in transcription from cryptic promoters within genes. In fact, mutations in many proteins associated with elongation cause cryptic transcription phenotypes [14]. In one interesting paper, the FACT complex was shown to deposit histones in a

nucleosome depleted region during transcription [151]. These findings suggest that both disassembly and assembly of nucleosomes are coupled to the transcription elongation machinery, perhaps independently.

The current model in the field suggests that histones H3 and H4 are acetylated in coding regions of transcribed genes by the histone exchange pathway and the presence of SAGA and NuA4. These acetylation marks are thought to recruit RSC and SWI/SNF to evict the nucleosomes in front of pol II. Chaperones like Spt6, FACT, and Asf1 reassemble the nucleosomes behind pol II. Some of this reassembly is likely to come from recycling the preexisting histones and the rest comes from histone exchange [150]. Behind pol II, Set2 methylates the nucleosomes at H3K36, which recruits the Rpd3S HDAC. Reassembly of nucleosomes behind pol II and deacetylation by Rpd3S maintains histone density in the coding regions and prevents cryptic transcription. Evidence suggests that the chromatin remodelers Isw1b and Chd1 function in the coding regions behind RNA pol II (Isw1b recognizes H3K36 methylation) to organize the chromatin and suppress histone exchange [152]. Refer to Figure 3 for a schematic of the model.

In vitro studies of elongation through chromatin have yielded insights into both the nature of the nucleosomal barrier and the mechanisms of nucleosome traversal by pol II. Results from several labs show that the strongest barriers to traversal are the histone-DNA contacts near the dyad of the nucleosome [15, 153-155]. Not surprisingly, the region near the dyad was shown to contain the strongest histone-DNA contacts [156]. Weakening histone-DNA contacts, with high ionic strength conditions or histone Sin mutations, stimulates elongation [157]. Studies under these conditions have shown that transcription of the nucleosome by pol II can displace the entire histone octamer or one H2A-H2B dimer [158]. Similar results were obtained using atomic force microscopy to observe the hexasome on individual templates after pol II passage [159].

The results of these experiments, and ones described below with the histone chaperone FACT, collectively point to formation of a hexasome as a key step in pol II transcription through a nucleosome.

In vitro studies have also demonstrated functions for proteins and histone modifications in specifically stimulating transcription by pol II on chromatin. Work from the Reinberg and Studitsky labs showed that hFACT is able to directly stimulate nucleosome traversal by pol II in a purified system. The current model is that hFACT interacts with the DNA binding surface of the H2A-H2B dimer. This interaction promotes uncoiling of the nucleosome during transcription and reassembly of a hexasome behind the polymerase [160]. In another study the human bromodomain-containing histone chaperones Brd2 and Brd3 specifically stimulated elongation on acetylated chromatin [161]. Finally, in the same system used in this dissertation, RSC and SWI/SNF were shown to utilize ATP to stimulate elongation by pol II in a reaction that was enhanced by histone acetylation by SAGA and NuA4 [15].

Next generation sequencing technologies have enabled the development of multiple methods for analyzing transcription by RNA pol II in the nucleus. One such development is the global nuclear run on (GRO-seq) assays. This method detects where actively engaged RNA pol II is present in the genome. This is in contrast to ChIP assays of RNA pol II that show where it is present, but cannot distinguish the actively transcribing pol II. Correlating GRO-seq data with genome wide ChIP data for histones showed that in mammalian cells active genes tend to have a large fraction of engaged RNA pol II paused proximal to the promoter and just upstream of a nucleosome [162], which suggested that the nucleosomal barrier may be a cause for this RNA pol II pausing. However, a higher resolution version of this technique (termed precision nuclear run on, or PRO-seq) used in *D. melanogaster* cells seemed to show that promoter proximal

pausing does not precisely correlate with the nucleosome, and thus the paused RNA pol II found in metazoans may be blocked by something other than the nucleosomal barrier [163].

In yeast a third approach was developed. Termed native elongating transcript sequencing (NET-seq), this technique involves purifying RNA pol II from cells, sequencing the nascent RNA, and then mapping it to the genome [164]. Churchman and Weissman used this method to create a map of transcription at single nucleotide resolution. In order to analyze transcriptional pausing, the authors did the analysis in cells lacking Dst1. Dst1 is the yeast homolog of TFIIIS, which is an elongation factor that stimulates the RNA pol II 3' cleavage activity. This activity is required for pol II to reengage in transcription after it backtracks at a barrier. Kireeva and colleagues demonstrated that this activity promotes pol II transcription through nucleosomes [153].

Therefore, by deleting Dst1, sites of pol II backtracking should be identifiable. The results of the NET-seq experiment show that pol II naturally pauses throughout gene bodies. When that data is correlated with nucleosome positioning data it shows a pattern of pausing right before the dyad axis in the second, third, and fourth nucleosome of transcribed genes [164]. This indicates that even in the context of a living cell, with all of the elongation factors, nucleosomes still generate a barrier to elongation that must be overcome.

Summary of Dissertation

The work in this dissertation falls into two categories. Chapters 2 and 3 address the questions of how RNA pol II is able to overcome the nucleosome barrier and how this process affects chromatin structure. A reconstituted system was used to test the activities of a variety of ATPases and histone chaperones in facilitating transcription elongation and maintaining chromatin structure. Chapters 4 and 5 investigate the properties of yeast heterochromatin in vitro and in vivo, with chapter 5 being a discovery-based project designed to identify new components of heterochromatin and analyze their function.

Chapter 2 of this dissertation is a reprint of work published in PNAS. This study screened the activities of the histone chaperones Nap1, Spt6, FACT, and Asf1 in stimulating transcription elongation with the ATPase RSC. Of these chaperones, NAP1 had the most profound effect on transcription. While RSC has the capacity to evict the histone octamer from the template, we found that in the presence of NAP1 only one H2A-H2B dimer is lost, leaving a hexasome on the template.

Chapter 3 is a reprint of work published in Current Biology. This study investigated the activities of the Rpd3S HDAC complex. The results showed that Rpd3S was repressive to elongation. It could both prevent octamer eviction by RSC and act as a histone chaperone to deposit histones onto DNA. In vivo experiments showed that Rpd3S functions to stabilize nucleosomes even without its catalytic HDAC activity.

Chapter 4 is a reprint of work published in Genes and Development. The main goal of this project was to investigate the phenomenon of telomeric position effect variegation in yeast. Major findings showed that the methylation of H3K79 was the critical difference between active and silenced genes in near the telomere. Surprisingly, Sir proteins were present at both the active and silenced loci. In vitro work confirmed that H3K79 methylation was sufficient to block the repressive activities of the Sir proteins even under conditions where their binding to the template was unaffected.

Chapter 5 is based on a project that started with the proteomic analysis of reconstituted yeast heterochromatin. In this project reconstituted chromatin and heterochromatin were incubated with yeast nuclear extract and the interacting proteins were identified by mass spectrometry. The comparison revealed that the Ino80 complex was one of the major complexes enriched in

heterochromatin. This interaction was confirmed by western blot and a genetic screen revealed that two subunits of the Ino80 complex, Arp5 and Ies6, were critical for maintaining silencing of the HML locus.

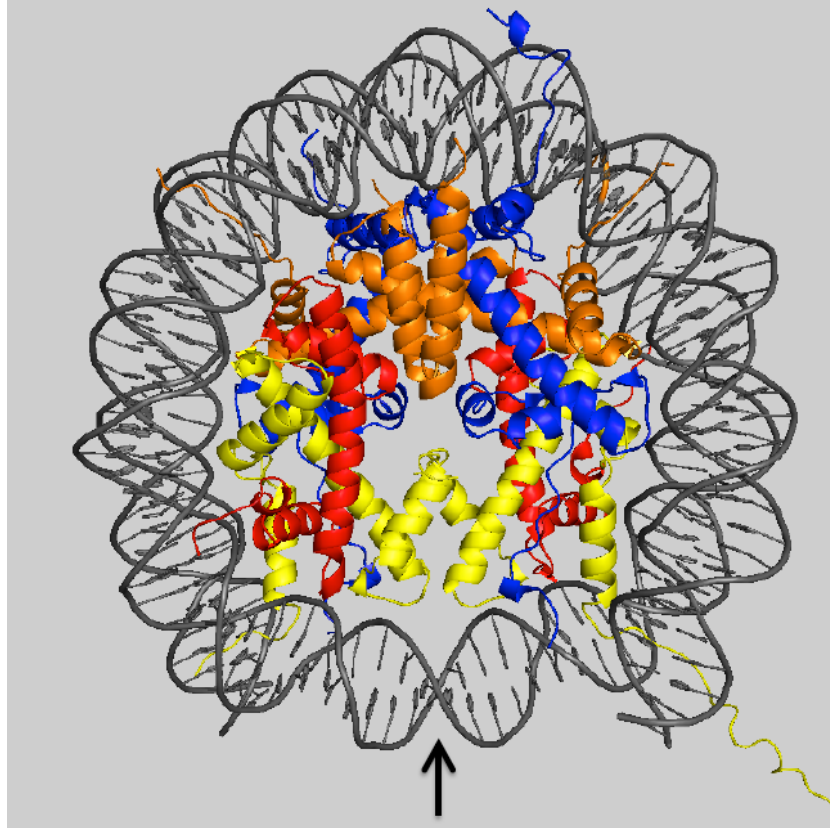


Figure 1. Crystal structure of the nucleosome core particle. The histone octamer, consisting of two copies each of H3 (yellow), H4 (red), H2A (blue), and H2B (orange) is shown wrapped by 146 bp of DNA (gray). The black arrow indicated the nucleosomal dyad.

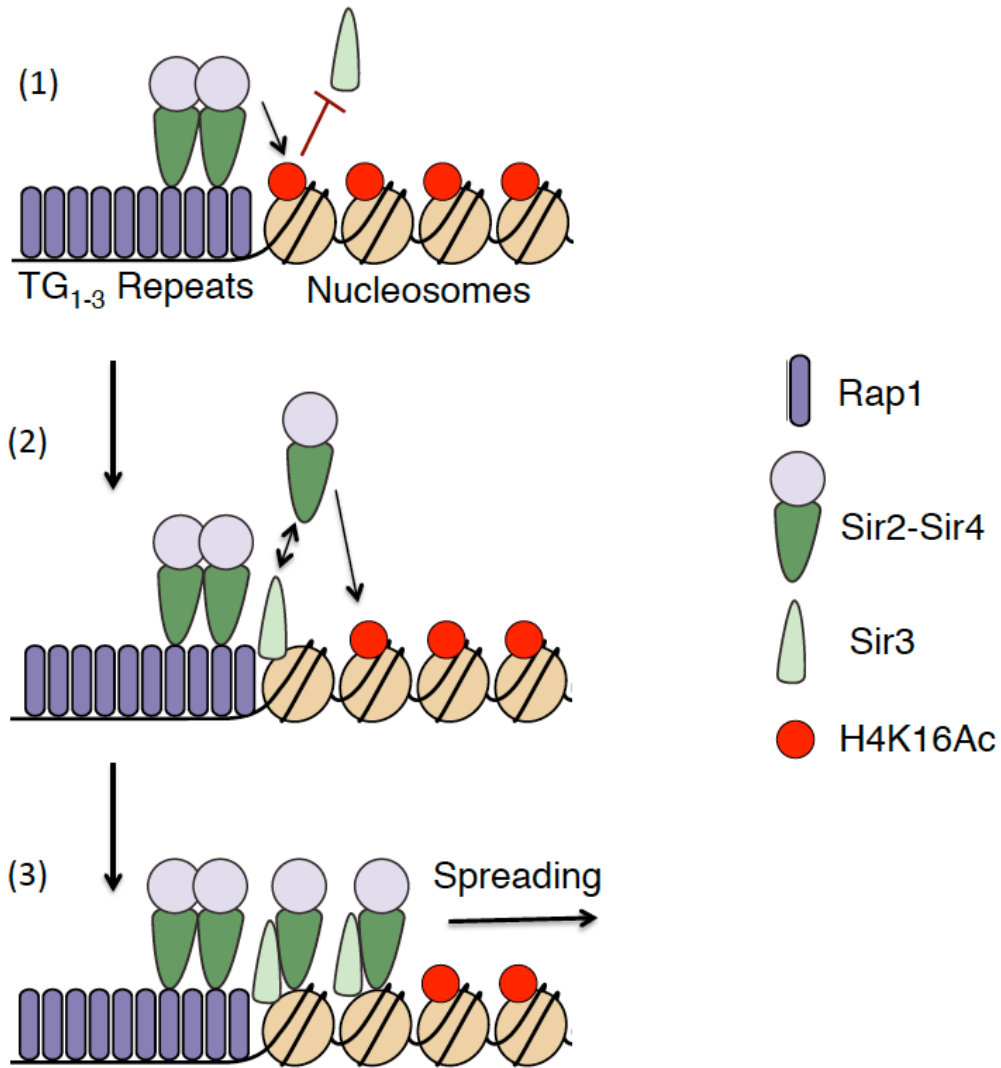


Figure 2. Model Sir complex spreading at the telomere. (1) Rap1 bound to the TG₁₋₃ repeats in the telomere directly interacts with Sir4 to bring in the Sir2-Sir4 dimer. Sir3 is unable to bind because of H4K16 acetylation. (2) Sir2 deacetylates H4K16, which allows Sir3 to bind. Sir3 then recruits more Sir2-Sir4. (3) The cycle repeats and spreading of heterochromatin occurs.

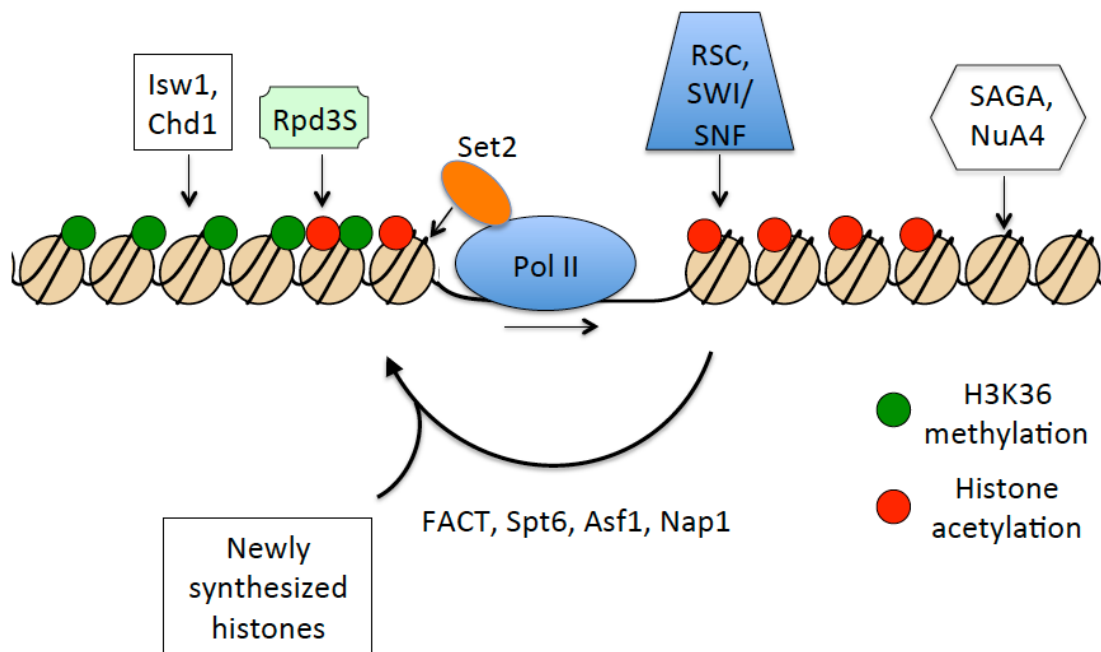


Figure 3. Model of nucleosome regulation during transcription elongation. Pol II is shown transcribing a nucleosomal array. In front of pol II, the SAGA and NuA4 HAT complexes acetylate nucleosomes. This acetylation recruits RSC and SWI/SNF ATPases, which coordinate with the elongating pol II and histone chaperones to facilitate nucleosomal transcription via nucleosome eviction and dimer exchange. Behind the polymerase, nucleosomes are assembled both in cis, with histones that were present before transcription, and in trans with newly synthesized histones. Set2, which is associated with the phosphorylated CTD of the transcribing pol II, methylates these nucleosomes at H3K36. H3K36 methylation recruits the Rpd3S HDAC complex to deacetylate nucleosomes behind pol II. The chromatin remodeling complexes Isw1 and Chd1 function behind the polymerase to organize chromatin in its wake.

References

1. Ptashne, M., *A Genetic Switch, Third Edition: Phage Lambda Revisited*. 2004, Cold Spring Harbor, NY: Cold Spring Harbor Laboratory Press.
2. Roeder, R.G. and W.J. Rutter, *Multiple forms of DNA-dependent RNA polymerase in eukaryotic organisms*. *Nature*, 1969. **224**(5216): p. 234-7.
3. Grummt, I., *Regulation of mammalian ribosomal gene transcription by RNA polymerase I*. *Prog Nucleic Acid Res Mol Biol*, 1999. **62**: p. 109-54.
4. Zawel, L. and D. Reinberg, *Common themes in assembly and function of eukaryotic transcription complexes*. *Annu Rev Biochem*, 1995. **64**: p. 533-61.
5. Willis, I.M., *RNA polymerase III. Genes, factors and transcriptional specificity*. *Eur J Biochem*, 1993. **212**(1): p. 1-11.
6. Groth, A., et al., *Chromatin challenges during DNA replication and repair*. *Cell*, 2007. **128**(4): p. 721-33.
7. Peterson, C.L. and J. Cote, *Cellular machineries for chromosomal DNA repair*. *Genes Dev*, 2004. **18**(6): p. 602-16.
8. Li, B., M. Carey, and J.L. Workman, *The role of chromatin during transcription*. *Cell*, 2007. **128**(4): p. 707-19.
9. Horn, P.J. and C.L. Peterson, *Molecular biology. Chromatin higher order folding--wrapping up transcription*. *Science*, 2002. **297**(5588): p. 1824-7.
10. McGhee, J.D. and G. Felsenfeld, *Nucleosome structure*. *Annu Rev Biochem*, 1980. **49**: p. 1115-56.
11. Kouzarides, T., *Chromatin modifications and their function*. *Cell*, 2007. **128**(4): p. 693-705.
12. Lee, T.I. and R.A. Young, *Transcription of eukaryotic protein-coding genes*. *Annu Rev Genet*, 2000. **34**: p. 77-137.
13. Workman, J.L. and R.E. Kingston, *Alteration of nucleosome structure as a mechanism of transcriptional regulation*. *Annu Rev Biochem*, 1998. **67**: p. 545-79.
14. Cheung, V., et al., *Chromatin- and transcription-related factors repress transcription from within coding regions throughout the *Saccharomyces cerevisiae* genome*. *PLoS Biol*, 2008. **6**(11): p. e277.
15. Carey, M., B. Li, and J.L. Workman, *RSC exploits histone acetylation to abrogate the nucleosomal block to RNA polymerase II elongation*. *Mol Cell*, 2006. **24**(3): p. 481-7.

16. Kuryan, B.G., et al., *Histone density is maintained during transcription mediated by the chromatin remodeler RSC and histone chaperone NAP1 in vitro*. Proc Natl Acad Sci U S A, 2012. **109**(6): p. 1931-6.
17. Chen, X.F., et al., *The Rpd3 core complex is a chromatin stabilization module*. Curr Biol, 2012. **22**(1): p. 56-63.
18. Heitz, E., *Das Heterochromatin der Moose*. I. Jahrb Wiss Bot, 1928. **69**: p. 762-818.
19. Elgin, S.C., *Heterochromatin and gene regulation in Drosophila*. Curr Opin Genet Dev, 1996. **6**(2): p. 193-202.
20. Kornberg, R.D., *Chromatin structure: a repeating unit of histones and DNA*. Science, 1974. **184**(4139): p. 868-71.
21. Olins, A.L. and D.E. Olins, *Spheroid chromatin units (v bodies)*. Science, 1974. **183**(4122): p. 330-2.
22. Oudet, P., M. Gross-Bellard, and P. Chambon, *Electron microscopic and biochemical evidence that chromatin structure is a repeating unit*. Cell, 1975. **4**(4): p. 281-300.
23. Woodcock, C.L., J.P. Safer, and J.E. Stanchfield, *Structural repeating units in chromatin. I. Evidence for their general occurrence*. Exp Cell Res, 1976. **97**: p. 101-10.
24. Finch, J.T. and A. Klug, *Solenoidal model for superstructure in chromatin*. Proc Natl Acad Sci U S A, 1976. **73**(6): p. 1897-901.
25. Cremer, T. and C. Cremer, *Rise, fall and resurrection of chromosome territories: a historical perspective. Part II. Fall and resurrection of chromosome territories during the 1950s to 1980s. Part III. Chromosome territories and the functional nuclear architecture: experiments and models from the 1990s to the present*. Eur J Histochem, 2006. **50**(4): p. 223-72.
26. Lieberman-Aiden, E., et al., *Comprehensive mapping of long-range interactions reveals folding principles of the human genome*. Science, 2009. **326**(5950): p. 289-93.
27. Luger, K., et al., *Crystal structure of the nucleosome core particle at 2.8 Å resolution*. Nature, 1997. **389**(6648): p. 251-60.
28. Tan, M., et al., *Identification of 67 histone marks and histone lysine crotonylation as a new type of histone modification*. Cell, 2011. **146**(6): p. 1016-28.
29. Wysocka, J., et al., *WDR5 associates with histone H3 methylated at K4 and is essential for H3 K4 methylation and vertebrate development*. Cell, 2005. **121**(6): p. 859-72.
30. Wysocka, J., et al., *A PHD finger of NURF couples histone H3 lysine 4 trimethylation with chromatin remodelling*. Nature, 2006. **442**(7098): p. 86-90.
31. Zeng, L. and M.M. Zhou, *Bromodomain: an acetyl-lysine binding domain*. FEBS Lett, 2002. **513**(1): p. 124-8.

32. Horn, P.J. and C.L. Peterson, *The bromodomain: a regulator of ATP-dependent chromatin remodeling?* Front Biosci, 2001. **6**: p. D1019-23.
33. Allfrey, V.G., R. Faulkner, and A.E. Mirsky, *ACETYLATION AND METHYLATION OF HISTONES AND THEIR POSSIBLE ROLE IN THE REGULATION OF RNA SYNTHESIS*. Proc Natl Acad Sci U S A, 1964. **51**: p. 786-94.
34. Brownell, J.E., et al., *Tetrahymena histone acetyltransferase A: a homolog to yeast Gcn5p linking histone acetylation to gene activation*. Cell, 1996. **84**(6): p. 843-51.
35. Taunton, J., C.A. Hassig, and S.L. Schreiber, *A mammalian histone deacetylase related to the yeast transcriptional regulator Rpd3p*. Science, 1996. **272**(5260): p. 408-11.
36. Rea, S., et al., *Regulation of chromatin structure by site-specific histone H3 methyltransferases*. Nature, 2000. **406**(6796): p. 593-9.
37. Shi, Y., et al., *Histone demethylation mediated by the nuclear amine oxidase homolog LSD1*. Cell, 2004. **119**(7): p. 941-53.
38. Ng, H.H., et al., *Ubiquitination of histone H2B by Rad6 is required for efficient Dot1-mediated methylation of histone H3 lysine 79*. J Biol Chem, 2002. **277**(38): p. 34655-7.
39. Dover, J., et al., *Methylation of histone H3 by COMPASS requires ubiquitination of histone H2B by Rad6*. J Biol Chem, 2002. **277**(32): p. 28368-71.
40. Sun, Z.W. and C.D. Allis, *Ubiquitination of histone H2B regulates H3 methylation and gene silencing in yeast*. Nature, 2002. **418**(6893): p. 104-8.
41. Briggs, S.D., et al., *Gene silencing: trans-histone regulatory pathway in chromatin*. Nature, 2002. **418**(6897): p. 498.
42. Jenuwein, T. and C.D. Allis, *Translating the histone code*. Science, 2001. **293**(5532): p. 1074-80.
43. Lee, J.S., E. Smith, and A. Shilatifard, *The language of histone crosstalk*. Cell, 2010. **142**(5): p. 682-5.
44. Loyola, A., et al., *PTMs on H3 variants before chromatin assembly potentiate their final epigenetic state*. Mol Cell, 2006. **24**(2): p. 309-16.
45. Campos, E.I., et al., *The program for processing newly synthesized histones H3.1 and H4*. Nat Struct Mol Biol, 2010. **17**(11): p. 1343-51.
46. Sobel, R.E., et al., *Conservation of deposition-related acetylation sites in newly synthesized histones H3 and H4*. Proc Natl Acad Sci U S A, 1995. **92**(4): p. 1237-41.
47. Li, Q., et al., *Acetylation of histone H3 lysine 56 regulates replication-coupled nucleosome assembly*. Cell, 2008. **134**(2): p. 244-55.
48. Chen, C.C., et al., *Acetylated lysine 56 on histone H3 drives chromatin assembly after repair and signals for the completion of repair*. Cell, 2008. **134**(2): p. 231-43.

49. Tsubota, T., et al., *Histone H3-K56 acetylation is catalyzed by histone chaperone-dependent complexes*. Mol Cell, 2007. **25**(5): p. 703-12.
50. Clemente-Ruiz, M., R. Gonzalez-Prieto, and F. Prado, *Histone H3K56 acetylation, CAF1, and Rtt106 coordinate nucleosome assembly and stability of advancing replication forks*. PLoS Genet, 2011. **7**(11): p. e1002376.
51. Shilatifard, A., *The COMPASS family of histone H3K4 methylases: mechanisms of regulation in development and disease pathogenesis*. Annu Rev Biochem, 2012. **81**: p. 65-95.
52. Avvakumov, N. and J. Cote, *The MYST family of histone acetyltransferases and their intimate links to cancer*. Oncogene, 2007. **26**(37): p. 5395-407.
53. Lauberth, S.M., et al., *H3K4me3 interactions with TAF3 regulate preinitiation complex assembly and selective gene activation*. Cell, 2013. **152**(5): p. 1021-36.
54. Sims, R.J., 3rd, et al., *Human but not yeast CHD1 binds directly and selectively to histone H3 methylated at lysine 4 via its tandem chromodomains*. J Biol Chem, 2005. **280**(51): p. 41789-92.
55. Lin, J.J., et al., *Mediator coordinates PIC assembly with recruitment of CHD1*. Genes Dev, 2011. **25**(20): p. 2198-209.
56. Krogan, N.J., et al., *The Paf1 complex is required for histone H3 methylation by COMPASS and Dot1p: linking transcriptional elongation to histone methylation*. Mol Cell, 2003. **11**(3): p. 721-9.
57. Wood, A., et al., *The Paf1 complex is essential for histone monoubiquitination by the Rad6-Bre1 complex, which signals for histone methylation by COMPASS and Dot1p*. J Biol Chem, 2003. **278**(37): p. 34739-42.
58. Briggs, S.D., et al., *Histone H3 lysine 4 methylation is mediated by Set1 and required for cell growth and rDNA silencing in Saccharomyces cerevisiae*. Genes Dev, 2001. **15**(24): p. 3286-95.
59. Terzi, N., et al., *H3K4 trimethylation by Set1 promotes efficient termination by the Nrd1-Nab3-Sen1 pathway*. Mol Cell Biol, 2011. **31**(17): p. 3569-83.
60. Margaritis, T., et al., *Two distinct repressive mechanisms for histone 3 lysine 4 methylation through promoting 3'-end antisense transcription*. PLoS Genet, 2012. **8**(9): p. e1002952.
61. Daniel, J.A. and P.A. Grant, *Multi-tasking on chromatin with the SAGA coactivator complexes*. Mutat Res, 2007. **618**(1-2): p. 135-48.
62. Ginsburg, D.S., C.K. Govind, and A.G. Hinnebusch, *NuA4 lysine acetyltransferase Esa1 is targeted to coding regions and stimulates transcription elongation with Gcn5*. Mol Cell Biol, 2009. **29**(24): p. 6473-87.

63. Kitada, T., et al., *Mechanism for epigenetic variegation of gene expression at yeast telomeric heterochromatin*. *Genes Dev*, 2012. **26**(21): p. 2443-55.
64. Nguyen, A.T. and Y. Zhang, *The diverse functions of Dot1 and H3K79 methylation*. *Genes Dev*, 2011. **25**(13): p. 1345-58.
65. Strahl, B.D., et al., *Set2 is a nucleosomal histone H3-selective methyltransferase that mediates transcriptional repression*. *Mol Cell Biol*, 2002. **22**(5): p. 1298-306.
66. Li, J., D. Moazed, and S.P. Gygi, *Association of the histone methyltransferase Set2 with RNA polymerase II plays a role in transcription elongation*. *J Biol Chem*, 2002. **277**(51): p. 49383-8.
67. Carrozza, M.J., et al., *Histone H3 methylation by Set2 directs deacetylation of coding regions by Rpd3S to suppress spurious intragenic transcription*. *Cell*, 2005. **123**(4): p. 581-92.
68. Bernstein, E., et al., *Mouse polycomb proteins bind differentially to methylated histone H3 and RNA and are enriched in facultative heterochromatin*. *Mol Cell Biol*, 2006. **26**(7): p. 2560-9.
69. Talbert, P.B. and S. Henikoff, *Histone variants--ancient wrap artists of the epigenome*. *Nat Rev Mol Cell Biol*, 2010. **11**(4): p. 264-75.
70. Dalal, Y., et al., *Tetrameric structure of centromeric nucleosomes in interphase Drosophila cells*. *PLoS Biol*, 2007. **5**(8): p. e218.
71. Santaguida, S. and A. Musacchio, *The life and miracles of kinetochores*. *EMBO J*, 2009. **28**(17): p. 2511-31.
72. Malik, H.S. and S. Henikoff, *Phylogenomics of the nucleosome*. *Nat Struct Biol*, 2003. **10**(11): p. 882-91.
73. Tagami, H., et al., *Histone H3.1 and H3.3 complexes mediate nucleosome assembly pathways dependent or independent of DNA synthesis*. *Cell*, 2004. **116**(1): p. 51-61.
74. Sakai, A., et al., *Transcriptional and developmental functions of the H3.3 histone variant in Drosophila*. *Curr Biol*, 2009. **19**(21): p. 1816-20.
75. Zlatanova, J. and A. Thakar, *H2A.Z: view from the top*. *Structure*, 2008. **16**(2): p. 166-79.
76. Suto, R.K., et al., *Crystal structure of a nucleosome core particle containing the variant histone H2A.Z*. *Nat Struct Biol*, 2000. **7**(12): p. 1121-4.
77. Zhang, H., D.N. Roberts, and B.R. Cairns, *Genome-wide dynamics of Htz1, a histone H2A variant that poises repressed/basal promoters for activation through histone loss*. *Cell*, 2005. **123**(2): p. 219-31.
78. Jin, C., et al., *H3.3/H2A.Z double variant-containing nucleosomes mark 'nucleosome-free regions' of active promoters and other regulatory regions*. *Nat Genet*, 2009. **41**(8): p. 941-5.

79. Thakar, A., et al., *H2A.Z and H3.3 histone variants affect nucleosome structure: biochemical and biophysical studies*. *Biochemistry*, 2009. **48**(46): p. 10852-7.
80. Millar, C.B., et al., *Acetylation of H2AZ Lys 14 is associated with genome-wide gene activity in yeast*. *Genes Dev*, 2006. **20**(6): p. 711-22.
81. Akey, C.W. and K. Luger, *Histone chaperones and nucleosome assembly*. *Curr Opin Struct Biol*, 2003. **13**(1): p. 6-14.
82. Park, Y.J. and K. Luger, *Histone chaperones in nucleosome eviction and histone exchange*. *Curr Opin Struct Biol*, 2008. **18**(3): p. 282-9.
83. Winkler, D.D. and K. Luger, *The histone chaperone FACT: structural insights and mechanisms for nucleosome reorganization*. *J Biol Chem*, 2011. **286**(21): p. 18369-74.
84. Orphanides, G., et al., *FACT, a factor that facilitates transcript elongation through nucleosomes*. *Cell*, 1998. **92**(1): p. 105-16.
85. Formosa, T., et al., *Defects in SPT16 or POB3 (yFACT) in Saccharomyces cerevisiae cause dependence on the Hir/Hpc pathway: polymerase passage may degrade chromatin structure*. *Genetics*, 2002. **162**(4): p. 1557-71.
86. Mason, P.B. and K. Struhl, *The FACT complex travels with elongating RNA polymerase II and is important for the fidelity of transcriptional initiation in vivo*. *Mol Cell Biol*, 2003. **23**(22): p. 8323-33.
87. Mayer, A., et al., *Uniform transitions of the general RNA polymerase II transcription complex*. *Nat Struct Mol Biol*, 2010. **17**(10): p. 1272-8.
88. Kaplan, C.D., L. Laprade, and F. Winston, *Transcription elongation factors repress transcription initiation from cryptic sites*. *Science*, 2003. **301**(5636): p. 1096-9.
89. Belotserkovskaya, R., et al., *FACT facilitates transcription-dependent nucleosome alteration*. *Science*, 2003. **301**(5636): p. 1090-3.
90. Schwabish, M.A. and K. Struhl, *Evidence for eviction and rapid deposition of histones upon transcriptional elongation by RNA polymerase II*. *Mol Cell Biol*, 2004. **24**(23): p. 10111-7.
91. Jamai, A., A. Puglisi, and M. Strubin, *Histone chaperone spt16 promotes redeposition of the original h3-h4 histones evicted by elongating RNA polymerase*. *Mol Cell*, 2009. **35**(3): p. 377-83.
92. Hartzog, G.A., et al., *Evidence that Spt4, Spt5, and Spt6 control transcription elongation by RNA polymerase II in Saccharomyces cerevisiae*. *Genes Dev*, 1998. **12**(3): p. 357-69.
93. Bortvin, A. and F. Winston, *Evidence that Spt6p controls chromatin structure by a direct interaction with histones*. *Science*, 1996. **272**(5267): p. 1473-6.

94. Sun, M., et al., *A tandem SH2 domain in transcription elongation factor Spt6 binds the phosphorylated RNA polymerase II C-terminal repeat domain (CTD)*. J Biol Chem, 2010. **285**(53): p. 41597-603.
95. Schneider, J., et al., *Rtt109 is required for proper H3K56 acetylation: a chromatin mark associated with the elongating RNA polymerase II*. J Biol Chem, 2006. **281**(49): p. 37270-4.
96. English, C.M., et al., *Structural basis for the histone chaperone activity of Asf1*. Cell, 2006. **127**(3): p. 495-508.
97. Schwabish, M.A. and K. Struhl, *Asf1 mediates histone eviction and deposition during elongation by RNA polymerase II*. Mol Cell, 2006. **22**(3): p. 415-22.
98. Takahata, S., Y. Yu, and D.J. Stillman, *FACT and Asf1 regulate nucleosome dynamics and coactivator binding at the HO promoter*. Mol Cell, 2009. **34**(4): p. 405-15.
99. Adkins, M.W. and J.K. Tyler, *The histone chaperone Asf1p mediates global chromatin disassembly in vivo*. J Biol Chem, 2004. **279**(50): p. 52069-74.
100. Green, E.M., et al., *Replication-independent histone deposition by the HIR complex and Asf1*. Curr Biol, 2005. **15**(22): p. 2044-9.
101. Del Rosario, B.C. and L.F. Pemberton, *Nap1 links transcription elongation, chromatin assembly, and messenger RNP complex biogenesis*. Mol Cell Biol, 2008. **28**(7): p. 2113-24.
102. Mosammaparast, N., C.S. Ewart, and L.F. Pemberton, *A role for nucleosome assembly protein 1 in the nuclear transport of histones H2A and H2B*. EMBO J, 2002. **21**(23): p. 6527-38.
103. Ishimi, Y. and A. Kikuchi, *Identification and molecular cloning of yeast homolog of nucleosome assembly protein I which facilitates nucleosome assembly in vitro*. J Biol Chem, 1991. **266**(11): p. 7025-9.
104. McBryant, S.J., et al., *Preferential binding of the histone (H3-H4)₂ tetramer by NAP1 is mediated by the amino-terminal histone tails*. J Biol Chem, 2003. **278**(45): p. 44574-83.
105. Andrews, A.J., et al., *A thermodynamic model for Nap1-histone interactions*. J Biol Chem, 2008. **283**(47): p. 32412-8.
106. Andrews, A.J., et al., *The histone chaperone Nap1 promotes nucleosome assembly by eliminating nonnucleosomal histone DNA interactions*. Mol Cell, 2010. **37**(6): p. 834-42.
107. Levchenko, V. and V. Jackson, *Histone release during transcription: NAP1 forms a complex with H2A and H2B and facilitates a topologically dependent release of H3 and H4 from the nucleosome*. Biochemistry, 2004. **43**(9): p. 2359-72.
108. Peterson, S., et al., *NAP1 catalyzes the formation of either positive or negative supercoils on DNA on basis of the dimer-tetramer equilibrium of histones H3/H4*. Biochemistry, 2007. **46**(29): p. 8634-46.

109. Clapier, C.R. and B.R. Cairns, *The biology of chromatin remodeling complexes*. Annu Rev Biochem, 2009. **78**: p. 273-304.
110. Vignali, M., et al., *ATP-dependent chromatin-remodeling complexes*. Mol Cell Biol, 2000. **20**(6): p. 1899-910.
111. Cote, J., et al., *Stimulation of GAL4 derivative binding to nucleosomal DNA by the yeast SWI/SNF complex*. Science, 1994. **265**(5168): p. 53-60.
112. Cairns, B.R., et al., *RSC, an essential, abundant chromatin-remodeling complex*. Cell, 1996. **87**(7): p. 1249-60.
113. Hassan, A.H., et al., *Selective recognition of acetylated histones by bromodomains in transcriptional co-activators*. Biochem J, 2007. **402**(1): p. 125-33.
114. Bao, Y. and X. Shen, *INO80 subfamily of chromatin remodeling complexes*. Mutat Res, 2007. **618**(1-2): p. 18-29.
115. Mizuguchi, G., et al., *ATP-driven exchange of histone H2AZ variant catalyzed by SWR1 chromatin remodeling complex*. Science, 2004. **303**(5656): p. 343-8.
116. Papamichos-Chronakis, M., et al., *Global regulation of H2A.Z localization by the INO80 chromatin-remodeling enzyme is essential for genome integrity*. Cell, 2011. **144**(2): p. 200-13.
117. Rusche, L.N., A.L. Kirchmaier, and J. Rine, *The establishment, inheritance, and function of silenced chromatin in Saccharomyces cerevisiae*. Annu Rev Biochem, 2003. **72**: p. 481-516.
118. Rine, J. and I. Herskowitz, *Four genes responsible for a position effect on expression from HML and HMR in Saccharomyces cerevisiae*. Genetics, 1987. **116**(1): p. 9-22.
119. Haber, J.E., *Mating-type genes and MAT switching in Saccharomyces cerevisiae*. Genetics, 2012. **191**(1): p. 33-64.
120. Holland, M.J., *Transcript abundance in yeast varies over six orders of magnitude*. J Biol Chem, 2002. **277**(17): p. 14363-6.
121. Liou, G.G., et al., *Assembly of the SIR complex and its regulation by O-acetyl-ADP-ribose, a product of NAD-dependent histone deacetylation*. Cell, 2005. **121**(4): p. 515-27.
122. Buchberger, J.R., et al., *Sir3-nucleosome interactions in spreading of silent chromatin in Saccharomyces cerevisiae*. Mol Cell Biol, 2008. **28**(22): p. 6903-18.
123. Onishi, M., et al., *Role of the conserved Sir3-BAH domain in nucleosome binding and silent chromatin assembly*. Mol Cell, 2007. **28**(6): p. 1015-28.
124. Armache, K.J., et al., *Structural basis of silencing: Sir3 BAH domain in complex with a nucleosome at 3.0 Å resolution*. Science, 2011. **334**(6058): p. 977-82.

125. Johnson, L.M., G. Fisher-Adams, and M. Grunstein, *Identification of a non-basic domain in the histone H4 N-terminus required for repression of the yeast silent mating loci*. EMBO J, 1992. **11**(6): p. 2201-9.
126. Johnson, A., et al., *Reconstitution of heterochromatin-dependent transcriptional gene silencing*. Mol Cell, 2009. **35**(6): p. 769-81.
127. Fourel, G., et al., *Cohabitation of insulators and silencing elements in yeast subtelomeric regions*. EMBO J, 1999. **18**(9): p. 2522-37.
128. Oki, M., et al., *Barrier proteins remodel and modify chromatin to restrict silenced domains*. Mol Cell Biol, 2004. **24**(5): p. 1956-67.
129. Sekinger, E.A. and D.S. Gross, *Silenced chromatin is permissive to activator binding and PIC recruitment*. Cell, 2001. **105**(3): p. 403-14.
130. Chen, L. and J. Widom, *Mechanism of transcriptional silencing in yeast*. Cell, 2005. **120**(1): p. 37-48.
131. Johnson, A., et al., *Heterochromatic gene silencing by activator interference and a transcription elongation barrier*. J Biol Chem, 2013. **288**(40): p. 28771-82.
132. Chang, J.S. and F. Winston, *Spt10 and Spt21 are required for transcriptional silencing in Saccharomyces cerevisiae*. Eukaryot Cell, 2011. **10**(1): p. 118-29.
133. Xu, F., et al., *Sir2 deacetylates histone H3 lysine 56 to regulate telomeric heterochromatin structure in yeast*. Mol Cell, 2007. **27**(6): p. 890-900.
134. Palladino, F., et al., *SIR3 and SIR4 proteins are required for the positioning and integrity of yeast telomeres*. Cell, 1993. **75**(3): p. 543-55.
135. Gotta, M., et al., *The clustering of telomeres and colocalization with Rap1, Sir3, and Sir4 proteins in wild-type Saccharomyces cerevisiae*. J Cell Biol, 1996. **134**(6): p. 1349-63.
136. Maillet, L., et al., *Evidence for silencing compartments within the yeast nucleus: a role for telomere proximity and Sir protein concentration in silencer-mediated repression*. Genes Dev, 1996. **10**(14): p. 1796-811.
137. Miele, A., K. Bystricky, and J. Dekker, *Yeast silent mating type loci form heterochromatic clusters through silencer protein-dependent long-range interactions*. PLoS Genet, 2009. **5**(5): p. e1000478.
138. Pokholok, D.K., N.M. Hannett, and R.A. Young, *Exchange of RNA polymerase II initiation and elongation factors during gene expression in vivo*. Mol Cell, 2002. **9**(4): p. 799-809.
139. Orphanides, G. and D. Reinberg, *A unified theory of gene expression*. Cell, 2002. **108**(4): p. 439-51.
140. Shilatifard, A., R.C. Conaway, and J.W. Conaway, *The RNA polymerase II elongation complex*. Annu Rev Biochem, 2003. **72**: p. 693-715.

141. Kim, M., et al., *Phosphorylation of the yeast Rpb1 C-terminal domain at serines 2, 5, and 7*. J Biol Chem, 2009. **284**(39): p. 26421-6.
142. Schwer, B. and S. Shuman, *Deciphering the RNA polymerase II CTD code in fission yeast*. Mol Cell, 2011. **43**(2): p. 311-8.
143. Ahn, S.H., M. Kim, and S. Buratowski, *Phosphorylation of serine 2 within the RNA polymerase II C-terminal domain couples transcription and 3' end processing*. Mol Cell, 2004. **13**(1): p. 67-76.
144. Li, B., et al., *The Set2 histone methyltransferase functions through the phosphorylated carboxyl-terminal domain of RNA polymerase II*. J Biol Chem, 2003. **278**(11): p. 8897-903.
145. Lorch, Y., J.W. LaPointe, and R.D. Kornberg, *Nucleosomes inhibit the initiation of transcription but allow chain elongation with the displacement of histones*. Cell, 1987. **49**(2): p. 203-10.
146. Han, M. and M. Grunstein, *Nucleosome loss activates yeast downstream promoters in vivo*. Cell, 1988. **55**(6): p. 1137-45.
147. Knezetic, J.A. and D.S. Luse, *The presence of nucleosomes on a DNA template prevents initiation by RNA polymerase II in vitro*. Cell, 1986. **45**(1): p. 95-104.
148. Kayne, P.S., et al., *Extremely conserved histone H4 N terminus is dispensable for growth but essential for repressing the silent mating loci in yeast*. Cell, 1988. **55**(1): p. 27-39.
149. Workman, J.L., *Nucleosome displacement in transcription*. Genes Dev, 2006. **20**(15): p. 2009-17.
150. Venkatesh, S., et al., *Set2 methylation of histone H3 lysine 36 suppresses histone exchange on transcribed genes*. Nature, 2012. **489**(7416): p. 452-5.
151. Perales, R., L. Zhang, and D. Bentley, *Histone occupancy in vivo at the 601 nucleosome binding element is determined by transcriptional history*. Mol Cell Biol, 2011. **31**(16): p. 3485-96.
152. Smolle, M., et al., *Chromatin remodelers Isw1 and Chd1 maintain chromatin structure during transcription by preventing histone exchange*. Nat Struct Mol Biol, 2012. **19**(9): p. 884-92.
153. Kireeva, M.L., et al., *Nature of the nucleosomal barrier to RNA polymerase II*. Mol Cell, 2005. **18**(1): p. 97-108.
154. Bondarenko, V.A., et al., *Nucleosomes can form a polar barrier to transcript elongation by RNA polymerase II*. Mol Cell, 2006. **24**(3): p. 469-79.
155. Bintu, L., et al., *Nucleosomal elements that control the topography of the barrier to transcription*. Cell, 2012. **151**(4): p. 738-49.

156. Hall, M.A., et al., *High-resolution dynamic mapping of histone-DNA interactions in a nucleosome*. Nat Struct Mol Biol, 2009. **16**(2): p. 124-9.
157. Hsieh, F.K., et al., *Histone Sin mutations promote nucleosome traversal and histone displacement by RNA polymerase II*. EMBO Rep, 2010. **11**(9): p. 705-10.
158. Kulaeva, O.I., et al., *Mechanism of chromatin remodeling and recovery during passage of RNA polymerase II*. Nat Struct Mol Biol, 2009. **16**(12): p. 1272-8.
159. Bintu, L., et al., *The elongation rate of RNA polymerase determines the fate of transcribed nucleosomes*. Nat Struct Mol Biol, 2011. **18**(12): p. 1394-9.
160. Hsieh, F.K., et al., *Histone chaperone FACT action during transcription through chromatin by RNA polymerase II*. Proc Natl Acad Sci U S A, 2013. **110**(19): p. 7654-9.
161. LeRoy, G., B. Rickards, and S.J. Flint, *The double bromodomain proteins Brd2 and Brd3 couple histone acetylation to transcription*. Mol Cell, 2008. **30**(1): p. 51-60.
162. Core, L.J., J.J. Waterfall, and J.T. Lis, *Nascent RNA sequencing reveals widespread pausing and divergent initiation at human promoters*. Science, 2008. **322**(5909): p. 1845-8.
163. Kwak, H., et al., *Precise maps of RNA polymerase reveal how promoters direct initiation and pausing*. Science, 2013. **339**(6122): p. 950-3.
164. Churchman, L.S. and J.S. Weissman, *Nascent transcript sequencing visualizes transcription at nucleotide resolution*. Nature, 2011. **469**(7330): p. 368-73.

Chapter 2

Histone density is maintained during transcription mediated by the chromatin remodeler RSC and histone chaperone NAP1 in vitro

Histone density is maintained during transcription mediated by the chromatin remodeler RSC and histone chaperone NAP1 in vitro

Benjamin G. Kuryan^a, Jessica Kim^a, Nancy Nga H. Tran^a, Sarah R. Lombardo^a, Swaminathan Venkatesh^b, Jerry L. Workman^b, and Michael Carey^{a,1}

^aDavid Geffen School of Medicine, Department of Biological Chemistry, 615 Charles E. Young Drive, University of California, Los Angeles, CA 90095-1737; and ^bStowers Institute for Medical Research, 1000 East 50th Street, Kansas City, MO 64110

Edited by Steven Henikoff, Fred Hutchinson Cancer Research Center, Seattle, WA, and approved December 20, 2011 (received for review June 20, 2011)

ATPases and histone chaperones facilitate RNA polymerase II (pol II) elongation on chromatin. In vivo, the coordinated action of these enzymes is necessary to permit pol II passage through a nucleosome while restoring histone density afterward. We have developed a biochemical system recapitulating this basic process. Transcription through a nucleosome in vitro requires the ATPase remodels structure of chromatin (RSC) and the histone chaperone nucleosome assembly protein 1 (NAP1). In the presence of NAP1, RSC generates a hexasome. Despite the propensity of RSC to evict histones, NAP1 reprograms the reaction such that the hexasome is retained on the template during multiple rounds of transcription. This work has implications toward understanding the mechanism of pol II elongation on chromatin.

Nucleosomes pose a strong barrier to RNA polymerase II (pol II) elongation (1–3). An understanding of how this barrier is overcome will reveal principles central to all eukaryotic organisms. Genome-wide chromatin immunoprecipitation analyses reveal that histone density is inversely proportional to transcriptional activity (4). However, with the exception of the heat shock loci (5), most genes maintain limited nucleosome density in the coding region during transcription. Maintenance of nucleosome density prevents cryptic transcription, which can have potentially deleterious effects on gene expression and genomic integrity (6).

Transcription through chromatin in vivo requires ATP-dependent remodeling machines, histone modification enzymes, and histone chaperones (7). ATP-dependent remodeling enzymes such as SWI/SNF and remodels structure of chromatin (RSC) can mobilize and/or evict nucleosomes to create an unimpeded DNA template for transcription (8). These enzymes are found at the promoters of genes and within ORFs (9–11). Furthermore, SWI/SNF has been shown to travel with pol II in vivo, evicting histones on active genes (12), and RSC has been shown to directly interact with the RNA pol subunit Rpb5 (13). In mammalian cells, pol II pauses at an artificially introduced 601 positioning sequence when SWI/SNF is knocked down by RNAi (14). Histone chaperones such as ASF1, SPT6, and FACT (SPT16/POB3) also travel with pol II throughout transcription and probably assist in the removal of histones in front of pol II and redeposition behind (15–17). Indeed, one study suggests that FACT redeposits the original histones behind pol II (18).

Studies of pol II elongation on chromatin in vitro have revealed insights into the mechanism. Experiments by Studitsky and coworkers showed that pol II frequently stalls and backtracks from the nucleosome (19). Higher ionic strength, which weakens DNA–histone contacts, abrogates the barrier allowing pol II to pass (20). The reaction is stimulated by TFIIS (19). Although nucleosomal passage by pol II occurs at physiological salt concentration (i.e., 150 mM), the efficiency increases with increasing ionic strength (20). Further, one orientation of the 601 positioned nucleosome is more permissive to transcription than the other (21). Studies by Reinberg and coworkers have shown that human FACT (SPT16/SSRP1) protein promotes pol II elongation on

chromatin in a system employing the general transcription factors (22). In a similar system, the bromodomain containing factors Brd2 and Brd3 facilitated elongation on acetylated chromatin substrates (23). In independent work, we found that the ATP-dependent RSC and SWI/SNF remodeling complexes from *Saccharomyces cerevisiae* were required for transcription of nucleosomal substrates in vitro and were stimulated by histone acetylation (24). In an effort to understand the role of histone chaperones, we purified and systematically analyzed the functions of ASF1, FACT, SPT6, and nucleosome assembly protein 1 (NAP1) during transcription of mononucleosomes in vitro. Surprisingly, among these, NAP1 was the most potent in stimulating transcription.

NAP1 is a homodimeric histone chaperone that binds to the histone folds of H3–H4 tetramers and H2A–H2B dimers and also interacts with the N-terminal tails of the H3–H4 tetramer (25, 26). The precise histone docking site on NAP1 is unknown but the crystal structure reveals an acidic surface (26). This surface may facilitate histone binding by neutralizing the basic charge of histones, as observed with other chaperones. NAP1 promotes nucleosome assembly by preventing nonnucleosomal histone–DNA interactions (27) and is found in the ORFs and promoters of *S. cerevisiae* and *Schizosaccharomyces pombe* genes by ChIP (28, 29). Deletion of NAP1 in *S. cerevisiae* affects expression of approximately 10% of the genome (30) and increases the H2A–H2B dimer density across genes (27). Some biochemical studies have supported the idea that NAP1 may play a role in transcription (31, 32). In vivo, NAP1 is recruited to sites of active transcription and functions in context with the TREX complex component YRA1, which is linked to mRNA biogenesis (28).

Previous studies had shown that NAP1 promotes the ability of RSC to evict the histone octamer from DNA (33). In our attempts to reproduce this phenomenon, we discovered that nanomolar concentrations of NAP1 and RSC promoted the loss of one H2A–H2B dimer, generating a hexasome. Under these conditions, NAP1 stimulated RSC-dependent pol II transcription of a nucleosomal template. Remarkably, under conditions where RSC would normally transfer the octamer to another DNA molecule, NAP1 promoted retention of the hexasome on the original DNA template. Hence, NAP1 and RSC coordinate to promote passage of pol II through a nucleosome, while maintaining partial nucleosome integrity.

Author contributions: B.G.K., S.V., J.L.W., and M.C. designed research; B.G.K., J.K., N.N.H.T., and S.V. performed research; J.K. and S.R.L. contributed new reagents/analytic tools; B.G.K. and M.C. analyzed data; and B.G.K. and M.C. wrote the paper.

The authors declare no conflict of interest.

This article is a PNAS Direct Submission.

¹To whom correspondence should be addressed. E-mail: mcarey@mednet.ucla.edu.

This article contains supporting information online at www.pnas.org/lookup/suppl/doi:10.1073/pnas.1109994109/-DCSupplemental.

Results

RSC-Dependent Pol II Elongation is Stimulated by Nucleosome Eviction. Our method for establishing pol II elongation complexes on chromatin involves the use of a single-stranded C tail attached to a DNA molecule bearing the 601 positioning sequence (Fig. S1A). The C tail serves as a binding site for pol II. Upon addition of nucleoside triphosphates, pol II transcribes into the double-stranded DNA containing the nucleosome assembled from recombinant octamers. The inclusion of RNase H prevents the formation of long DNA–RNA hybrids and allows pol II to establish a transcription bubble (34). The tailed-template approach was used to obtain the first crystal structures pol II elongation complexes (35, 36). The proteins used in this study included four chaperones (ASF1, NAP1, FACT, and SPT6), two ATP-dependent remodeling machines (SWI/SNF and RSC), and pol II. All were purified to near homogeneity (Fig. S1B). Pol II binds well to the template in both the free and nucleosomal forms as shown by EMSA (Fig. S1C).

Our previous work demonstrated that RSC facilitates elongation by pol II on nucleosomal templates in an ATP-dependent manner, both enhancing the overall levels of RNA synthesis and decreasing the pausing at the nucleosome (24). Although RSC alone stimulates transcription on the nucleosome, the strongest effects are dependent on the presence of unlabeled supercoiled plasmid DNA containing the 601 sequence (termed acceptor DNA) in the reaction. At 2 nM RSC, a fivefold increase in full-length transcript was observed with the enzyme alone, but this increased to a 152-fold stimulation upon the addition of acceptor DNA (Fig. 1A). The fold-stimulation varied only twofold in numerous experiments and correlated with small differences in the amount of free DNA remaining in different nucleosome preparations.

Previous studies have shown that RSC transfers the octamer from one DNA template to another (37). We performed chromatin remodeling reactions with RSC, in the presence and absence of acceptor DNA, on nucleosomes assembled with a ³²P-labeled 601 DNA sequence. After the remodeling reaction, RSC was competed from remodeled nucleosomes with poly(dI:dC) and the nucleosomal products were separated on native gels. The data in Fig. 1B show that in the presence of a supercoiled acceptor DNA molecule, RSC initially remodels the nucleosome. Higher levels of RSC lead to eviction of the octamer, generating free ³²P-labeled DNA. At 6 nM RSC, approximately 70% of the octamer is evicted. In contrast, in reactions lacking acceptor DNA, most of the octamer is retained on the template in the remodeled state. The data suggest that the effect of RSC on transcription in vitro is associated with its ability to evict the octamer from the template. However, an important caveat is that RSC generated a product migrating faster than the remodeled nucleosome in reactions bearing acceptor DNA. We will comment on the nature of this product below because it was also associated with the action of RSC and NAP1.

NAP1 Allows RSC-Dependent Elongation Without Nucleosome Eviction. We hypothesized, based on biochemical and genetic data, that histone chaperones would substitute for acceptor DNA and permit efficient RSC-dependent elongation. Chaperones known to be involved in transcription were purified (Fig. S1B) and tested in the elongation reaction. All of the proteins displayed some nucleosome assembly activity, the hallmark of chaperones, and FACT and NAP1 displayed the most potent effects (Fig. S2).

We next screened these histone chaperones in our in vitro transcription assay (Fig. 1C and Fig. S3A). Of the chaperones tested, NAP1 was most efficient in the ability to promote pol II elongation in the absence of acceptor DNA. NAP1 displayed a 69-fold stimulation of full-length RNA compared to the 71-fold average stimulation by acceptor DNA. ASF1 and SPT6 also stimulated slightly, but FACT did not. This result was surprising because

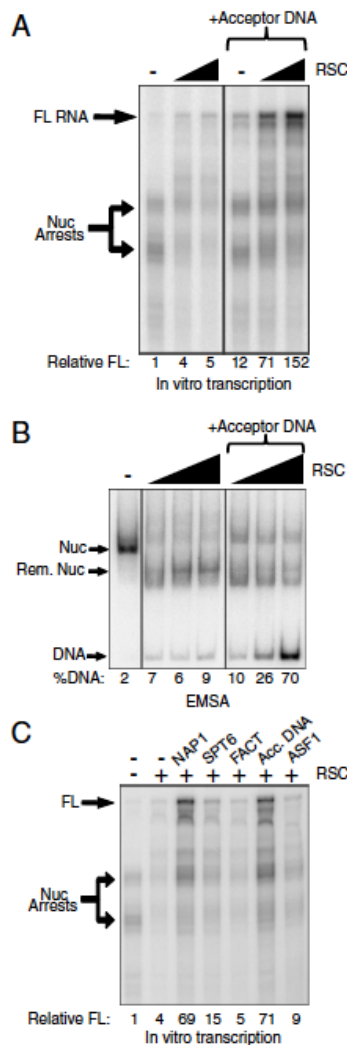


Fig. 1. RSC-dependent elongation requires a histone acceptor. (A) In vitro transcription with RSC in the presence or absence of acceptor DNA. Reactions containing 1 ng (0.3 nM) of C-tailed nucleosome template, 0.9 nM pol II, and 0, 0.2, or 2 nM RSC were incubated with ATP in the presence or absence of 10 ng pGEM3Z601R for 60 min. Nucleoside triphosphates containing ³²P-CTP were added for 15 min and the products were resolved on a 7 M urea 10% acrylamide gel. A PhosphorImage is shown. FL indicates the full-length transcript and arrows point to the nucleosomal arrests. Quantitation of the full-length product is indicated below each lane. (B) Nucleosome remodeling/eviction reactions with RSC in the presence or absence of acceptor DNA. Reactions containing 0.3 nM of ³²P-labeled mononucleosome template and 0, 0.6, 2, or 6 nM RSC were incubated with 2 mM ATP in the presence or absence of 10 ng pGEM3Z601R for 60 min, poly(dI:dC) was added, and the products were resolved by 4.5% native PAGE. An autoradiograph is shown. Quantitation of free DNA is shown below the gel. (C) In vitro transcription assay screening various histone chaperones. Transcription reactions with 0.9 nM pol II contained, from left to right, no addition, 2 nM RSC, and 2 nM RSC with either 42 nM NAP1, 53 nM SPT6, 49 nM FACT, 10 ng pGEM3Z601R, or 44 nM ASF1. The mean amount of FL RNA from two independent experiments is shown below each lane. A bar graph display of the data is shown in Fig. S3B.

studies by Reinberg and coworkers had shown that human FACT stimulates pol II elongation through nucleosomes (22). Formosa et al. have suggested that NHP6 facilitates the function of yeast FACT by substituting for the HMG domain of mammalian SSRP1 (38). However, addition of NHP6A to yeast FACT sup-

pressed rather than stimulated transcription and strongly inhibited the ability of RSC to evict histones both in the presence and absence of FACT (Fig. S4). This result is consistent with experiments that suggest NHP6 functions to stabilize nucleosomes in vivo (39). It is also consistent with the observation that mutations of yeast FACT lead to the cryptic transcription phenotype (16). Cryptic transcription is hypothesized to be due to an inability to properly assemble nucleosomes in transcribed regions (3).

To rule out the possibility that NAP1 was stimulating transcription independent of RSC, we performed a reciprocal titration of RSC and NAP1 in our transcription assay (Fig. 2A). We found that stimulation by NAP1 requires RSC and that both proteins display dose-dependent effects. A time course of the reaction suggests that the template undergoes continuous transcription for up to 45 min (Fig. 2B and Fig. S3B). These data implicate the combinatorial action of RSC and NAP1 in optimal transcription. Stimulation of transcription was also observed with NAP1 and SWI/SNF, a member of the same class of chromatin remodelers as RSC (Fig. S5).

To further study the mechanism by which NAP1 stimulates elongation, we employed a nucleosome remodeling assay. We found that NAP1 does not facilitate RSC-dependent nucleosome eviction in the absence of acceptor DNA (Fig. 2C). However, NAP1 with RSC promotes formation of a faster-migrating band in the gel (labeled “?”), representing a unique remodeled species or a partially disassembled nucleosome. These results were in contrast to a previous study that showed NAP1 was sufficient for nucleosome eviction by RSC (33). The discrepancy may be due to our use of lower concentrations of NAP1 (43 nM as opposed to 2.4 μ M) and recombinant *Xenopus laevis* histones rather than rat liver histones.

Because NAP1 is a nucleosome assembly protein, we hypothesized that histones evicted by RSC might be reassembled back onto the template, explaining the lack of nucleosome eviction. To examine this possibility, we tested whether NAP1 could facilitate RSC-dependent octamer transfer to acceptor DNA. If histones were fully evicted and then reassembled onto DNA, they should be redeposited onto the supercoiled acceptor DNA, which is in significant excess over the template. Surprisingly, NAP1 blocked RSC-dependent octamer transfer and instead produced the faster-migrating species described above (Fig. 2D).

NAP1 and RSC Generate a Hexasome. To determine the composition of the remodeled intermediate, we developed a sensitive assay to quantitate the relative amounts of H2A-H2B dimers and H3-H4 tetramers present at the subnanogram amounts in our assay. We fused protein kinase A (PKA) phosphorylation sites onto the N terminus of H3 and the C terminus of H2A (Fig. S64). We assembled these separately into octamers and then into nucleosomes. In the presence of PKA and γ^{32} P-ATP, the PKA-tagged histones within the context of the nucleosome could be labeled to high specific activity enabling facile detection on gels. The labeling was specific as measured by two criteria (Fig. S6B and C). First, only the PKA-tagged histone within the nucleosome was 32 P-labeled, as shown in the SDS gel of Fig. S6B, even though all four histones were present in the octamer. Second, only nucleosomes bearing a PKA-tagged histone were labeled as shown in the native gel of Fig. S6C. The presence of the PKA tag, either phosphorylated or unphosphorylated, did not affect the remodeling reaction or the distribution of remodeled products (Fig. S6D).

To determine the relative amounts of H2A-H2B dimer and H3-H4 tetramer in the nucleosomes remodeled by RSC and NAP1, we performed remodeling assays on nucleosomes in which the DNA, H3, or H2A were 32 P-labeled (*DNA, *H3, *H2A). We quantitated the NAP1-dependent remodeling product using ImageQuant TL. The results show that the remodeled species generated by NAP1 is still present in reactions in which DNA, H3, or H2A are separately labeled with 32 P (Fig. 3.4). We noted,

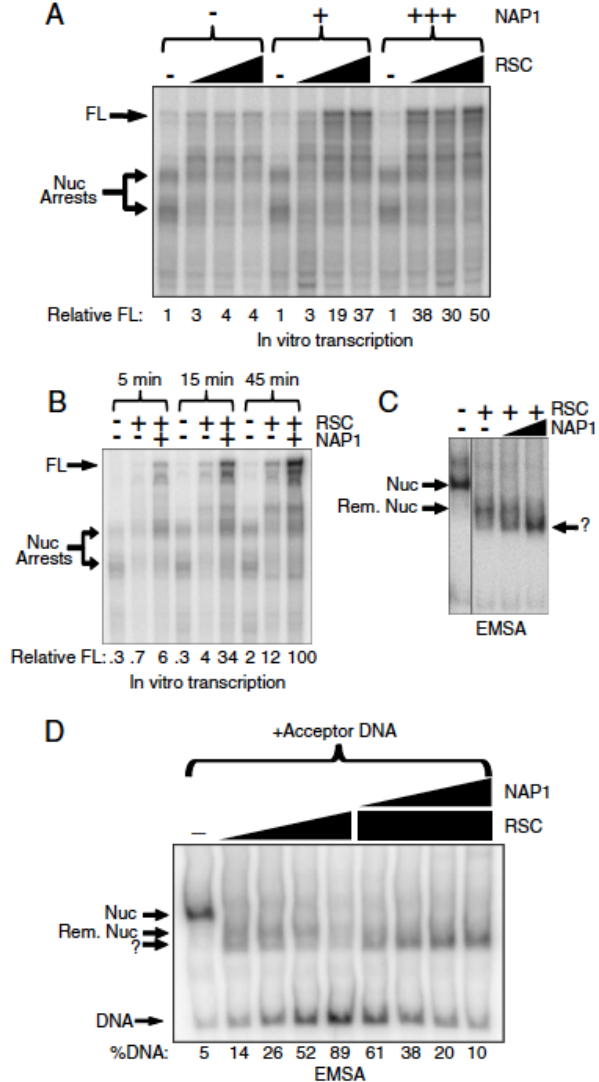


Fig. 2. NAP1-dependent elongation requires RSC, but not nucleosome eviction. (A) In vitro transcription reactions were performed with 0, 0.2, 0.7, or 2 nM RSC and 14 nM (+) or 43 nM (+++) NAP1. Quantitation of full-length RNA is shown below the gel. (B) Time course of in vitro transcription with 2 nM pol II, 2 nM RSC, and 43 nM NAP1. Quantitation of full-length (FL) RNA from three independent experiments is indicated below the gel. A bar graph of the quantitation is displayed in Fig. S3B. (C) Nucleosome remodeling assay with 0.6 nM RSC and 1.3 or 13 nM NAP1. No acceptor DNA was added. The question mark (?) indicates a NAP1-dependent product. (D) A nucleosome eviction assay with NAP1 was performed with 10 ng acceptor DNA and 0.6–17 nM RSC. NAP1, 4.8–130 nM, was titrated into reactions containing 17 nM RSC. Quantitation of free DNA is shown below the gel.

however, that in the reactions containing 32 P-labeled H2A, the remodeled species generated by NAP1 appeared lighter relative to the untreated nucleosome or nucleosome remodeled by RSC alone. To quantitate the remodeled species generated by NAP1, we divided the intensity of that band by the intensity of the untreated nucleosome for 32 P-labeled DNA, which normalizes the amount of nucleosome converted to the NAP1 remodeled species. We then obtained the same ratios for the reactions in which H3 or H2A were 32 P-labeled. We then divided those ratios by the ratio obtained with 32 P-labeled DNA because, in principle,

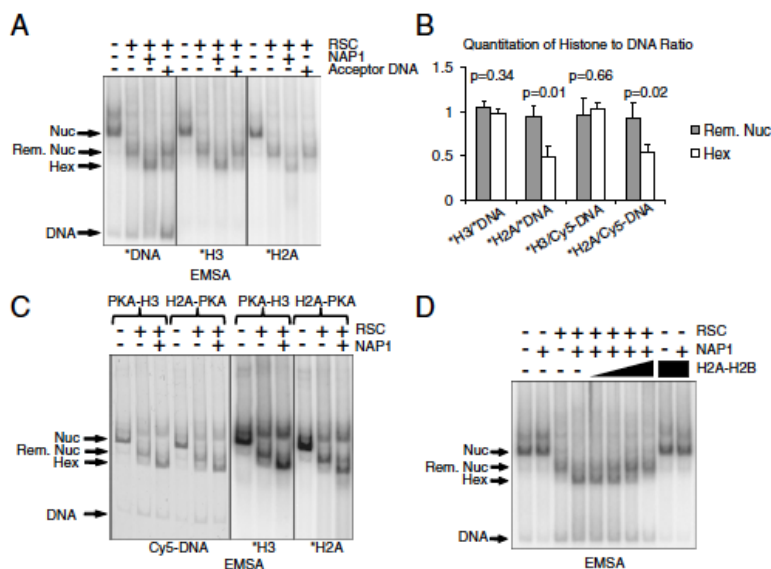


Fig. 3. NAP1 stimulates RSC-dependent hexasome formation. (A) Remodeling assay with NAP1 using nucleosomal substrates containing labeled DNA (*DNA), H3 (*H3), or H2A (*H2A) where indicated. Reactions contained 2 nM RSC, 43 nM NAP1, and 10 ng acceptor DNA where indicated. The hexasome migrates below the remodeled nucleosome ("Hex"). Because of differences in the labeling efficiency, a darker exposure of H3 is shown. (B) Quantitation of the histone to DNA ratios of the remodeled nucleosome and hexasome from A and C. The means from three independent experiments are displayed with the standard deviations as error bars. The ratios were calculated by dividing the intensity for each remodeled nucleosome or hexasome by the intensity of untreated nucleosome (Rem. Nuc/Nuc or Hex/Nuc). The value obtained for either *H3 or *H2A was then normalized to the value obtained for DNA as measured by Cy5 or ^{32}P label. *P* values were calculated using a two-tailed Student's *t* test. (C) Remodeling assay as in A using Cy5 labeled DNA with ^{32}P -H3 (*H3) or ^{32}P -H2A (*H2A). Left panels measure fluorescence intensities of Cy5 DNA template, whereas right panels are Phosphorimages of *H3 or *H2A. As in A, a darker exposure of H3 is shown. (D) Remodeling assay with 0.3, 1, 4, or 16 nM H2A-H2B dimer added to reactions containing 2 nM RSC and 43 nM NAP1.

if all of the histones are retained in the NAP1-generated remodeled species, then the resulting ratio should be one. Indeed in reactions containing ^{32}P -labeled H3, the ratio was very close to one (Fig. 3B; *H3/*DNA). However, in reactions containing ^{32}P -labeled H2A, the ratio was approximately 0.5 (Fig. 3B; *H2A/*DNA). In contrast, when we quantitated the nucleosome remodeled with RSC alone, the ratio was approximately one irrespective of whether H3 or H2A was ^{32}P -labeled. We argue that the species generated by RSC and NAP1 lacks half of the amount of H2A (and probably H2B), and is therefore a hexasome. To further validate our quantitation methodology, we repeated the reactions with ^{32}P -labeled histones assembled onto Cy5 labeled DNA templates (Fig. 3C). This technique allowed us to internally measure the DNA amounts within the ^{32}P -labeled nucleosomes using fluorescence, rather than comparing them to a separate reaction. Not surprisingly, the results were essentially identical. The ratios obtained with *H3/*DNA and *H2A/*DNA were equivalent to those obtained with *H3/Cy5-DNA and *H2A/Cy5-DNA, respectively (Fig. 3B). Similar results were obtained using a mononucleosome containing the natural 5S positioning sequence (Fig. S7A and B), indicating that this effect is not specific to the 601 sequence.

We performed the remodeling reactions with RSC and NAP1 in the presence of excess H2A-H2B dimer. This approach was previously employed independently by the Kornberg and Reinberg laboratories to study the composition of partially disassembled nucleosomes (33, 40). We found that increasing amounts of the H2A-H2B dimer converts the NAP1 generated remodeled species into a remodeled nucleosome (Fig. 3D). These data strengthen our argument that the remodeled species is a hexasome. Note that our inclusion of (poly)dl:dC after the reaction does not influence the appearance of the products, but is necessary to remove RSC so we can observe the hexasome (Fig. S7C and D). Also, at high concentration of *H2A, we

do observe the previously reported complex of NAP1 with H2A-H2B (25), but it migrates below the hexasome in our gels (Fig. S8) and is only weakly visible in reactions containing 0.3 nM nucleosome.

Pol II Forms Active Elongation Complexes on the Hexasome. To obtain a snapshot of pol II in the act of transcribing the hexasomal template, we captured the elongation complexes on native polyacrylamide gels. In this experiment, complexes were detected in separate reactions containing ^{32}P -labeled *DNA, *H3, and *H2A (Fig. 4A). The pol II complexes with nucleosome or DNA migrate with slower but unique mobilities versus the nucleosome or free DNA alone (Fig. S1B). The complexes of pol II on the remodeled nucleosome or hexasome migrate between the pol II:DNA and pol II:Nuc complexes (see blowup of Fig. 4A in Fig. S9A). Importantly, the amount of pol II:DNA under NAP1-dependent transcription conditions did not increase when compared to RSC alone but did increase in reactions lacking NAP1 but containing RSC and acceptor DNA (Fig. 4A). This observation supports the idea that pol II is transcribing a hexasomal template in the presence of RSC and NAP1. We do not understand the precise mechanics by which pol II passes through a hexasome but it may be similar to the mechanism proposed by Studitsky and coworkers (41).

The time course experiment in Fig. 4B shows that pol II remains bound to the hexasomal template throughout an extended time frame during which RNA accumulates linearly (Fig. 2B and Fig. S3B). Note that, in Figs. 4A and 4B, reactions containing RSC and NAP1 displayed a decrease in H2A signal. Quantitation of that signal by comparing the pol II:Hex to pol II:Nuc ratio of labeled histone with that of labeled DNA, revealed that the hexasomes contain approximately the same amount of H3 as DNA but approximately half the amount of H2A (Fig. 4C and D).

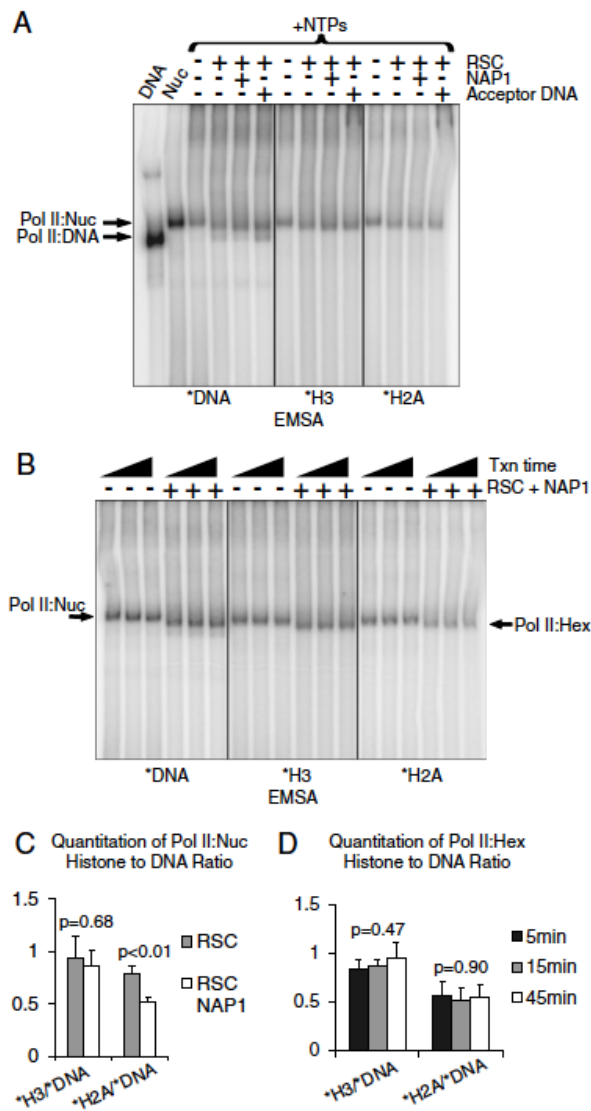


Fig. 4. Hexasome is maintained during transcription. (A) In vitro transcription reactions with C-tailed nucleosomal templates 32 P-labeled on DNA, *H3, or *H2A. The reactions contained unlabeled nucleoside triphosphates (NTPs), with 2 nM pol II, 2 nM RSC, 43 nM NAP1, and/or 10 ng acceptor DNA, where indicated. After addition of poly(dI:dC), the products were resolved by 4.5% native PAGE. A PhosphorImage of the gel is shown. As in Fig. 3, a darker exposure of H3 is shown. (B) In vitro transcription time course (5, 15, or 45 min) as in Fig. 2B with 32 P-labeled nucleosomal templates (*DNA, *H3, or *H2A) (Txn time, transcription time). (C) Quantitation of A. The histone to DNA ratios for the pol II:Nuc band (which migrates slightly faster when remodeled by RSC) was quantified for each condition. Calculations were performed as in Fig. 3C. *P* values were calculated as in Fig. 3B. (D) Quantitation of B. Histone to DNA ratios for the pol II:Hex band were calculated as in Fig. 3B. *P* values were calculated using an ANOVA test.

To further strengthen this argument, we added a C-tail oligonucleotide to compete pol II off of the hexasomal templates during transcription. In principle, once pol II has transcribed the template, fallen off, and become bound by the C-tail oligonucleotide, it should release the hexasome, which should allow us to determine whether the hexasome remains intact over an extended time course. Indeed, at both short (5 min) and long (45 min) times,

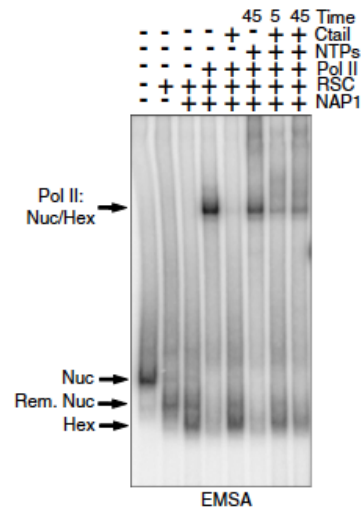


Fig. 5. Hexasomes are continually present. In vitro transcription reactions were performed as in Fig. 4B using 32 P-labeled DNA templates. After transcription for the indicated times, C-tail competitor was added and the products were separated by 4.5% native PAGE. A PhosphorImage is shown.

the hexasome is released (Fig. 5). This result argues that the hexasome is maintained during continuous transcription by pol II in the presence of RSC and NAP1. We also note that the pol II:Hex complexes become more resistant to C-tail oligonucleotide competition over time, which may reflect the accumulation of arrested pol II elongation complexes trapped in an inactive state.

It is plausible that the hexasome generates a tetrasome intermediate during transcription. To address this idea, we assembled tetrasomes using purified H3-H4 tetramers and examined transcription in the presence of combinations of RSC, NAP1, and acceptor DNA (Fig. S9B). The tetrasome blocked full-length transcription under all conditions indicating that H2A-H2B dimers within the hexasome are required for RSC and NAP1-stimulated elongation. These data diminish the likelihood of a tetrasomal intermediate during transcription. Our work is consistent with a previous study, which reported that tetrasomes, like intact nucleosomes, are refractory to transcription elongation (42).

Discussion

ATP-dependent remodeling enzymes, histone chaperones, and chromatin modifying enzymes work in concert to allow pol II to transcribe nucleosomal DNA in vivo (7). Our efforts to reproduce the basic enzymatic requirements in vitro led to the discovery that NAP1 and RSC coordinate to allow pol II transcription through a nucleosome while maintaining a hexasome on the template. Although RSC alone displays a propensity to evict the octamer, the addition of NAP1 prevents RSC-mediated eviction but not remodeling. The formation of the hexasome seems likely to be causal for pol II transcription, as previous biochemical analyses, where transcription was stimulated by elevated salt concentrations, revealed hexasomes. Apparently, the elevated ionic strength, in conjunction with the translocase activity of pol II, promotes release of an H2A-H2B dimer during transcription (20). Hexasomes constructed with the H2A-H2B dimer at either the proximal or the distal position, relative to the oncoming pol II, revealed that the proximal H2A-H2B dimer is critical for promoting reassembly of the nucleosome behind pol II via the "0-loop intermediate" (41). In this model, the proximal H2A-H2B dimer nucleates reassembly of the nucleosome by interacting with DNA trailing the transcribing pol II. Moreover, human FACT generates a hexasome in a transcription system that does

not require ATP-dependent remodeling proteins (40). Taken together, our study and others collectively point to the hexasome as an intermediate that allows the nucleosome to remain partially assembled during transcription.

We were surprised that other chaperones tested did not efficiently substitute for NAP1. SPT6 and ASF1 slightly stimulated transcription, whereas FACT had almost no effect. We note that the process of elongation *in vivo* involves coordinated histone and pol II modifications. In addition to histone acetylation, the pol II is phosphorylated at serines 2, 5, and 7 by Cdk7 (KIN28), BUR1, and CTK1 kinases that coordinate RNA processing with transcription at the beginning and end of the gene (43). Further, chromatin is methylated at H3K4 by COMPASS near the start of a gene and at H3K36 by SET2 and at H3K79 by DOT1 within the coding region. Therefore, a large number of coordinated modifications are necessary for proper gene control. Hence, chaperones may function only at specific steps and their action may be difficult to recapitulate without the other proteins and modifications involved.

Nevertheless, NAP1 faithfully recapitulated some chaperone-mediated processes. For example, NAP1 reprogrammed RSC to allow remodeling while simultaneously preventing nucleosome eviction, similar to the phenomenon observed by Strubin and coworkers (18), where SPT16 (FACT) apparently redeposits the original histones evicted during pol II elongation. In that study, H3 and H4 were evicted and replaced by new H3-H4 tetramers in SPT16 mutants. Our data are also consistent with the notion that

ATP-dependent remodeling enzymes and chaperones function in concert. Schwabish and Struhl have shown that SWI/SNF travels in coding regions with pol II and that SWI2 mutant strains suppress cryptic transcription phenotypes caused by mutations in SPT16 (12).

Finally, the deletion of NAP1 was shown to increase the density of histone H2A and H2B in the promoter and coding regions of GAL genes *in vivo* (27). It was proposed that this effect was due to NAP1 preventing nonnucleosomal H2A-H2B dimer interactions with DNA. However, the data are also consistent with a model in which NAP1 facilitates hexasome formation. A loss of NAP1 would result in H2A-H2B dimer enrichment due to failure of converting nucleosomes into hexasomes. We favor a model where RSC can destabilize one H2A-H2B dimer, which NAP1 then removes.

Materials and Methods

See *SI Materials and Methods* for the details of experimental methods for purification of yeast proteins, preparation of PKA-tagged histones, chromatin assembly and template preparation, *in vitro* transcription assays, nucleosome eviction and remodeling assays, and EMSA of pol II.

ACKNOWLEDGMENTS. We thank Reid C. Johnson (University of California, Los Angeles, CA) for the generous gift of NHP6A. This research was supported by National Institutes of Health Grants GM085002 and GM074701 (to M.C.) and GM047867 (to J.L.W.). B.G.K. was supported by Ruth L. Kirschstein National Research Service Award GM007185.

- Izban MG, Luse DS (1991) Transcription on nucleosomal templates by RNA polymerase II *in vitro*: Inhibition of elongation with enhancement of sequence-specific pausing. *Genes Dev* 5:683–696.
- Studitsky VM, Walter W, Kireeva M, Kashlev M, Felsenfeld G (2004) Chromatin remodeling by RNA polymerases. *Trends Biochem Sci* 29:127–135.
- Workman JL (2006) Nucleosome displacement in transcription. *Genes Dev* 20:2009–2017.
- Lee C-K, Shibata Y, Rao B, Strahl BD, Lieb JD (2004) Evidence for nucleosome depletion at active regulatory regions genome-wide. *Nat Genet* 36:900–905.
- Zhao J, Herrera-Diaz J, Gross DS (2005) Domain-wide displacement of histones by activated heat shock factor occurs independently of Swi5/Nf and is not correlated with RNA polymerase II density. *Mol Cell Biol* 25:8985–8999.
- Lee J-S, Shilatifard A (2007) A site to remember: H3K36 methylation a mark for histone deacetylation. *Mutat Res* 618:130–134.
- Li B, Carey M, Workman JL (2007) The role of chromatin during transcription. *Cell* 128:707–719.
- Clapier CR, Cairns BR (2009) The biology of chromatin remodeling complexes. *Annu Rev Biochem* 78:273–304.
- Ng HH, Robert Fo, Young RA, Struhl K (2002) Genome-wide location and regulated recruitment of the RSC nucleosome-remodeling complex. *Genes Dev* 16:806–819.
- Venters BJ, Pugh BF (2009) A canonical promoter organization of the transcription machinery and its regulators in the *Saccharomyces* genome. *Genome Res* 19:360–371.
- Floer M, et al. (2010) A RSC/nucleosome complex determines chromatin architecture and facilitates activator binding. *Cell* 141:407–418.
- Schwabish MA, Struhl K (2007) The Swi/Snf complex is important for histone eviction during transcriptional activation and RNA polymerase II elongation *in vivo*. *Mol Cell Biol* 27:6987–6995.
- Soutourina J, et al. (2006) Rsc4 connects the chromatin remodeler RSC to RNA polymerases. *Mol Cell Biol* 26:4920–4933.
- Subtil-Rodriguez A, Reyes JC (2010) BRG1 helps RNA polymerase II to overcome a nucleosomal barrier during elongation, *in vivo*. *EMBO Rep* 11:751–757.
- Mason PB, Struhl K (2003) The FACT complex travels with elongating RNA polymerase II and is important for the fidelity of transcriptional initiation *in vivo*. *Mol Cell Biol* 23:8323–8333.
- Kaplan CD, Laprade L, Winston F (2003) Transcription elongation factors repress transcription initiation from cryptic sites. *Science* 301:1096–1099.
- Schwabish MA, Struhl K (2006) Asf1 mediates histone eviction and deposition during elongation by RNA polymerase II. *Mol Cell* 22:415–422.
- Jamal A, Puglisi A, Strubin M (2009) Histone chaperone Spt16 promotes redeposition of the original H3-H4 histones evicted by elongating RNA polymerase. *Mol Cell* 35:377–383.
- Kireeva ML, et al. (2005) Nature of the nucleosomal barrier to RNA polymerase II. *Mol Cell* 18:97–108.
- Kireeva ML, et al. (2002) Nucleosome remodeling induced by RNA polymerase II: Loss of the H2A/H2B dimer during transcription. *Mol Cell* 9:541–542.
- Bondarenko VA, et al. (2006) Nucleosomes can form a polar barrier to transcript elongation by RNA polymerase II. *Mol Cell* 24:469–479.
- Orphanides G, LeRoy G, Chang C-H, Luse DS, Reinberg D (1998) FACT, a factor that facilitates transcript elongation through nucleosomes. *Cell* 92:105–116.
- LeRoy G, Rickards B, Flint SJ (2008) The double bromodomain proteins Brd2 and Brd3 couple histone acetylation to transcription. *Mol Cell* 30:51–60.
- Carey M, Li B, Workman JL (2006) RSC exploits histone acetylation to abrogate the nucleosomal block to RNA polymerase II elongation. *Mol Cell* 24:481–487.
- McBryant SJ, et al. (2003) Preferential binding of the histone (H3-H4)₂ tetramer by NAP1 is mediated by the amino-terminal histone tails. *J Biol Chem* 278:44574–44583.
- Park Y-J, Luger K (2006) The structure of nucleosome assembly protein 1. *Proc Natl Acad Sci USA* 103:1248–1253.
- Andrews AJ, Chen X, Zevin A, Stargell LA, Luger K (2010) The histone chaperone Nap1 promotes nucleosome assembly by eliminating nonnucleosomal histone DNA interactions. *Mol Cell* 37:834–842.
- Del Rosario BC, Pemberton LF (2008) Nap1 links transcription elongation, chromatin assembly, and messenger RNP complex biogenesis. *Mol Cell Biol* 28:2113–2124.
- Walfridsson J, Khorosjutina O, Matikainen P, Gustafsson CM, Ekwall K (2007) A genome-wide role for CHD remodelling factors and Nap1 in nucleosome disassembly. *EMBO J* 26:2868–2879.
- Ohkuni K, Shirahige K, Kikuchi A (2003) Genome-wide expression analysis of NAP1 in *Saccharomyces cerevisiae*. *Biochem Biophys Res Commun* 306:5–9.
- Levchenko V, Jackson V (2004) Histone release during transcription: NAP1 forms a complex with H2A and H2B and facilitates a topologically dependent release of H3 and H4 from the nucleosome. *Biochemistry* 43:2359–2372.
- Peterson S, Danowitz R, Wunsch A, Jackson V (2007) NAP1 catalyzes the formation of either positive or negative supercoils on DNA on basis of the dimer-tetramer equilibrium of histones H3/H4. *Biochemistry* 46:8634–8646.
- Lorch Y, Maier-Davis B, Kornberg RD (2006) Chromatin remodeling by nucleosome disassembly *in vitro*. *Proc Natl Acad Sci USA* 103:3090–3093.
- Kane CM (1988) Renaturation and ribonuclease H: A novel mechanism that influences transcript displacement by RNA polymerase II *in vitro*. *Biochemistry* 27:3187–3196.
- Pogltisch CL, et al. (1999) Electron crystal structure of an RNA polymerase II transcription elongation complex. *Cell* 98:791–798.
- Gnatt AL, Cramer P, Fu J, Bushnell DA, Kornberg RD (2001) Structural basis of transcription: An RNA polymerase II elongation complex at 3.3 Å resolution. *Science* 292:1876–1882.
- Lorch Y, Zhang M, Kornberg RD (1999) Histone octamer transfer by a chromatin-remodeling complex. *Cell* 96:389–392.
- Formosa T, et al. (2001) Spt16-Pob3 and the HMG protein Nhp6 combine to form the nucleosome-binding factor SPN. *EMBO J* 20:3506–3592.
- Dowell NL, Sperling AS, Mason MJ, Johnson RC (2010) Chromatin-dependent binding of the *S. cerevisiae* HMGB protein Nhp6A affects nucleosome dynamics and transcription. *Genes Dev* 24:2031–2042.
- Belotserkovskaya R, et al. (2003) FACT facilitates transcription-dependent nucleosome alteration. *Science* 301:1090–1093.
- Kulaeva OI, et al. (2009) Mechanism of chromatin remodeling and recovery during passage of RNA polymerase II. *Nat Struct Mol Biol* 16:1272–1278.
- Chang C-H, Luse DS (1997) The H3/H4 tetramer blocks transcript elongation by RNA polymerase II *in vitro*. *J Biol Chem* 272:23427–23434.
- Buratowski S (2009) Progression through the RNA polymerase II CTD cycle. *Mol Cell* 36:541–546.

Supporting Information

Kuryan et al. 10.1073/pnas.1109994109

SI Materials and Methods

Purification of Yeast Proteins. Remodels structure of chromatin (RSC), RNA polymerase II (pol II), SWI/SNF, ASF1, SPT6, and FACT were purified using tandem affinity purification (TAP) from the TAP-tagged *Saccharomyces cerevisiae* library as previously described (1). Yeast nucleosome assembly protein 1 (NAP1) was cloned into pGEX4T-1 and expressed as GST-fusion in *Escherichia coli* strain BL21. NAP1 was cleaved from the resin by incubation with bovine thrombin (Sigma). Typically 1 L of bacteria was grown to log phase, lysed by sonication, cleared by centrifugation, and bound to glutathione Sepharose as described by the manufacturer (General Electric). Recombinant NHP6A was a gift from Reid C. Johnson (University of California, Los Angeles, CA).

Preparation of Protein Kinase A (PKA)-Tagged Histones. The PKA tag (RRASV) was added on to the N terminus of H3.1 or the C terminus of H2A from *Xenopus laevis* (2) in the pET21a vector. Proteins were expressed in *E. coli* strain BL21 (DE3) and purified as previously described (2).

Chromatin Assembly and Template Preparation. C-tail template from pGEM3Z601R (3) was prepared as previously described (4). The 263-bp template used in remodeling and eviction assays was the PCR fragment used for C-tail template preparation. For PCR of the Cy5 template, a Cy5-labeled 3' primer was used. The 174-bp template used in Fig. S2 was made with a forward oligonucleotide primer closer to the 601 positioning sequence (CCCCCG-GATCCACAGGATGTATATATCTGACACGTGCC). The 5S mononucleosome template was generated by PCR of EcoRI digested G5E4 5S (5) using forward primer ATAAAGTGTAAGCCTGGGGTGCCTAATGA CAACGAATAACTTCCAGG and reverse primer GGTATTCCCAGGCGGACAGTTACCAATGCTTAATCAGTGAGGCAC. Chromatin was assembled by salt dilution essentially as described (6) using recombinant *X. laevis* histone octamers or tetramers (2) and diluting with chromatin storage buffer (50 mM Hepes pH 7.5, 1 mM EDTA, 100 µg/mL BSA, 10% glycerol, 0.1% Nonidet P-40, 5 mM DTT). Typical chromatin assembly reactions contained 100 ng DNA template and equimolar histone octamer. PKA-tagged nucleosomes were labeled as described in Fig. S6B with 1 µg PKA in 50 µL of 1× transcription buffer A (25 mM Hepes pH 7.5, 10 mM MgCl₂, 50 mM KCl, 10% glycerol) with 1 mM DTT and 250 ng/µL BSA. The reactions were desalted over VWR

G50 microspin columns equilibrated in chromatin storage buffer with 0.2 M NaCl. One microgram of free octamer was labeled under essentially the same conditions for Fig. S8.

In Vitro Transcription Assays. Transcription assays contain 1 ng (0.3 nM) DNA template (free or nucleosomal) as described (4) with the addition of recombinant *E. coli* RNase H. Templates were pretreated in remodeling reactions (as described below) for 60 min in the presence of either 0.9 or 2 nM pol II and RNase H at 30 °C. After the pretreatment, 500 µM nucleoside triphosphates containing 2.5 µCi ³²P-CTP were added and transcription was allowed to proceed typically for 15 min, unless otherwise indicated in the legends. Reactions were terminated with the addition of 100 µL stop buffer (0.3 M NaOAc, 5 mM EDTA, 0.1% SDS, 50 µg/mL yeast tRNA). After phenol extraction and ethanol precipitation, the RNA was resuspended in formamide dye and resolved by 7 M Urea/10% PAGE. The gels were dried, exposed to a PhosphorImager cassette, and quantitated using ImageQuant TL software.

Nucleosome Eviction and Remodeling Assays. For each reaction, 1 ng (0.3 nM), or 3 ng (0.9 nM) for the Cy5-labeled template, of nucleosome was incubated in 1× transcription buffer A with 2 mM ATP, 1 mM DTT, and 250 ng/µL BSA. Eviction reactions also contained 10 ng of pGEM3Z601R acceptor DNA. After 60 min at 30 °C, 400 ng poly (dIdC) was added to terminate the reaction. The 20-µL reactions mixtures were resolved by 4.5% native PAGE in 0.5× TBE (1×, 89 mM Tris base, 89 mM boric acid, 2 mM EDTA, pH 8.0) at 4 °C. The gels were dried and exposed to a PhosphorImager cassette, and quantitated using ImageQuant TL software as described in the text. For the Cy5-labeled template, the wet gel was scanned in the appropriate channel before drying and processing as described.

EMSA of Pol II. Pol II complexes of free DNA and nucleosomes were formed as described for remodeling and evictions assays with the addition of 2 nM pol II. The mixtures were loaded onto 20 cm 4.5% native polyacrylamide gels as described above and electrophoresed for 1,500 V hours. Gels were dried and processed as described above. For reactions with C-tail competition, 3 µL of 40 µM hybridized C-tail oligonucleotide was added to reactions and allowed to incubate for 15 min before resolving by PAGE.

1. Li B, Howe L, Anderson S, Yates JR, Workman JL (2003) The Set2 histone methyltransferase functions through the phosphorylated carboxyl-terminal domain of RNA polymerase II. *J Biol Chem* 278:8897–8903.
2. Luger K, Rechsteiner TJ, Flaus AJ, Wayne MMY, Richmond TJ (1997) Characterization of nucleosome core particles containing histone proteins made in bacteria. *J Mol Biol* 272:301–311.
3. Lowary PT, Widom J (1998) New DNA sequence rules for high affinity binding to histone octamer and sequence-directed nucleosome positioning. *J Mol Biol* 276:19–42.

4. Carey M, Li B, Workman JL (2006) RSC exploits histone acetylation to abrogate the nucleosomal block to RNA polymerase II elongation. *Mol Cell* 24:481–487.
5. Utley RT, et al. (1998) Transcriptional activators direct histone acetyltransferase complexes to nucleosomes. *Nature* 394:498–502.
6. Carrozza MJ, Hassan AH, Workman JL (2003) Assay of activator recruitment of chromatin-modifying complexes. *Methods Enzymol* 371:536–544.

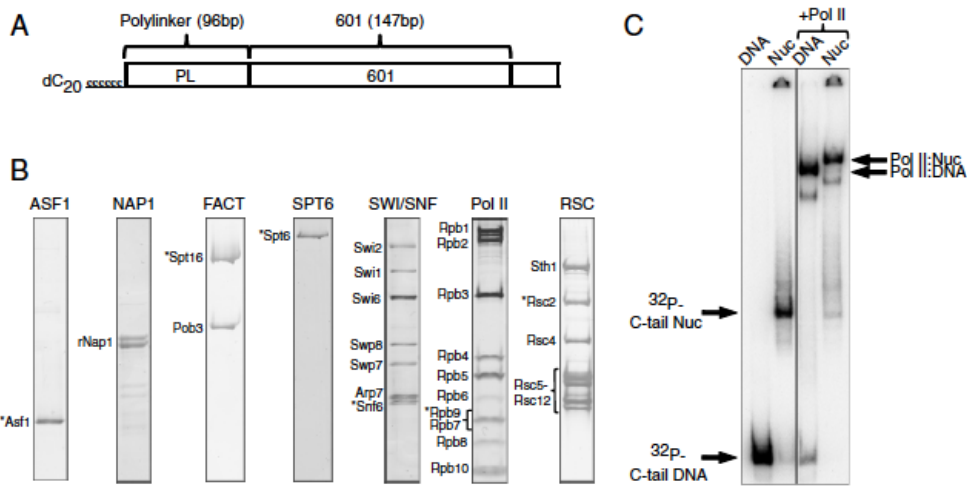


Fig. S1. Biochemical transcription elongation system. (A) Diagram of the C-tail template. A 264-bp template bearing the 601 positioning sequence and a 20-nucleotide single-stranded C tail. The template was used as either free DNA or nucleosomal. (B) Coomassie (NAP1 only) and silver stain gels of purified protein complexes. *S. cerevisiae* NAP1 was expressed and purified in bacteria. Other proteins were purified from the Open Biosystems (Thermo) *S. cerevisiae* TAP-tagged library. The asterisk * indicates tagged subunit. (C) EMSA of C-tail template and pol II. The C-tail template was end-labeled with ³²P and assembled into nucleosomes. DNA and nucleosomal (Nuc) templates were incubated with and without pol II and resolved by 4.5% native PAGE. An autoradiograph of the dried gel is shown.

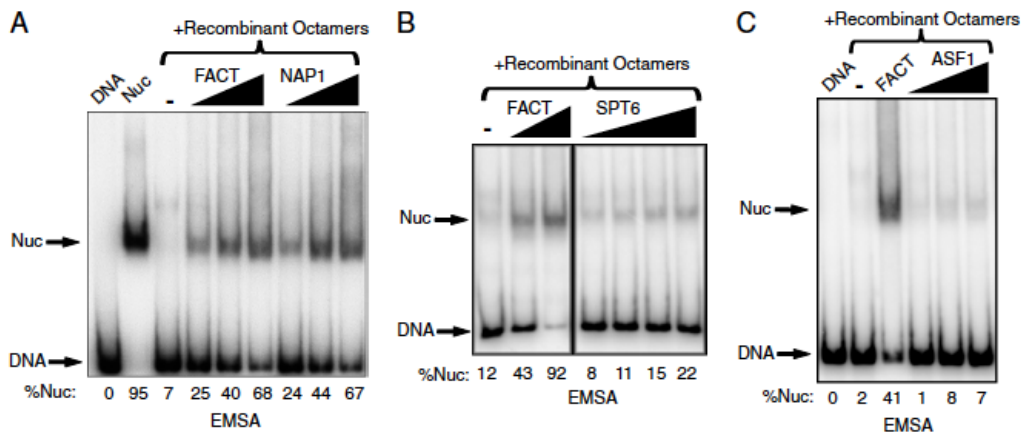


Fig. S2. Histone chaperone activity assay. Reactions contained 1 ng (0.4 nM) of a 174-bp ³²P-labeled 601 template, 7.3 nM recombinant *X. laevis* octamers, and varying concentrations of histone chaperone proteins. The chaperones were preincubated with octamers for 30 min before addition of DNA. The reactions proceeded for 60 min, competitor DNA was added, and the products were resolved by 4.5% native PAGE. A quantitation of the percent nucleosome (as calculated by input DNA minus free DNA) is indicated below each lane. (A) Assay with 4.8–42 nM NAP1 and 0.6–2 nM FACT. (B) Assay with 5–16 nM FACT and 9–53 nM SPT6. (C) Assay with 49 nM FACT and 4.9–44 nM ASF.

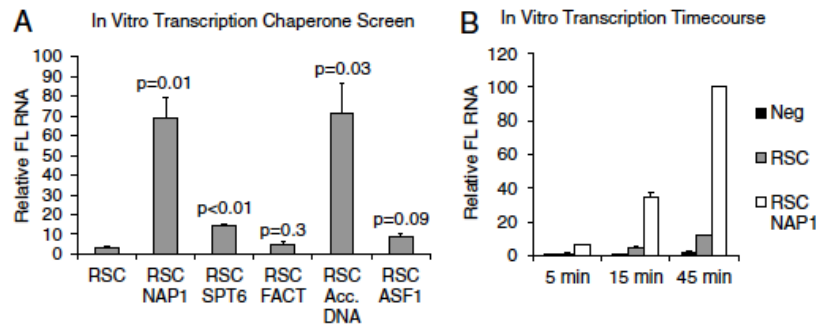


Fig. 53. Quantitation of in vitro transcription. (A) Bar graph representation of the in vitro transcription chaperone screen from Fig. 1C. The average (mean) from two independent experiments is displayed with the error bars representing the standard deviation. A two-tailed Student's *t* test was used to determine the *P* values for the various conditions relative to RSC alone. (FL, full length.) (B) Bar graph representation of data from Fig. 2B. The average (mean) from three independent experiments is displayed with the error bars representing the standard deviation. FL RNA transcription from the nucleosome alone (Neg) is compared with reactions containing RSC or RSC and NAP1. The 45 min time point average is normalized to 100.

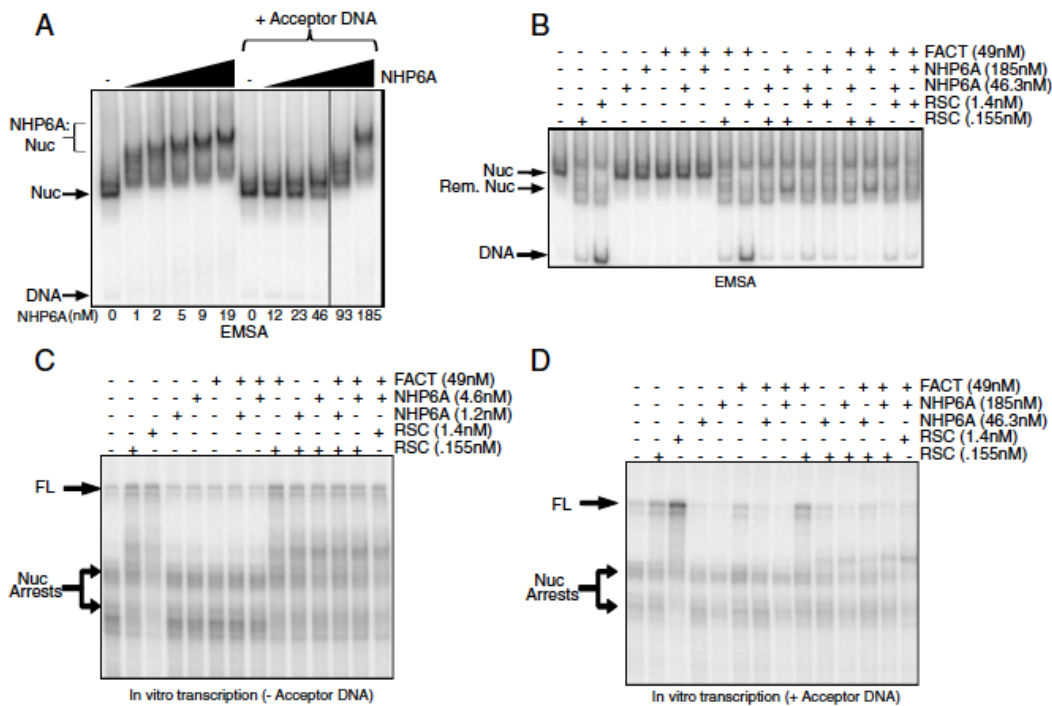


Fig. 54. NHP6A blocks RSC mediated eviction and transcription. (A) NHP6A electrophoretic mobility shift assay. NHP6A was incubated at the indicated concentrations with 1 ng (0.3 nM) labeled nucleosomes for 60 min, and the complexes were resolved by 4.5% PAGE. A PhosphorImage is shown. (B) Nucleosome eviction assay as in Fig. 1B with the indicated concentrations of RSC, NHP6A, FACT, and 10 ng supercoiled pGEM3Z601R. (C) In vitro transcription with RSC, NHP6A, and FACT in the absence of acceptor DNA. Reactions were performed as in Fig. 1C with the concentrations indicated. (D) In vitro transcription with RSC, NHP6A, and FACT in the presence of acceptor DNA. The same reactions conditions were used as in C, but with 10 ng of supercoiled pGEM3Z601R and the indicated concentrations of proteins. (FL, full length.)

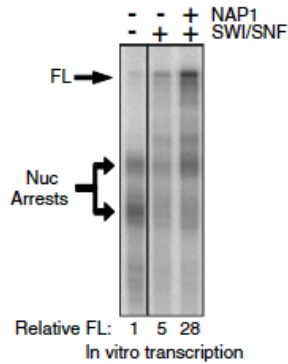


Fig. S5. NAP1 stimulates SWI/SNF-mediated transcription. In vitro transcription was performed as in Fig. 1C. NAP1 (43 nM) stimulates SWI/SNF (0.3 nM) dependent transcription by pol II (0.9 nM). The quantitation of relative full-length (FL) RNA is shown below the gel normalized to pol II alone, which was assigned a value of one.

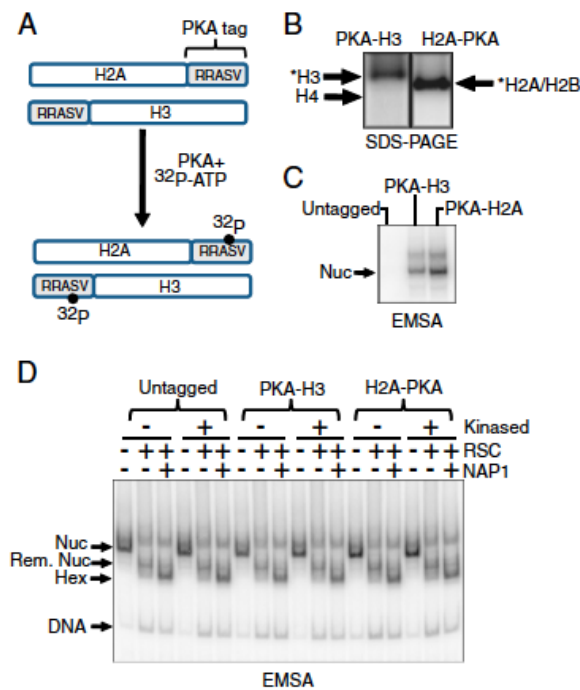


Fig. S6. PKA-tagged histones. (A) Schematic of PKA-tagged histones. (B) Nucleosomes (37 ng) containing PKA-H3 or H2A-PKA were labeled with PKA and γ - 32 P-ATP for 3 h at 30 °C. One nanogram of each labeled nucleosome was resolved by 15% SDS-PAGE. The position of H4, which did not label, is also shown. (C) Untagged, PKA-H3, or H2A-PKA nucleosomes were labeled as in Fig. S6B. One nanogram of each nucleosome was resolved by 4.5% native PAGE. (D) Nucleosome remodeling assay on PKA-tagged substrates. Nucleosomes (1 ng or 0.3 nM each) containing 32 P-labeled DNA with untagged, PKA-H3, or H2A-PKA histones were treated with PKA in the presence or absence of cold ATP, incubated for 1 h with RSC (2 nM) and NAP1 (43 nM), where indicated, and the products were resolved by 4.5% native PAGE. Phosphorimages of the dried gels are shown.

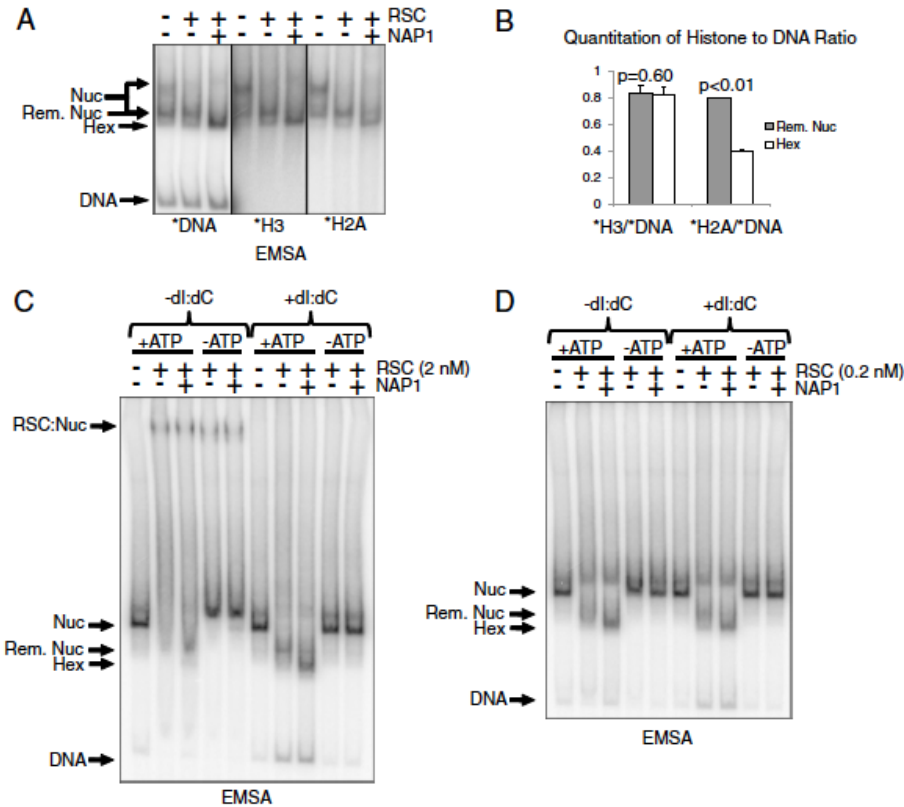


Fig. 57. Chromatin remodeling on 5S nucleosomal template and the effect of poly(dl:dC) on remodeling reactions. (A) Chromatin remodeling reactions with DNA- and histone-labeled mononucleosomes reconstituted on the 5S nucleosome position sequence. Note that the nucleosome assumes two distinct positions on 5S DNA (arrows), one near the middle and one near the end of the sequence. Because RSC translocates the nucleosome to the end, the final remodeled nucleosome migrates similarly to the end-positioned nucleosome. Nevertheless, RSC and NAP1 generate a new species that migrates lower and represents a hexasome. (B) Quantitation of the histone:DNA ratios from A. Bars show the mean from duplicate reactions with the error bars representing the standard deviation. A two-tailed Student's *t* test was performed to determine *p* values. (C) Nucleosome remodeling reactions on 601 template with 2 nM RSC and 43 nM NAP1 were performed in the presence or absence of ATP with and without (poly)dl:dC competitor DNA, where indicated. (D) Remodeling reactions as in C except with 0.2 nM RSC. Phosphorimages of the dried gels are shown.

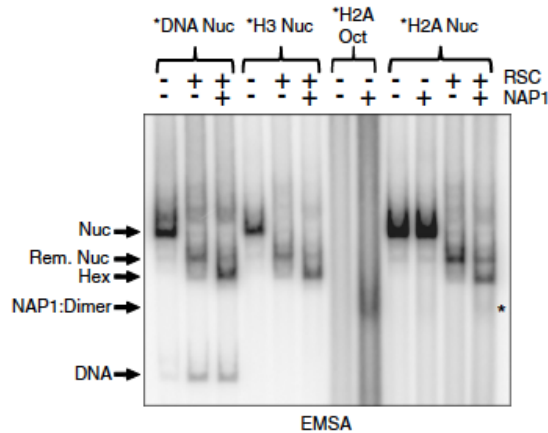


Fig. 58. NAP1 binds to the released H2A:H2B dimer. Nucleosome remodeling reactions were performed with 2 nM RSC and 43 nM NAP1 on ³²P-labeled DNA (*DNA), PKA-H3 (*H3), or H2A-PKA (*H2A) nucleosomal templates, where indicated. Additionally, ³²P-labeled H2A-PKA octamer (5 nM) was incubated with NAP1 to determine the mobility of the NAP1:dimer complex. This complex is weakly present in reactions containing RSC, NAP1, and *H2A nucleosome (noted by the *).

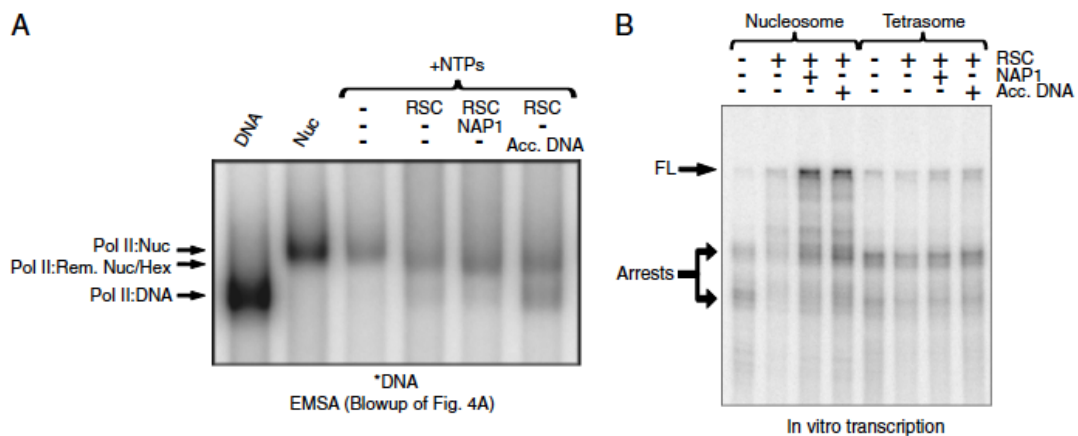


Fig. 59. Blowup from Fig. 4A and in vitro transcription on tetrasome templates. (A) The *DNA panel from Fig. 4A was enlarged to show the mobilities of the pol II:Nuc and pol II:Rem. Nuc/Hex bands. The complexes of pol II with remodeled nucleosome and pol II with hexasome migrate similarly and are hence labeled together as pol II:Rem. Nuc/Hex. (B) In vitro transcription with nucleosome and tetrasome templates. Reactions with 0.9 nM pol II contained 2 nM RSC, 43 nM NAP1, and 10 ng acceptor DNA where indicated. (FL, full length).

Contribution

The work presented in this chapter was my primary project. I generated all of the data found in this chapter except for Supplemental Figure 4. Jessica Kim, Nancy Tran, Sarah Lombardo helped to purify some of the reagents used in this project. Nancy Tran generated the data in Supplemental Figure 4

Chapter 3

The Rpd3 Core Complex is a Chromatin Stabilization Module

The Rpd3 Core Complex Is a Chromatin Stabilization Module

Xiao-Fen Chen,¹ Benjamin Kuryan,¹ Tasuku Kitada,¹ Nancy Tran,¹ Jing-Yu Li,¹ Siavash Kurdistani,¹ Michael Grunstein,¹ Bing Li,² and Michael Carey^{1,*}

¹Department of Biological Chemistry, 351A Biomedical Sciences Research Building, David Geffen School of Medicine, University of California, Los Angeles, Los Angeles, CA 90095-1737, USA

²Department of Molecular Biology, University of Texas Southwestern Medical Center at Dallas, 5323 Harry Hines Blvd, Dallas, TX 75390, USA

Summary

The *S. cerevisiae* Rpd3 large (Rpd3L) and small (Rpd3S) histone deacetylase (HDAC) complexes are prototypes for understanding transcriptional repression in eukaryotes [1]. The current view is that they function by deacetylating chromatin, thereby limiting accessibility of transcriptional factors to the underlying DNA. However, an Rpd3 catalytic mutant retains substantial repression capability when targeted to a promoter as a LexA fusion protein [2]. We investigated the HDAC-independent properties of the Rpd3 complexes biochemically and discovered a chaperone function, which promotes histone deposition onto DNA, and a novel activity, which prevents nucleosome eviction but not remodeling mediated by the ATP-dependent RSC complex. These HDAC-independent activities inhibit Pol II transcription on a nucleosomal template. The functions of the endogenous Rpd3 complexes can be recapitulated with recombinant Rpd3 core complex comprising Sin3, Rpd3, and Ume1. To test the hypothesis that Rpd3 contributes to chromatin stabilization in vivo, we measured histone H3 density genomewide and found that it was reduced at promoters in an Rpd3 deletion mutant but partially restored in a catalytic mutant. Importantly, the effects on H3 density are most apparent on RSC-enriched genes [3]. Our data suggest that the Rpd3 core complex could contribute to repression via a novel nucleosome stabilization function.

Results and Discussion

Rpd3S Contains H3K36me3-Independent Histone Chaperone and Nucleosome Stabilization Functions

The Rpd3 HDAC is the prototype for understanding gene repression on chromatin [4]. HDACs function by removing acetyl marks placed on histone tails by histone acetyltransferases such as SAGA and NuA4 [5]. Acetylated histones decondense chromatin directly [6] and/or serve as targets for ATP-dependent remodeling enzymes including SWI/SNF [7] and RSC [8]. Bromodomains within these enzymes recruit them to acetylated chromatin and enhance their remodeling function [9]. In yeast, Rpd3L and Rpd3S share three subunits: Rpd3, Sin3, and Ume1 [10, 11]. Rpd3L contains numerous additional subunits [12] and is targeted to promoters by

sequence-specific DNA binding proteins like Ume6 [13, 14]. Importantly, the Rpd3 HDAC activity contributes to but is not essential for repression on promoters when targeted as a LexA fusion [2]. The Rpd3S complex contains two additional subunits, Rco1 and Eaf3, which target it to H3K36 trimethylated (H3K36me3) nucleosomes in the ORF [15]. Set2 catalyzes H3K36me3 and associates with Pol II [16]. Rpd3S maintains a hypoacetylated state in the ORF and suppresses cryptic transcription [10, 11, 17]. Recently, Rpd3S was reported to interact with elongating Pol II, and its recruitment to transcribed regions was dependent on phosphorylation of the carboxy-terminal domain of Rpb1 [18].

Several aspects of Rpd3 function were of interest to us. First, the in vivo roles of both Rpd3S and Rpd3L were consistent with a nucleosome stability function. Second, in addition to Rpd3, the two complexes share two other subunits, Ume1 and Sin3. In yeast and mammalian cells, Sin3 has a long history of correlating with repression of transcription on chromatin [19]. Finally, the observation that Rpd3 catalytic mutants retain some repression capabilities when targeted via LexA fusions suggested that some other aspect of the protein was contributing to its function [2]. This is not to say that the deacetylase is unessential, only that other aspects of Rpd3 complexes may cooperate with the HDAC to ensure full repression. To explore the HDAC-independent functions of Rpd3, we considered the possibility that it might affect nucleosome remodeling. For example, a previous study by Kingston and colleagues revealed that human SWI/SNF ATPases copurified with a Sin3/HDAC complex and that their remodeling activities were compromised by the HDAC [20].

We initiated our study with Rpd3S because of our continuing interest in the mechanism of Pol II elongation on nucleosomal templates, which in our system requires nucleosome remodeling and octamer eviction by RSC. Because we began with Rpd3S, we also asked whether H3K36me3 would affect nucleosome remodeling. Tandem affinity purification (TAP) was employed to purify the RSC and Rpd3S proteins from *S. cerevisiae* (Figure 1A) [21]. H3K36me3 histones were generated with the methyl-lysine analog (MLA) technology [22]. H3K36 was first mutated to cysteine (H3K36C) and then alkylated with (2-bromoethyl) trimethylammonium bromide to form a methyl-lysine analog or MLA (H3K36C-me3). We will refer to the MLA as H3K36me3 for convenience. The MLA is recognized in a western blotting experiment by an H3K36me3 antibody (Figure S1A available online). Subsequently, unmethylated (naive) or H3K36me3 mononucleosomes were reconstituted on a ³²P-labeled DNA fragment containing the 601 nucleosome positioning sequence [23, 24]. Rpd3S bound to both nucleosomes in an EMSA assay and displayed a higher affinity for H3K36me3 nucleosomes as shown previously [25] (Figure S1B).

The assembled nucleosomes were incubated with RSC in the presence or absence of Rpd3S and analyzed by native gel electrophoresis. RSC mobilized the histone octamer as indicated by the faster migration of the 601 nucleosome on a native gel. However, Rpd3S did not significantly inhibit this activity (Figure 1B). Similar effects were observed on H3K36me3 nucleosomes (Figure S1C). We conclude that

*Correspondence: mcarey@mednet.ucla.edu

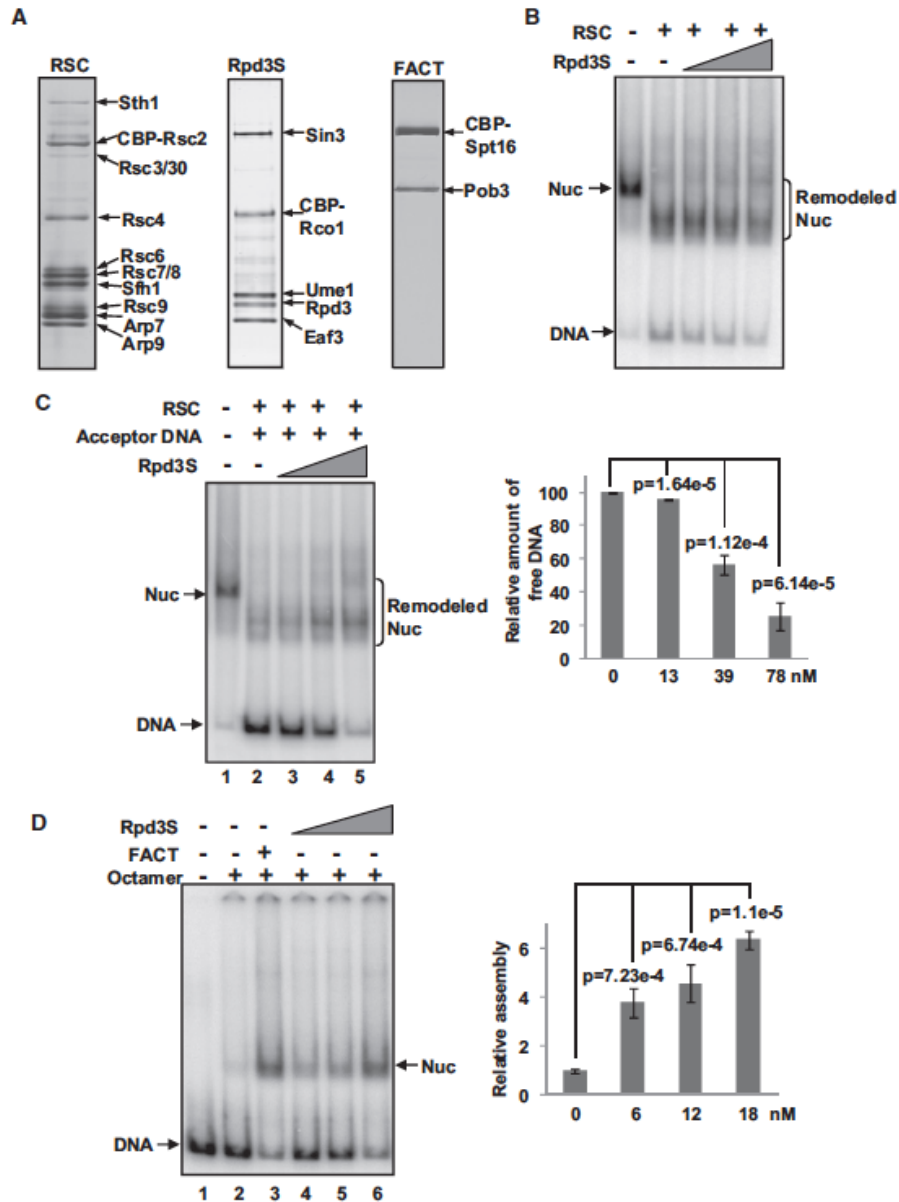


Figure 1. Rpd3S Inhibits RSC-Dependent Nucleosome Eviction and Promotes Nucleosome Assembly In Vitro

(A) Silver stain gel of TAP-purified RSC2, Rpd3S, and FACT complexes.

(B) The effect of Rpd3S on RSC-dependent nucleosome remodeling. 2 nM RSC was incubated with 0.3 nM 32 P-labeled mononucleosome and 0, 13, 39, or 78 nM Rpd3S. The remodeling products were fractionated by native PAGE. A phosphorimage of the gel is shown. See also Figures S1A–S1C for the effect of H3K36me3 on Rpd3S in binding and RSC-mediated nucleosome remodeling reactions.

(C) The effect of Rpd3S on RSC-dependent nucleosome eviction. Left, 6 nM RSC was incubated with 0.3 nM mononucleosome and 0, 13, 39, or 78 nM Rpd3S in the presence of 10 ng of pGEM3Z601R acceptor DNA. Bar graph on the right represents quantitation by ImageQuant TL (GE) of the three independent experiments. The relative amounts of free DNA generated by eviction were plotted as a bar graph normalized to that generated by 6 nM RSC alone, which was assigned a value of 100. The error bars show \pm standard deviation (SD). The p value is calculated by Student's t test. See also Figure S1D for the effect of H3K36me3 on Rpd3S in RSC-mediated nucleosome eviction.

(D) Rpd3S-mediated chromatin assembly assay. Left, the reaction contained 18 nM FACT, or 6, 12, 18 nM of Rpd3S, respectively, with recombinant *Xenopus* octamers and a 32 P-labeled 601 DNA fragment. A phosphorimage of a native gel is shown. Graph on the right represents quantitation of the amounts of assembled nucleosomes by Rpd3S relative to no Rpd3S control (i.e., octamers alone). The free DNA and assembled nucleosome are indicated. The error bars show \pm standard deviation (SD). The p value is calculated with Student's t test. For chaperone assays see also Figure S1E for the effect of H3K36me3 on Rpd3S, Figure S1F for the effect of Rpd3S mutants, and Figure S1G for the effect of trichostatin.

Rpd3S does not inhibit nucleosome remodeling under the experimental conditions tested in our assays.

As reported previously [26], RSC has the ability to transfer a histone octamer from one DNA molecule to another, often termed an acceptor. This octamer transfer capability, referred to as eviction, is important for RSC's function [8]. Upon addition of an unlabeled supercoiled acceptor DNA to our remodeling reactions, RSC transferred the majority of octamers from the labeled DNA probe to the unlabeled DNA, thereby generating substantial amounts of free ^{32}P -DNA (Figure 1C, lane 2). Importantly, the amount of eviction, as measured by accumulation of free DNA, decreased significantly with increasing doses of Rpd3S (Figure 1C, lanes 3–5 and accompanying bar graph), while the amount of remodeled nucleosome increased. Similar effects on remodeling and eviction were observed at similar Rpd3S concentrations on H3K36me3 chromatin (Figures S1C and S1D). We conclude that Rpd3S inhibits RSC-mediated octamer eviction in an H3K36me3-independent manner *in vitro*.

Inhibition of ATP-dependent octamer eviction is an activity that may act to maintain nucleosome stability and histone density over a regulatory region and gene. Another activity that could serve a similar role would be the ability of Rpd3S to act as a chaperone by assembling histones onto DNA. Histone chaperones such as FACT, Nap1, Asf1, and Spt6 play important roles in transcription regulation in yeast [27, 28]. To address this possibility, Rpd3S was first incubated with unmodified, naive octamers to allow protein-protein interactions, followed by incubation with a ^{32}P -labeled DNA bearing the 601 positioning sequence. Nucleosome formation was analyzed on a native gel (Figure 1D). To verify the efficiency of our *in vitro* system, we compared Rpd3S with the well-studied histone chaperone FACT (Figure 1A) [27], which is known to specifically load histones onto DNA. As reported previously [29], FACT strongly stimulated nucleosome formation (Figure 1D, lane 3). Importantly, Rpd3S also promoted nucleosome assembly in a dose-dependent manner (Figure 1D, lanes 4–6). Surprisingly, the concentration of Rpd3S necessary to assemble nucleosomes was measurably lower than that required to inhibit eviction. H3K36me3 did not enhance and even inhibited the chaperone function of Rpd3S (Figure S1E). Moreover, an Rpd3S mutant lacking the PHD domain of Rco1 and the chromo domain (CHD) of Eaf3, both of which target Rpd3S to H3K36me3 [25], displayed similar relative nucleosome assembly activity as did the wild-type protein. H3K36me3 negatively affected the mutant's chaperone function similar to its effect on wild-type Rpd3S (Figure S1F). We conclude that the Rpd3S complex acts as a histone chaperone to promote histone deposition onto DNA *in vitro* in an H3K36me3-independent manner.

The inhibition of chaperone function by H3K36me3 was quite interesting given that Rpd3S normally targets this modification for binding within an ORF. However, the effect was also observed in a mutant of Rpd3S lacking the targeting domains suggesting that H3K36me3 inhibits a specific aspect of the chaperone function. For example, H3K36me3 also negatively affected the chaperone activity of FACT (data not shown). Collectively, the chaperone and eviction data suggest that Rpd3S possesses a chromatin stabilization function, which is independent of the specific H3K36me3 targeting function. Although our assays utilized unacetylated histones, it remained a remote possibility that the HDAC function of Rpd3 might somehow contribute. However, Rpd3S promoted nucleosome formation at the same efficiency in the absence

or presence of trichostatin concentrations sufficient to inhibit 90% of Rpd3's HDAC activity (Figure S1G).

The 3-Subunit Core of Rpd3L and Rpd3S Mediates the Nucleosome Stabilization Function

We next asked whether the Rpd3L complex exhibited similar properties as Rpd3S because the two enzymes share a set of three core subunits [10, 11]. To address this question, we TAP purified the Rpd3L complex (Figure 2A) and tested its effect on RSC-dependent remodeling (data not shown) and octamer eviction (Figure 2B). Like Rpd3S, Rpd3L had little effect on remodeling but significantly inhibited octamer eviction as indicated by the reduced amounts of free DNA observed with increased amounts of protein (Figure 2B). Moreover, like Rpd3S, Rpd3L stimulated nucleosome assembly with naive octamers (Figure 2C).

Because Rpd3L shares a 3-subunit core complex (3-core) with Rpd3S, we next asked whether this module contributes to the nucleosome stabilization function. The 3-subunit core complex was reconstituted by coexpression of *S. cerevisiae* Ume1, Rpd3, and Sin3 in Sf9 cells via a baculovirus system. Sin3 was tagged with the FLAG epitope and the complex was purified with a two-step procedure involving an anti-FLAG immuno-affinity column followed by gel filtration chromatography. The final products were relatively pure except for an unknown protein that copurified (Figure 2D). We observed a significant and dose-dependent inhibition of RSC-mediated octamer eviction by the 3-subunit core complex (Figure 2E). The core complex also enhanced nucleosome formation in a chaperone assay, similar to Rpd3S and Rpd3L (Figure 2C).

In an attempt to identify the subunit responsible for nucleosome stabilization, we used FLAG-affinity chromatography to purify each of the individual subunits (Figure S2A). In side-by-side purifications of similar scale and yield, only Ume1 purified to near homogeneity as a single species. Sin3 was degraded slightly and Rpd3 copurified with several higher molecular weight bands. Nevertheless, the amounts of full-length subunits were sufficient for testing. Surprisingly, no individual subunit inhibited RSC-mediated octamer eviction (Figure S2B) or assembled nucleosomes to any significant extent (Figure S2C). We conclude that the entire Rpd3 core complex (Sin3, Ume1, and Rpd3) is necessary and sufficient for the chromatin stabilization function *in vitro*.

The Nucleosome Stabilization Function Inhibits Nucleosomal Transcription *In Vitro*

To further study the nucleosome stabilization function of Rpd3 HDACs, we performed *in vitro* transcription. Previously, we established a system to study Pol II transcription through a nucleosome by using a "C-tail" template bearing a single-stranded stretch of dC ligated to a DNA fragment encompassing the 601 positioning sequence (Figure 3A) [30]. Pol II employs the C-tail as a promoter and elongates into the 601 nucleosome. RSC was shown to stimulate Pol II elongation through the nucleosomal barrier [30]. Our current view is that RSC stimulates transcription by evicting the nucleosome. We wished to determine whether the nucleosome stabilization function of Rpd3 was potent enough to prevent RSC-mediated transcription. Consistent with our previous study, transcription with TAP-purified yeast Pol II generated only small amounts of full-length (FL) transcripts (Figure 3B, lane 1). Pol II arrested at discrete locations and short transcripts were produced. In the presence of ATP and acceptor DNA,

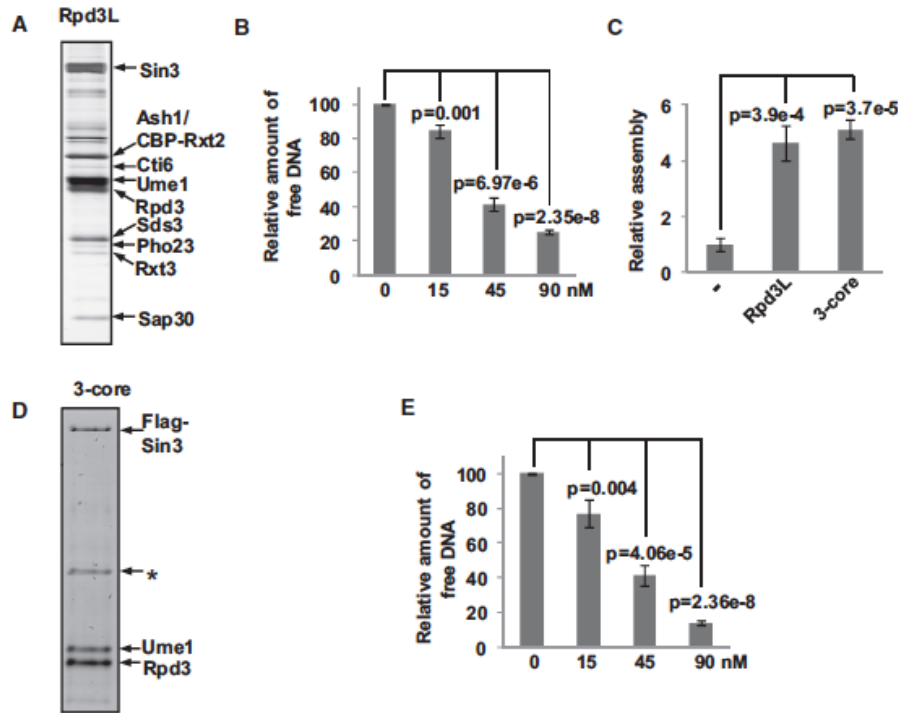


Figure 2. Rpd3L and 3-Subunit Core Complex Prevent RSC-Dependent Nucleosome Eviction and Promote Nucleosome Assembly In Vitro

(A) Silver stain gel of TAP-purified Rpd3L.

(B) The effect of Rpd3L on RSC-dependent nucleosome eviction. 6 nM RSC was incubated with 0, 15, 45, 90 nM Rpd3L, respectively, and analyzed as described in Figure 1C legend.

(C) Nucleosome assembly with *Xenopus* octamers and 18 nM Rpd3L or 3-subunit core complex, respectively, as in Figure 1D legend.

(D) Silver stain gel of recombinant 3-subunit core complex. The asterisk indicates an unknown protein that copurified with the 3-subunit core complex.

(E) The effect of 3-subunit core complex on RSC-dependent nucleosome eviction. 6 nM RSC was incubated with 601 nucleosome and 0, 15, 45, 90 nM of recombinant core complex, respectively, and analyzed as in Figure 1C legend. See also Figure S2A for silver-stained gels of the individual subunits, Figure S2B for their effect on RSC-mediated nucleosome eviction, and Figure S2C for chaperone assays.

RSC strongly stimulated transcription as reflected by the decrease in arrested transcripts and by increased production of full-length (FL) transcripts (Figure 3B, lane 2). The addition of the Rpd3 HDACs, in the form of either Rpd3S, Rpd3L, or the 3-subunit core complex, all diminished transcription in a dose-dependent manner on naive chromatin (Figure 3B, lanes 3–8). However, the presence of the chaperone FACT, which has no effect on RSC eviction (data not shown), did not affect the production of full-length transcripts (Figure 3B, lanes 9–10). The inhibition of transcription by Rpd3 HDACs was specific to a nucleosomal template as shown by the fact that they did not inhibit transcription on naked DNA (Figure 3C). Because Rpd3S displayed a higher affinity for H3K36me3 nucleosomes [25], we compared the inhibitory effect of Rpd3S and 3-subunit core complex on transcription with naive or H3K36me3 nucleosomal template. The H3K36me3 nucleosomes enhanced repression by Rpd3S but not by the 3-subunit core complex (Figure 3D). The results are consistent with the higher affinity of Rpd3S for H3K36me3 nucleosomes. These data indicate that the Rpd3 complexes antagonize RSC-mediated stimulation of Pol II transcription elongation through a nucleosome in vitro. The inhibition of transcription elongation by Rpd3S is consistent with an in vivo study showing that deletion of Rpd3 bypasses the requirement of positive elongation factor Burt1/Bur2 [11].

Our approach does not indicate whether Rpd3S, for example, can block an elongating Pol II molecule in vivo. It is not known how Pol II elongation occurs in living cells and whether there are situations where it would encounter Rpd3S-bound nucleosomes. Indeed, the current model, for which there is little experimental support, suggests that Rpd3S-bound nucleosomes accumulate behind Pol II [15]. Nevertheless, our assay provides a measure of the stability of the nucleosome conferred by Rpd3 in the presence of the strong ATP-dependent remodeling activity of RSC and the potent NTP-dependent DNA translocase activity of Pol II.

Rpd3 Affects H3 Density Preferentially at RSC-Bound Genes in Vivo

The ability of the two Rpd3 complexes to stabilize nucleosomes independent of HDAC activity suggested that they might play similar roles in vivo. To address this hypothesis, we prepared strains of yeast with the endogenous Rpd3 gene deleted but bearing an empty vector or vectors expressing either the wild-type or H150A catalytically inactive Rpd3 [2]. The mutant and wild-type Rpd3p were expressed at similar levels (Figure S3A). The H150A mutation appears to be completely defective for histone deacetylase activity as shown previously via an in vitro assay. However, it still interacts with Sin3 and partially retains the transcription repression

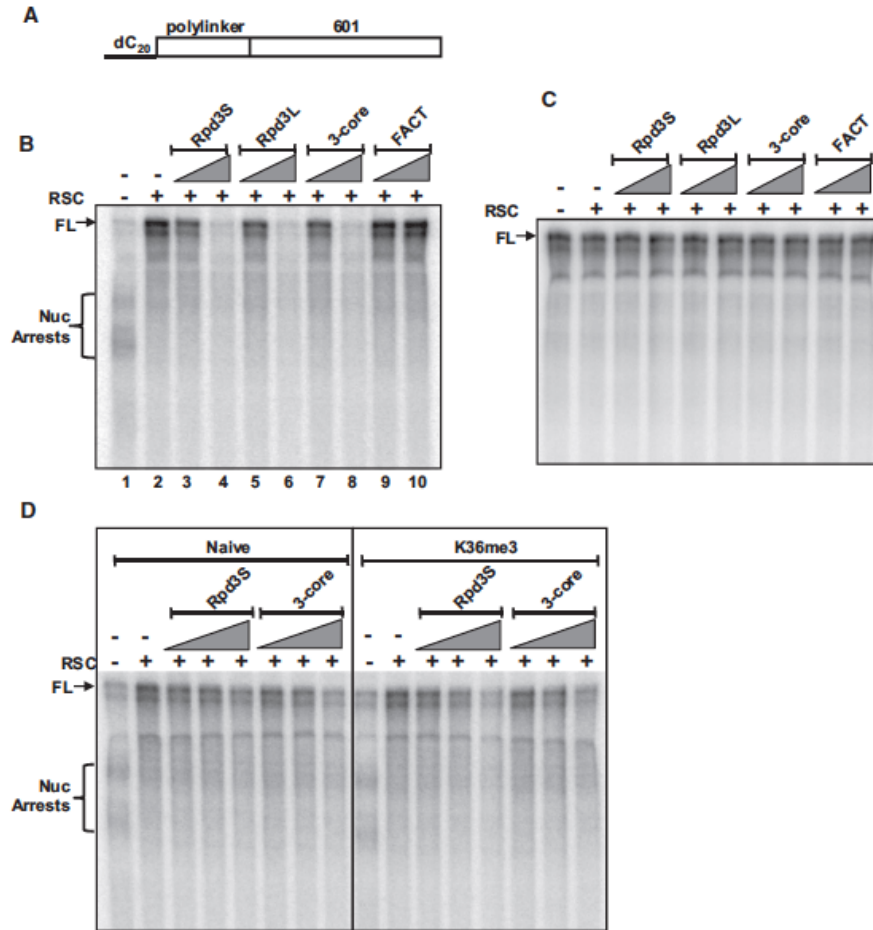


Figure 3. Rpd3 HDACs Inhibit RSC-Mediated Activation of Nucleosome Transcription

(A) Schematic of the C-tail template. The template contains the 601 positioning sequence and a 20-nucleotide single-stranded C-tail with an intervening polylinker from pGEM3Z601R. Pol II initiates from the C-tail.

(B) The template was assembled into a mononucleosome with naive recombinant *Xenopus* octamers and then preincubated with 3 nM RSC in the presence or absence of 30 or 60 nM Rpd3S, Rpd3L, 3-subunit core complex, or FACT for 1 hr at 30°C. Pol II, α - 32 P]CTP, NTPs, and RNase H were then added for 15 min at 30°C. The 32 P-labeled RNA products were fractionated on a 10% polyacrylamide/urea gel. A phosphorimage of the gel is shown.

(C) Same assay as performed in (B), except that naked C-tail DNA template was used instead of nucleosomal template.

(D) In vitro transcription was performed on naive or H3K36me3 nucleosomes. 3 nM RSC was incubated with 0, 5, 15, 45 nM Rpd3S or recombinant 3-subunit core complex, respectively.

function [2]. To test the effect in vivo, we chose two known targets of Rpd3, histone H3K18ac and H4K5ac [31]. The data demonstrate that the H150A and null Rpd3 mutants lead to similar levels of H3K18 and H4K5 hyperacetylation, suggesting that the point mutant is largely inactive in vivo (Figure S3B). Finally, we measured histone H3 density genome-wide in each of these three strains by using Agilent tiling arrays. Upon deletion of Rpd3, we observed a significant decrease in H3 density at intergenic/promoter regions genome-wide, while the coding regions/ORFs were less affected (Figure 4A) although still significant in some regions (data not shown). Importantly, however, the H150A derivative maintained significantly higher H3 density than in Rpd3-deletion cells (empty vector), although not as high as in Rpd3 wild-type cells. The data suggest a global role of Rpd3 in affecting histone density although the effect is more apparent in promoter regions.

Our biochemical studies showed that Rpd3 complexes prevent RSC from evicting histones on chromatin (Figures 1 and 2). We hypothesized that the observed changes in H3 density upon Rpd3 mutation might be more evident on genes that are bound by RSC in vivo. To test this hypothesis, we compared our data with that of the published genome-wide distribution of five subunits of the RSC1 and RSC2 complexes in *S. cerevisiae* [3]. We analyzed intergenic/promoter regions scored for high RSC binding by the authors (as measured via all five subunits; $p < 0.001$ for each region) and compared them with a similar number of targets displaying the least RSC binding (Figure 4B). We then analyzed the H3 density changes observed upon Rpd3 mutation in these same two subsets of targets. The deletion or mutation of Rpd3 minimally impaired H3 occupancy at low RSC-bound targets, while a more significant decrease was observed at

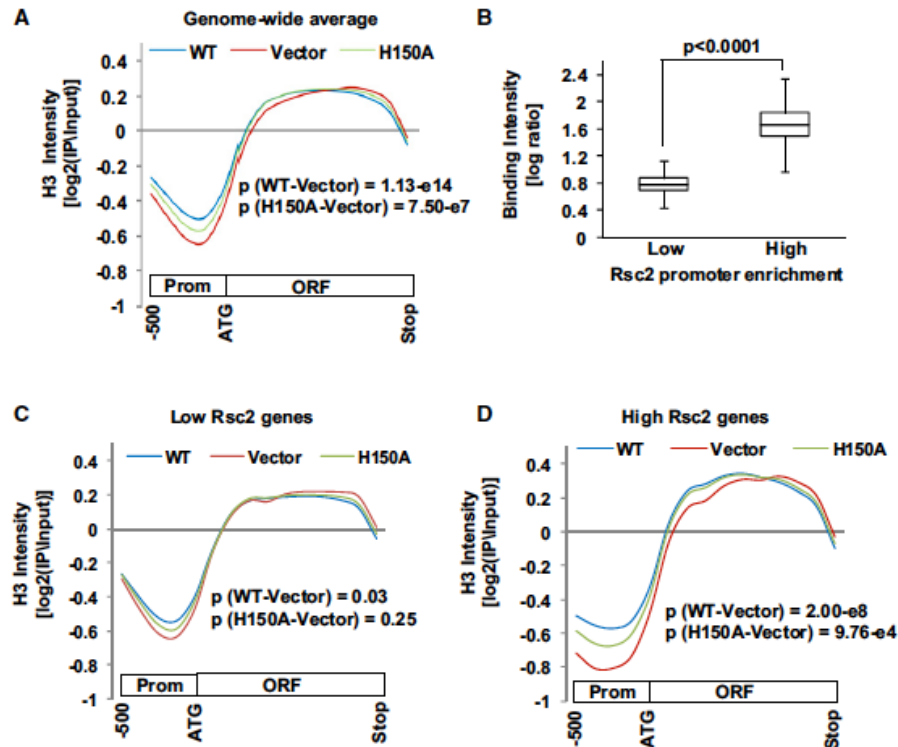


Figure 4. Rpd3 Complexes Stabilize Chromatin In Vivo

(A) H3 levels were measured by ChIP in wild-type (WT), *rpd3* H150A (H150A), and *rpd3Δ* (Vector) cells. ChIP DNA of Histone H3 and inputs were amplified, labeled, and hybridized to Agilent Tiling arrays. The average binding of 6,572 annotated genes and their upstream 500 bp regions are shown. Enrichment of H3 ChIP DNA is shown as the log₂ ratios of ChIP versus input DNA. p values for the promoters were calculated with the Mann-Whitney test. See also Figure S3A for Rpd3 native versus H150A protein levels, Figure S3B for global acetylation levels of H3K18 and H4K5 in Rpd3 native, H150A, and null backgrounds, and Figures S3C and S3D for Rpd3 association with Pol II and H3.

(B) Box and whisker plot for two subsets of targets that have high or low Rsc2 enrichment. Each subset has 495 and 506 targets, respectively. The p values are calculated by Student's t test.

(C and D) H3 levels of the low (C) and high (D) Rsc2 targets were measured in wild-type, *rpd3* H150A, and *rpd3Δ* cells. p values for the promoters were calculated by the Mann-Whitney test.

the RSC-enriched targets (Figures 4C and 4D). Importantly, the largest difference in H3 density between wild-type and either the null or H150A Rpd3 mutant was observed at RSC-enriched regions. The data suggest the possibility that the Rpd3 complex can somehow influence nucleosome stability at RSC-enriched promoter regions in vivo. It is unclear how this would affect gene expression because recent findings suggest that the nucleosome occupancy of Rpd3 targets is not always correlated with transcription frequency [32–34]. Additionally, Rpd3 affects transcription of full length and cryptic transcripts [10, 17], making it complicated to determine the true effect.

Conclusions and Perspectives

We have demonstrated that Rpd3S and Rpd3L possess a previously unrecognized capacity to promote nucleosome assembly like a histone chaperone. Additionally, both Rpd3 HDAC complexes prevent RSC-dependent histone eviction from nucleosomes, possibly through their histone chaperone activity. However, we note that the eviction and chaperone functions displayed different concentration dependence. We were also able to establish that the three common subunits of Rpd3S and Rpd3L formed a subcomplex, which contributed to the shared activities of the small and large Rpd3 HDACs. We

speculate that the combination of a histone chaperone activity and inhibition of RSC eviction facilitate chromatin stability and complement the transcriptional repression function of the Rpd3 HDAC.

The diminished density of H3 in strains upon Rpd3 deletion or mutation was significant mainly on the promoter/intergenic regions. Despite the observation that transcription level is inversely correlated with H3 density [35], the levels of H3 in transcribed regions significantly exceed those in promoter regions. It remains a possibility that although Rpd3S is found primarily in ORFs, the normally high histone density masks its stabilization function. Histone density and chromatin stabilization in the ORF is known to involve numerous proteins, including chaperones such as Spt6 and FACT, many of which generate a cryptic transcription phenotype when mutated [36–38]. Hence the role of Rpd3's stabilization function in the ORF regions may be less apparent and require more sensitive assays or combinatorial mutations of other chaperones to become more evident. Alternately, the ability of H3K36me3 to inhibit Rpd3's chaperone function may disable that function in ORFs.

A prediction of the role of Rpd3, as either a chaperone or in chromatin stabilization, is that it should copurify with substantial amounts of H3. Indeed, we observed that Rpd3

complexes, purified with an Rpd3-TAP strain, contained a significant amount of H3 and less, but still detectable, amounts of Pol II. Stoichiometry measurements revealed that the ratio of Rpd3:H3:Pol II is 10:4.5:1 (Figures S3C and S3D). This result was obtained with concentrations of heparin and ethidium bromide, which are known to disfavor protein-DNA interactions. In the case of H3, these data are consistent with a chaperone function. In the case of Pol II, these data are consistent with the direct interaction of Pol II and Rpd3S proposed by Hinnebusch and colleagues [18].

It should be pointed out that our unpublished microarray data show that deletion of Rpd3 causes upregulation and downregulation of many genes as reported [39] (data not shown). Although it would be easy to dismiss the downregulated genes as indirect effects, the result belies a complex role of Rpd3 in transcription. For example, little is known about the mechanisms underlying global histone deacetylation and what role it plays. Additionally, Rpd3 has been shown to be directly required for activation of stress-inducible genes, and in some cases, the effect requires the catalytic activity [32–34]. In such scenarios, nucleosome density and the chromatin stabilization function may not always correlate with Rpd3 occupancy. Therefore, although our results reveal an additional function for Rpd3, which may have implications for the function of these proteins in higher eukaryotes, much remains to be learned of how this protein functions in genomic regulation.

Accession Numbers

The raw data have been deposited into the Gene Expression Omnibus (GEO) database (accession # GSE33829).

Supplemental Information

Supplemental Information includes Supplemental Experimental Procedures and three figures and can be found with this article online at doi:10.1016/j.cub.2011.11.042.

Acknowledgments

This work was supported by the National Institute of General Medical Sciences grant (1R01GM085002) to M.C. B.L. is a W.A. "Tex" Moncrief, Jr., Scholar in Medical Research and is supported by grants from the National Institutes of Health (R01GM090077), the Welch Foundation (I-1713), the March of Dimes Foundation, and the American Heart Association. We are grateful to K. Struhl at Harvard Medical School for providing the Rpd3 wild-type and H150A plasmids. We thank Y. Guo for her initial experimental contributions to this work.

Received: September 29, 2011

Revised: November 21, 2011

Accepted: November 21, 2011

Published online: December 15, 2011

References

1. Yang, X.J., and Seto, E. (2008). The Rpd3/Hda1 family of lysine deacetylases: from bacteria and yeast to mice and men. *Nat. Rev. Mol. Cell Biol.* 9, 206–218.
2. Kadosh, D., and Struhl, K. (1998). Histone deacetylase activity of Rpd3 is important for transcriptional repression in vivo. *Genes Dev.* 12, 797–805.
3. Ng, H.H., Robert, F., Young, R.A., and Struhl, K. (2002). Genome-wide location and regulated recruitment of the RSC nucleosome-remodeling complex. *Genes Dev.* 16, 806–819.
4. Taunton, J., Hassig, C.A., and Schreiber, S.L. (1996). A mammalian histone deacetylase related to the yeast transcriptional regulator Rpd3p. *Science* 272, 408–411.

5. Saha, A., Wittmeyer, J., and Cairns, B.R. (2006). Chromatin remodelling: the industrial revolution of DNA around histones. *Nat. Rev. Mol. Cell Biol.* 7, 437–447.
6. Peterson, C.L., and Laniel, M.A. (2004). Histones and histone modifications. *Curr. Biol.* 14, R546–R551.
7. Fry, C.J., and Peterson, C.L. (2001). Chromatin remodeling enzymes: who's on first? *Curr. Biol.* 11, R185–R197.
8. Clapier, C.R., and Cairns, B.R. (2009). The biology of chromatin remodeling complexes. *Annu. Rev. Biochem.* 78, 273–304.
9. Yang, X.J. (2004). Lysine acetylation and the bromodomain: a new partnership for signaling. *Bioessays* 26, 1076–1087.
10. Carrozza, M.J., Li, B., Florens, L., Suganuma, T., Swanson, S.K., Lee, K.K., Shia, W.J., Anderson, S., Yates, J., Washburn, M.P., and Workman, J.L. (2005). Histone H3 methylation by Set2 directs deacetylation of coding regions by Rpd3S to suppress spurious intragenic transcription. *Cell* 123, 581–592.
11. Keogh, M.C., Kurdistani, S.K., Morris, S.A., Ahn, S.H., Podolny, V., Collins, S.R., Schuldiner, M., Chin, K., Punna, T., Thompson, N.J., et al. (2005). Cotranscriptional set2 methylation of histone H3 lysine 36 recruits a repressive Rpd3 complex. *Cell* 123, 593–605.
12. Florens, L., Carrozza, M.J., Swanson, S.K., Fournier, M., Coleman, M.K., Workman, J.L., and Washburn, M.P. (2006). Analyzing chromatin remodeling complexes using shotgun proteomics and normalized spectral abundance factors. *Methods* 40, 303–311.
13. Kadosh, D., and Struhl, K. (1998). Targeted recruitment of the Sin3-Rpd3 histone deacetylase complex generates a highly localized domain of repressed chromatin in vivo. *Mol. Cell Biol.* 18, 5121–5127.
14. Rundlett, S.E., Camen, A.A., Suka, N., Tumer, B.M., and Grunstein, M. (1998). Transcriptional repression by UME6 involves deacetylation of lysine 5 of histone H4 by RPD3. *Nature* 392, 831–835.
15. Li, B., Carey, M., and Workman, J.L. (2007). The role of chromatin during transcription. *Cell* 128, 707–719.
16. Lee, J.S., and Shilatifard, A. (2007). A site to remember: H3K36 methylation a mark for histone deacetylation. *Mutat. Res.* 618, 130–134.
17. Li, B., Gogol, M., Carey, M., Pattenden, S.G., Seidel, C., and Workman, J.L. (2007). Infrequently transcribed long genes depend on the Set2/Rpd3S pathway for accurate transcription. *Genes Dev.* 21, 1422–1430.
18. Govind, C.K., Qiu, H., Ginsburg, D.S., Ruan, C., Hofmeyer, K., Hu, C., Swaminathan, V., Workman, J.L., Li, B., and Hinnebusch, A.G. (2010). Phosphorylated Pol II CTD recruits multiple HDACs, including Rpd3C(S), for methylation-dependent deacetylation of ORF nucleosomes. *Mol. Cell* 39, 234–246.
19. Grzenda, A., Lomber, G., Zhang, J.S., and Urrutia, R. (2009). Sin3: master scaffold and transcriptional corepressor. *Biochim. Biophys. Acta* 1789, 443–450.
20. Sif, S., Saurin, A.J., Imbalzano, A.N., and Kingston, R.E. (2001). Purification and characterization of mSin3A-containing Brg1 and hBrm chromatin remodeling complexes. *Genes Dev.* 15, 603–618.
21. Ghaemmaghami, S., Huh, W.K., Bower, K., Howson, R.W., Belle, A., Dephoure, N., O'Shea, E.K., and Weissman, J.S. (2003). Global analysis of protein expression in yeast. *Nature* 425, 737–741.
22. Simon, M.D., Chu, F., Racki, L.R., de la Cruz, C.C., Burlingame, A.L., Panning, B., Narlikar, G.J., and Shokat, K.M. (2007). The site-specific installation of methyl-lysine analogs into recombinant histones. *Cell* 128, 1003–1012.
23. Lowary, P.T., and Widom, J. (1998). New DNA sequence rules for high affinity binding to histone octamer and sequence-directed nucleosome positioning. *J. Mol. Biol.* 276, 19–42.
24. Steger, D.J., and Workman, J.L. (1999). Transcriptional analysis of purified histone acetyltransferase complexes. *Methods* 19, 410–416.
25. Li, B., Gogol, M., Carey, M., Lee, D., Seidel, C., and Workman, J.L. (2007). Combined action of PHD and chromo domains directs the Rpd3S HDAC to transcribed chromatin. *Science* 316, 1050–1054.
26. Lorch, Y., Zhang, M., and Kornberg, R.D. (1999). Histone octamer transfer by a chromatin-remodeling complex. *Cell* 96, 389–392.
27. Das, C., Tyler, J.K., and Churchill, M.E. (2010). The histone shuffle: histone chaperones in an energetic dance. *Trends Biochem. Sci.* 35, 476–489.
28. Etoku, M., Sato, L., Senda, T., and Horikoshi, M. (2008). Histone chaperones: 30 years from isolation to elucidation of the mechanisms of nucleosome assembly and disassembly. *Cell. Mol. Life Sci.* 65, 414–444.

29. Belotserkovskaya, R., Oh, S., Bondarenko, V.A., Orphanides, G., Studitsky, V.M., and Reinberg, D. (2003). FACT facilitates transcription-dependent nucleosome alteration. *Science* 301, 1090-1093.
30. Carey, M., Li, B., and Workman, J.L. (2006). RSC exploits histone acetylation to abrogate the nucleosomal block to RNA polymerase II elongation. *Mol. Cell* 24, 481-487.
31. Rundlett, S.E., Carmen, A.A., Kobayashi, R., Bavykin, S., Turner, B.M., and Grunstein, M. (1996). HDA1 and RPD3 are members of distinct yeast histone deacetylase complexes that regulate silencing and transcription. *Proc. Natl. Acad. Sci. USA* 93, 14503-14508.
32. Alejandro-Osorio, A.L., Huebert, D.J., Porcaro, D.T., Sonntag, M.E., Nillasithanukroh, S., Will, J.L., and Gasch, A.P. (2009). The histone deacetylase Rpd3p is required for transient changes in genomic expression in response to stress. *Genome Biol.* 10, R57.
33. Ruiz-Roig, C., Viéitez, C., Posas, F., and de Nadal, E. (2010). The Rpd3L HDAC complex is essential for the heat stress response in yeast. *Mol. Microbiol.* 76, 1049-1062.
34. Sertil, O., Vemula, A., Salmon, S.L., Morse, R.H., and Lowry, C.V. (2007). Direct role for the Rpd3 complex in transcriptional induction of the anaerobic DAN/TIR genes in yeast. *Mol. Cell. Biol.* 27, 2037-2047.
35. Lee, C.K., Shibata, Y., Rao, B., Strahl, B.D., and Lieb, J.D. (2004). Evidence for nucleosome depletion at active regulatory regions genome-wide. *Nat. Genet.* 36, 900-905.
36. Bortvin, A., and Winston, F. (1996). Evidence that Spt16p controls chromatin structure by a direct interaction with histones. *Science* 272, 1473-1476.
37. Duina, A.A., Ruffange, A., Bracey, J., Hall, J., Nourani, A., and Winston, F. (2007). Evidence that the localization of the elongation factor Spt16 across transcribed genes is dependent upon histone H3 integrity in *Saccharomyces cerevisiae*. *Genetics* 177, 101-112.
38. Kaplan, C.D., Laprade, L., and Winston, F. (2003). Transcription elongation factors repress transcription initiation from cryptic sites. *Science* 301, 1096-1099.
39. Bemstein, B.E., Tong, J.K., and Schreiber, S.L. (2000). Genomewide studies of histone deacetylase function in yeast. *Proc. Natl. Acad. Sci. USA* 97, 13708-13713.

Supplemental Information

The Rpd3 Core Complex Is

a Chromatin Stabilization Module

Xiao-Fen Chen, Benjamin Kuryan, Tasuku Kitada, Nancy Tran, Jing-Yu Li, Siavash Kurdistani, Michael Grunstein, Bing Li, and Michael Carey

Inventory of Supplemental Materials

- 1. Figures S1, Related to Figure 1**
- 2. Figure S2, related to Figure 2**
- 3. Figure S3, Related to Figure 4**
- 4. Experimental Procedures**
- 5. Supplemental References**

Figure S1, related to Figure 1, Chen et al.,

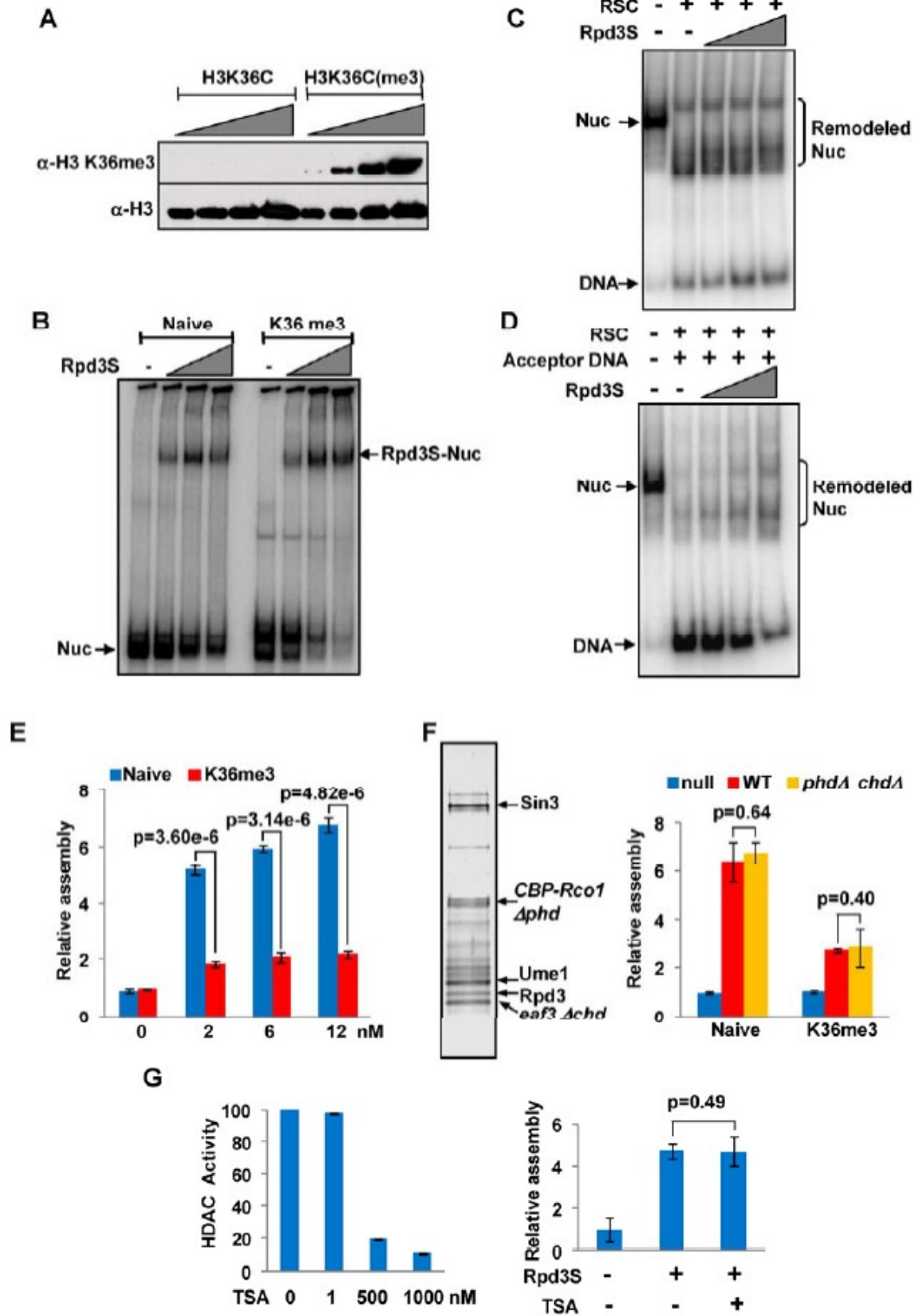


Figure S1, related to Figure 1

Rpd3S Stabilizes Nucleosome Structure Independent of H3K36me3 or HDAC Activity.

(A) Methyl lysine analogues (H3K36Cme3) and their precursors (H3K36C) are immunoblotted against H3 (ab1791) or H3K36me3 antibody (ab9050).

(B) EMSA of Rpd3S binding to naïve or H3K36me3 nucleosomes. 0.67, 2 or 6 nM of Rpd3S were incubated with naïve or H3K36me3 nucleosomes and fractionated on native polyacrylamide gels. A phosphorimage of the gel is shown.

(C) RSC dependent remodeling on H3K36me3 nucleosomes in the presence or absence of Rpd3S. 2nM RSC was incubated with ³²P-labeled nucleosomes and 0, 13, 39, 78 nM Rpd3S. The products were fractionated by native PAGE. A phosphorimage of the gel is shown.

(D) RSC-dependent eviction on H3K36me3 nucleosomes in the presence or absence of Rpd3S. 6 nM RSC was analyzed with 0, 13, 39 or 78 nM Rpd3S in the presence of 10 ng pGEM3Z601R acceptor DNA and analyzed as in (C).

(E) Rpd3S-mediated chromatin assembly with naïve or H3K36me3 octamers. 20 ng of naïve or H3K36me3 octamers were incubated with 0, 2, 6 or 12 nM Rpd3S and a ³²P-labeled 601 DNA fragment. The graph quantitates the amounts of assembled nucleosome mediated by Rpd3S relative to no Rpd3S control (octamers alone). The error bars show +/- standard deviation (SD). The P value is calculated using Student's t-test.

(F) Left panel, silver stain gel of TAP-purified mutant Rpd3S with combined deletion of CHD and PHD domains. Right panel, comparison of wild-type (WT) and mutant Rpd3S (*phdΔ chdΔ*) in mediating chromatin assembly using naïve or H3K36me3 octamers. 12 nM of wild-type or mutant Rpd3S was incubated with 20 ng naïve or H3K36me3 octamers. Bar graph from 3 independent experiments representing the relative amount of assembled nucleosomes normalized to no Rpd3S control (null). The error bars show +/- standard deviation (SD). P values are from Student's t-test.

(G) Left panel, histone deacetylation assay with TSA. The deacetylase activity of 20 nM Rpd3S in the presence of 0, 1, 500, 1000 nM TSA was analyzed using an HDAC fluorometric activity assay kit (BIOMOL). Bar graph from 3 independent experiments representing the relative activity of Rpd3S HDAC normalized to the no TSA control. The error bars show +/- standard deviation (SD). Right panel, the effect of TSA on Rpd3S-mediated chromatin assembly. 12 nM Rpd3S with or without 1000 nM TSA was incubated with 20 ng of naïve octamers and analyzed as in (E).

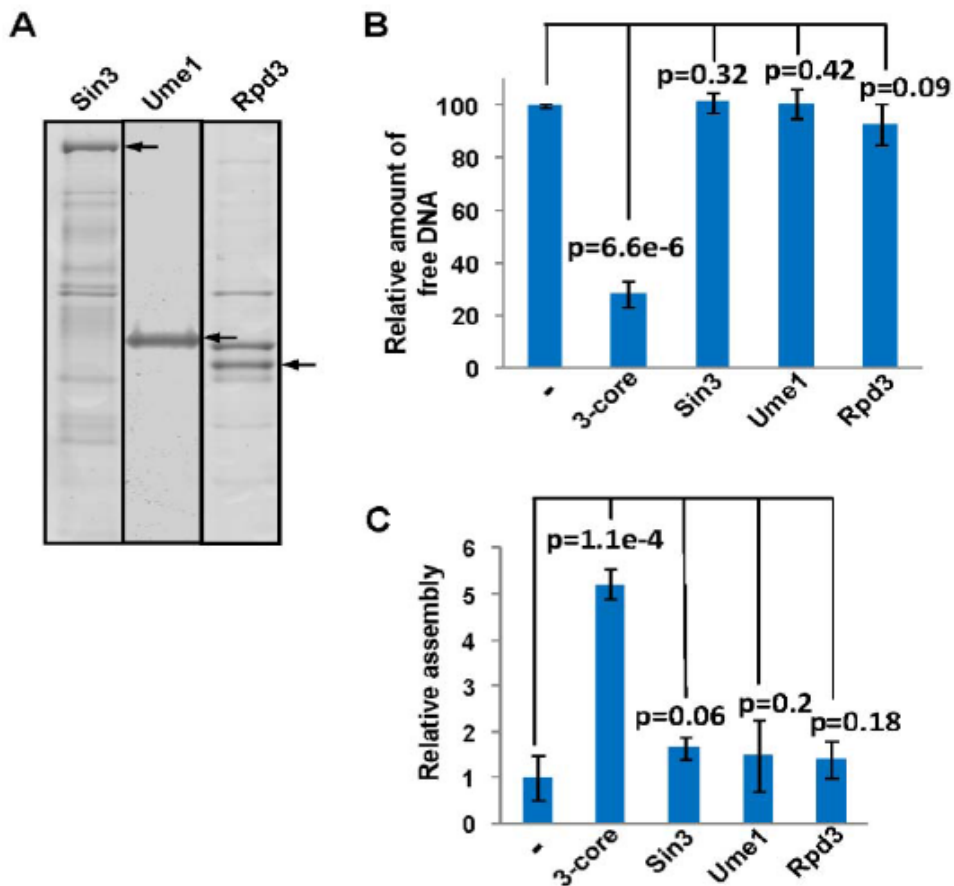


Figure S2, related to Figure 2

Individual Subunits of the 3-subunit Core Complex Do Not Stabilize Nucleosome Structure.

(A) Silver stained gel of recombinant Sin3, Ume1, Rpd3 expressed in a baculovirus system.

(B) RSC-dependent eviction on naive nucleosomes in the presence or absence of 3-core, Sin3, Ume1, Rpd3. 6 nM RSC was analyzed with or without 90 nM of 3-core, Sin3, Ume1, Rpd3. Data were analyzed as in legend of Figure 1C.

(C) Chromatin assembly assay. 20ng of naive octamers were assayed with or without 12 nM of 3-subunit core, Sin3, Ume1, Rpd3. Data were analyzed as in Figure S1E.

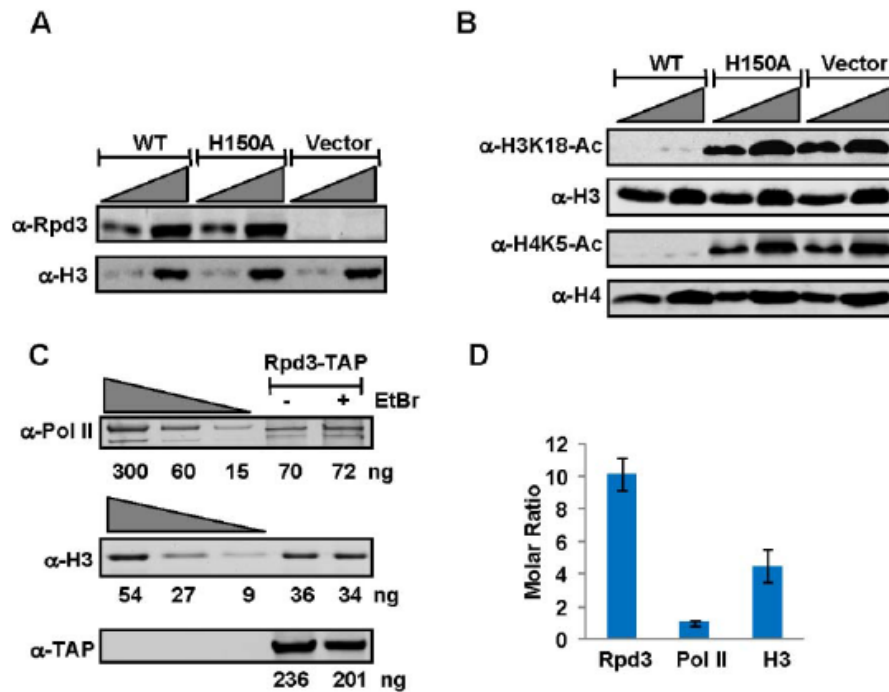


Figure S3, related to Figure 4

(A and B) *rpd3* mutation (H150A) induces histone H3 and H4 hyperacetylation similar to *rpd3*-deletion (Vector).

(A) Rpd3p or Rpd3p (H150A) levels were measured by western blotting in extracts of wild-type (WT), *rpd3* H150A (H150A), and *rpd3* Δ (Vector) cells. The histone H3 blot serves as loading control.

(B) Relative histone acetylation levels in wild-type (WT), *rpd3* H150A (H150A), and *rpd3* Δ (Vector) cells were determined by blotting with antibodies specific for H3 acetyl-lysine 18 or H4 acetyl-lysine 5. H3 and H4 blots serve as loading controls.

(C and D) Rpd3 Co-purifies with Pol II and Histone H3 In Vivo.

(C) Western blot shows TAP-purified Rpd3 co-purifies with Pol II and H3. A standard curve (left three lanes) was generated using 300, 60, and 15 ng of TAP-purified Pol II, and 54, 27, and 9 ng of recombinant H3. Rpd3 was quantified by silver staining.

(D) Bar graph shows the molar ratio of Pol II, H3, and Rpd3 in the Rpd3-TAP purification. Data from 3 replicates were averaged and graphed. The error bars show +/- standard deviation (SD).

Supplemental Experimental Procedures

TAP Strains and TAP Purification

TAP-tagged strains for Rco1, Rsc2, Spt16 and Rxt2 are from the Open Biosystems Yeast-TAP Fusion Library. *eaf3Δchd rco1Δphd*-TAP tagged strain was a gift from Bing Li. TAP purification was performed as previously described with minor modifications [1].

Recombinant Histone Purification and Nucleosome Reconstitution

Recombinant *Xenopus laevis* histones (H3K36C, H3, H4, H2A, and H2B) were individually expressed in BL21 (DE3) cells and purified as described [2]. Methyl-lysine analog histones (H3K36Cme3) were prepared as described previously [3]. DNA templates used in the nucleosome assembly assays were PCR amplified from the pGEM3Z601R plasmid [4]. Mononucleosomes were reconstituted via the serial salt dilution method [5].

RSC-Dependent Nucleosome Remodeling and Eviction Assays

Nucleosomes were end-labeled with Polynucleotide kinase and $\gamma^{32}\text{P}$ -ATP on 601 DNA, and then incubated with RSC and Rpd3 complex in reaction buffer (25mM HEPES, pH 7.5, 10 mM MgCl₂, 50 mM KCl, 0.25 mg/mL BSA, 10% Glycerol, 1mM DTT, 2mM ATP). For eviction assays, 10 ng of pGEM3Z601R plasmid was added as acceptor DNA. After 1hr at 30°C, 400 ng Poly(dI-dC) and 100 ng of pGEM3Z601R plasmid DNA were added for 15 min at 30°C to compete RSC and

Rpd3 off the nucleosomes. The nucleosomal products were separated on a 5% (29:1) polyacrylamide gel, dried and exposed to a Phosphor imaging screen (GE).

Chaperone-dependent Chromatin Assembly

20 ng of *Xenopus laevis* octamers were incubated with FACT or Rpd3 complexes in a 10- μ L reaction mixture containing 25 mM HEPES pH7.5, 10 mM MgCl₂, 50 mM KCl, 0.25 mg/mL BSA, 10% Glycerol, and 1 mM DTT. After 30 min at 30°C, 1 ng of ³²P-end-labeled 174-bp DNA template in 10 μ l of the same buffer above was added. After 1 h at 30°C, 400 ng of Poly(dI-dC) and 100 ng of pGEM3Z601R plasmid DNA were added for an additional 15 min. The products were separated by 5% (29:1) native PAGE, dried and exposed to a Phosphor imaging screen (GE).

Purification of Recombinant 3-Subunit Core Complex and Individual Subunits from SF9 Cells

Sf9 insect cells were grown at 27 °C in suspension cultures in Sf-900™ II SFM (Invitrogen). Recombinant baculoviruses were generated in Sf9 cells using the BacPAK™ Baculovirus Expression System (Clontech). For 3-subunit core purification, SF9 cells were co-transfected with Flag-Sin3, Rpd3 and Ume1 baculoviruses and harvested after 48 h. The cell pellets were lysed in lysis buffer (50 mM HEPES at pH 7.9, 300 mM NaCl, 2 mM MgCl₂, 0.2% Triton, 10% Glycerol, 0.5 mM EDTA). The recombinant 3-subunit core complex was then purified using M1 FLAG antibody affinity resin (Sigma) following the

manufacturer's instructions. The Flag-affinity eluate was fractionated on a Superose 12 HR 10/30 gel filtration column (Amersham Biosciences). For the Sin3, Ume1, Rpd3 purifications, each subunit was Flag-tagged, and affinity-purified using FLAG antibody resin.

In Vitro Transcription

Transcription reactions were performed as previously described [6] with the addition of 0.8U RNase H to prevent formation of DNA-RNA hybrids during transcription.

Chromatin Immunoprecipitation and Genome-Wide Mapping

Yeast strains for ChIP assays were constructed in RMY200 with myc-H3 as described previously [7]. RPD3 was deleted using a PCR-based gene disruption strategy [8, 9]. Centromeric plasmids were constructed bearing wild-type *RPD3*, *rpd3* H150A or vector alone and transformed into the *rpd3Δ* myc-H3 yeast cells. ChIP assays were performed as previously described [10]. Briefly, formaldehyde cross-linked, sonicated whole-cell extract was incubated overnight with antibodies directed against myc-H3 (9E10, Abcam). The ChIP and input DNA were amplified, labeled, and hybridized to two-color Agilent 244-k tiling arrays (G4491A) as previously described [11]. Hybridization and washing were performed according to the manufacturer's instructions. Following array scanning, the data were analyzed using Agilent Feature Extraction and normalized using Agilent ChIP Analytics with the default settings. Average probe signal was

extracted within bins as described in the figure legends. The raw data have been deposited into the Gene Expression Omnibus (GEO) database (Accession # GSE33829).

Data Analysis

The data from two biological replicates were combined using Agilent ChIP analytics 1.3 software. The RSC genome-wide occupancy data were downloaded from <http://web.wi.mit.edu/young/datadownload.htm>. We selected 506 intergenic regions with a combined P-value less than 0.001 as high RSC-bound targets. We arranged the combined P-values of the RSC dataset in descending order and selected 495 genes with the highest P values as low RSC-bound targets. The data were verified by comparing the Rsc2 intensity in these two subsets of targets. The H3 densities of these two subsets were compared in wild-type, *rpd3* H150A, and *rpd3* Δ cells.

Supplemental References

1. Ghaemmaghami, S., Huh, W.K., Bower, K., Howson, R.W., Belle, A., Dephoure, N., O'Shea, E.K., and Weissman, J.S. (2003). Global analysis of protein expression in yeast. *Nature* 425, 737-741.
2. Luger, K., Rechsteiner, T.J., Flaus, A.J., Wayne, M.M., and Richmond, T.J. (1997). Characterization of nucleosome core particles containing histone proteins made in bacteria. *J Mol Biol* 272, 301-311.
3. Simon, M.D., Chu, F., Racki, L.R., de la Cruz, C.C., Burlingame, A.L., Panning, B., Narlikar, G.J., and Shokat, K.M. (2007). The site-specific installation of methyl-lysine analogs into recombinant histones. *Cell* 128, 1003-1012.
4. Lowary, P.T., and Widom, J. (1998). New DNA sequence rules for high affinity binding to histone octamer and sequence-directed nucleosome positioning. *J Mol Biol* 276, 19-42.
5. Li, B., Pattenden, S.G., Lee, D., Gutierrez, J., Chen, J., Seidel, C., Gerton, J., and Workman, J.L. (2005). Preferential occupancy of histone variant H2AZ at inactive promoters influences local histone modifications and chromatin remodeling. *Proc Natl Acad Sci U S A* 102, 18385-18390.
6. Carey, M., Li, B., and Workman, J.L. (2006). RSC exploits histone acetylation to abrogate the nucleosomal block to RNA polymerase II elongation. *Mol Cell* 24, 481-487.
7. Mann, R.K., and Grunstein, M. (1992). Histone H3 N-terminal mutations allow hyperactivation of the yeast GAL1 gene in vivo. *EMBO J* 11, 3297-3306.
8. Baudin, A., Ozier-Kalogeropoulos, O., Denouel, A., Lacroute, F., and Cullin, C. (1993). A simple and efficient method for direct gene deletion in *Saccharomyces cerevisiae*. *Nucleic Acids Res* 21, 3329-3330.
9. Wach, A., Brachat, A., Pohlmann, R., and Philippsen, P. (1994). New heterologous modules for classical or PCR-based gene disruptions in *Saccharomyces cerevisiae*. *Yeast* 10, 1793-1808.
10. Hecht, A., Strahl-Bolsinger, S., and Grunstein, M. (1996). Spreading of transcriptional repressor SIR3 from telomeric heterochromatin. *Nature* 383, 92-96.
11. Robyr, D., and Grunstein, M. (2003). Genomewide histone acetylation microarrays. *Methods* 31, 83-89.

Contribution

The work presented in this chapter started out as a secondary project of mine, but was finished by Xiao-Fen Chen. I contributed by developing assays, generating preliminary data, and making reagents critical to the project. I directly provided the data for Supplemental Figure 1A.

Chapter 4

Mechanism for epigenetic variegation of gene expression at yeast
telomeric heterochromatin

Mechanism for epigenetic variegation of gene expression at yeast telomeric heterochromatin

Tasuku Kitada,^{1,2} Benjamin G. Kuryan,^{1,2} Nancy Nga Huynh Tran,^{1,2} Chunying Song,^{1,2} Yong Xue,^{1,2} Michael Carey,^{1,2} and Michael Grunstein^{1,2,3}

¹Department of Biological Chemistry, David Geffen School of Medicine, ²the Molecular Biology Institute, University of California at Los Angeles, Los Angeles, California 90095, USA

Yeast contains heterochromatin at telomeres and the silent mating-type loci (*HML/HMR*). Genes positioned within the telomeric heterochromatin of *Saccharomyces cerevisiae* switch stochastically between epigenetically bistable ON and OFF expression states. Important aspects of the mechanism of variegated gene expression, including the chromatin structure of the natural ON state and the mechanism by which it is maintained, are unknown. To address this issue, we developed approaches to select cells in the ON and OFF states. We found by chromatin immunoprecipitation (ChIP) that natural ON telomeres are associated with Rap1 binding and, surprisingly, also contain known characteristics of OFF telomeres, including significant amounts of Sir3 and H4K16 deacetylated nucleosomes. Moreover, we found that H3K79 methylation (H3K79me), H3K4me, and H3K36me, which are depleted from OFF telomeres, are enriched at ON telomeres. We demonstrate in vitro that H3K79me, but not H3K4me or H3K36me, disrupts transcriptional silencing. Importantly, H3K79me does not significantly reduce Sir complex binding in vivo or in vitro. Finally, we show that maintenance of H3K79me at ON telomeres is dependent on transcription. Therefore, although Sir proteins are required for silencing, we propose that epigenetic variegation of telomeric gene expression is due to the bistable enrichment/depletion of H3K79me and not the fluctuation in the amount of Sir protein binding to nucleosomes.

[*Keywords:* epigenetics; position effect variegation; silencing; telomeres; histones; Sir complex]

Supplemental material is available for this article.

Received July 13, 2012; revised version accepted September 7, 2012.

Epigenetics is traditionally defined as “the study of mitotically and/or meiotically heritable changes in gene function that cannot be explained by changes in DNA sequence” (Riggs et al. 1996). Position effect variegation (PEV), discovered in the fruit fly *Drosophila melanogaster*, is a classic example of an epigenetic phenomenon (Girton and Johansen 2008). PEV is characterized by the reversible and stochastic switching of a gene positioned within heterochromatin between ON and OFF states. Telomere position effect (TPE), at the heterochromatin of telomeres in budding yeast, is a form of PEV (Supplemental Fig. S1; Gottschling et al. 1990; Mondoux and Zakian 2006). TPE involves the variegated expression of genes positioned near telomeres at the boundary of heterochromatin and euchromatin. Although TPE in yeast was discovered more than two decades ago (Gottschling et al. 1990), how the variegated gene expression pattern arises at telomeres

is still poorly understood (Ptashne 2002; Mondoux and Zakian 2006; Madhani 2007).

The formation of telomeric and silent mating-type locus heterochromatin has been well characterized, and current data are consistent with a model in which yeast heterochromatin proteins assemble and spread along histones in a stepwise manner (Hecht et al. 1996; Rusche et al. 2003; Mondoux and Zakian 2006). In this process, Rap1 bound at the telomeric TG₁₋₃ repeats (Buchman et al. 1988; Klein et al. 1992) recruits Sir4 through direct protein-protein interaction (Moretti et al. 1994; Hoppe et al. 2002; Luo et al. 2002). Sir4 in turn recruits Sir2 (Moazed et al. 1997; Strahl-Bolsinger et al. 1997), an NAD-dependent histone deacetylase (HDAC) with specificity for histone H4K16 acetylation (H4K16ac) (Imai et al. 2000; Landry et al. 2000; Smith et al. 2000). Deacetylation of H4K16ac generates a high-affinity binding site for the Sir3 protein (Johnson et al. 1990; Liou et al. 2005), which in turn recruits more Sir4 and Sir2 (Hecht et al. 1996; Hoppe et al. 2002; Luo et al. 2002). Cycles of H4K16 deacetylation and Sir3 recruitment enable spreading of

³Corresponding author
E-mail mg@mbi.ucla.edu

Article is online at <http://www.genesdev.org/cgi/doi/10.1101/gad.201095.112>.

the Sir complex along telomeric heterochromatin. The spreading of the Sir complex is eventually blocked by H4K16ac in adjacent euchromatin by the histone acetyltransferase Sas2 (Kimura et al. 2002; Suka et al. 2002). Sas2-mediated acetylation of H4K16 is also thought to enhance the incorporation of the histone H2A variant Htz1/H2AZ (Shia et al. 2006), which may act as an additional barrier to Sir complex spreading (Meneghini et al. 2003).

Similarly, H3K4 methylation (H3K4me), H3K36me, and H3K79me have also been proposed to contribute to the boundary between heterochromatin and euchromatin, but the exact role that each modification plays in this process is less well defined (Verzijlbergen et al. 2009). It has been suggested, using histone point mutant and methyltransferase deletion strains, that the presence of H3K4me or H3K36me prevents ectopic binding of Sir proteins in euchromatin (Santos-Rosa et al. 2004; Tompa and Madhani 2007). More critically, the overexpression of the H3K79 methyltransferase Dot1 has been shown to disrupt gene silencing *in vivo*, and it has been proposed that H3K79me may block Sir complex binding to antagonize subtelomeric silencing *in vivo* (Singer et al. 1998; van Leeuwen et al. 2002; Ng et al. 2003; Katan-Khaykovich and Struhl 2005; Altaf et al. 2007; Fingerman et al. 2007; Onishi et al. 2007). Genetic, biochemical, and structural studies have shown that unmethylated H3K79 is a contact site for Sir3 and that methylation of H3K79 can disrupt that interaction between the H3K79 region and Sir3 *in vitro* (Ng et al. 2002; Altaf et al. 2007; Fingerman et al. 2007; Johnson et al. 2009; Martino et al. 2009; Armache et al. 2011; Ehrentraut et al. 2011). Moreover, removal of H3K79me has been shown to facilitate *de novo* establishment of silencing at the silent mating-type locus *HML* (Osborne et al. 2009). Although it has been reported that H3K79 methylation by Dot1 does not play a role in natural silencing at *HML* or at most subtelomeres (Takahashi et al. 2011), the study asked whether the genome-wide depletion of H3K79me would derepress heterochromatin silencing instead of directly addressing the function of H3K79me at heterochromatin *per se*.

The precise mechanism by which heterochromatin prevents the transcription of a gene is not known. However, it has been proposed that the Sir complex can prevent gene activation by either blocking the assembly of the preinitiation complex (PIC; general transcription factors and RNA polymerase II [RNAPII]) or regulating the transition between transcription initiation and RNAPII elongation (Sekinger and Gross 2001; Chen and Widom 2005; Gao and Gross 2008). Additionally, it has been shown that the abnormal lengthening of telomeres can increase the strength of gene silencing (Kyrion et al. 1993; Li and Lustig 1996; Mishra and Shore 1999; Park and Lustig 2000).

In contrast to the formation of the OFF state of telomeric heterochromatin, the chromatin structure of the natural ON state has not been well characterized. Potentially, the natural ON state could result from the absence of Rap1 binding to telomeric repeats or loss of interaction between the Sir complex and nucleosomes due to H4K16ac

or H3K79me (Ng et al. 2003; Moazed 2011). However, this is not necessarily the case, as it has been shown that a telomeric gene can be derepressed in the presence of Sir complex binding in an H4K16R Sir2-345 catalytic mutant strain (Yang et al. 2008), an H3K56 mutant strain (Xu et al. 2007), an H3 Δ 4-30 tail deletion mutant strain (Sperling and Grunstein 2009), and a strain with a Gal4-Sir1 fusion protein artificially recruited to a synthetic *HMR* silent mating-type locus prior to the establishment of silencing (Kirchmaier and Rine 2006).

Therefore, to decipher the basis of epigenetic variegation, we sought to identify the molecular factors that determine the natural ON state of budding yeast TPE. To accomplish this, we first developed a method for isolating populations of cells with telomeres in the ON and OFF states. This approach is conceptually different from most previous studies in which mixed populations of cells with ON and OFF telomeres were compared with heterochromatin mutant strains with telomeres that are artificially ON (Rusche et al. 2003). We then assessed the structural differences in chromatin at the ON and OFF telomeres *in vivo*. Additionally, by *in vitro* reconstitution of heterochromatin, we asked whether any of the differences observed *in vivo* were sufficient to disrupt gene silencing using yeast nuclear extracts. Surprisingly, we found that Rap1 binding, Sir complex binding to nucleosomes, and H4K16 deacetylation were largely similar between the ON and OFF states *in vivo*. Instead, we demonstrate that H3K79me enables the disruption of gene silencing and inheritance of the natural ON state of the telomere by a transcription-mediated positive feedback loop despite the spreading of the Sir complex along nucleosomes. We conclude that H3K79me and not the difference in the amount of Sir complex binding to nucleosomes *per se* is the epigenetic basis for variegation at telomeres.

Results

Isolation of ON and OFF cells by medium selection

To determine the differences between the ON and OFF chromatin states, it was necessary to separate ON and OFF cells in bulk. To accomplish this, we employed a yeast strain harboring a *URA3* reporter gene at a telomere at the left arm of chromosome VII (TEL07L). We isolated ON and OFF cells, respectively, by culturing the strain in medium lacking uracil (SD-ura) or medium containing the drug 5-FOA (SD+FOA), which is toxic to cells with *Ura3* activity (Fig. 1A; Boeke et al. 1987). For comparison, *YFR057W*, a native gene located near a different telomere (native TEL06R), was monitored as a control.

A recent study had shown that the *URA3*-FOA assay may identify false positive hits when used in screens for detecting silencing mutants, making it necessary to confirm the expression of *URA3* using quantitative RT-PCR (qRT-PCR) (Rossmann et al. 2011). As shown in Figure 1B, the mRNA level of *URA3* was low in cells cultured in SD+FOA and high in SD-ura when measured by qRT-PCR. In fact, the *URA3* expression level of cells grown in SD-ura was comparable with that of a Δ *sir3*

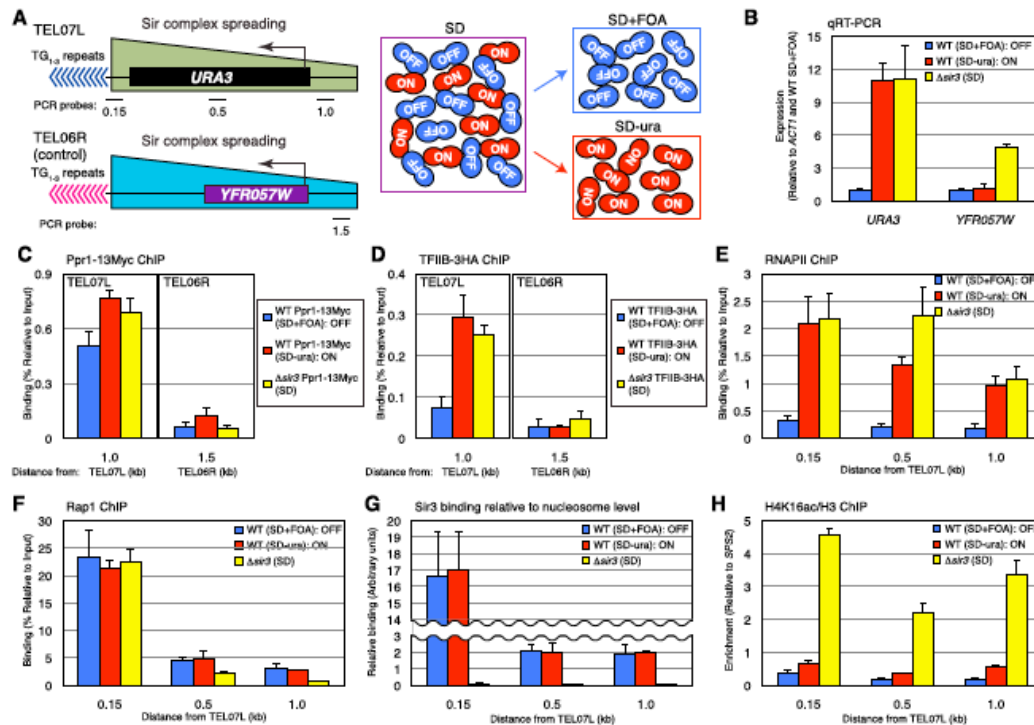


Figure 1. Rap1 binding to DNA and Sir protein binding to nucleosomes are not different between ON and OFF telomeres. (A) Schematic of the medium selection approach to isolate ON and OFF telomeres. Probes were ~0.15, 0.5, and 1.0 kb away from the telomeric repeats of *URA3*-TEL07L and ~1.5 kb from native TEL06R. (B) qRT-PCR of *URA3* at TEL07L and *YFR057W* at native TEL06R in wild-type (WT) *SIR3* cells grown in SD+FOA (blue bars) and SD-ura (red bars) and $\Delta sir3$ cells grown in SD (yellow bars). Data are presented as mean \pm standard deviation (SD). (C, D) ChIP of Ppr1-13Myc (C) and TFIIIB-3HA (D) depicted as in B except Ppr1 and TFIIIB were tagged with 13Myc and 3HA, respectively. (E-H) ChIP of RNAPII (E), Rap1 (F), Sir3 binding relative to nucleosome level (G), and H4K16ac/H3 (H) at *URA3*-TEL07L depicted as in B.

control strain in which heterochromatin is completely disrupted (Fig. 1B; Strahl-Bolsinger et al. 1997). Therefore, by the direct measurement of *URA3* mRNA using qRT-PCR, we found that our medium-based selection approach is capable of separating ON and OFF cells in bulk.

TPE is regulated at the RNAPII PIC assembly step

Previous studies had reported, in a contradictory manner, that heterochromatin prevents transcription by blocking either PIC assembly (Chen and Widom 2005) or the transition between initiation of transcription and RNAPII elongation (Sekinger and Gross 2001; Gao and Gross 2008). Therefore, we wished to clarify which step of the transcription process differed in our wild-type ON and OFF cells separated by medium selection. To accomplish this, we measured the binding of the *URA3* activator Ppr1 (Myc-tagged), general transcription factor TFIIIB (HA-tagged), and RNAPII at *URA3*-TEL07L by chromatin immunoprecipitation (ChIP) in ON cells, OFF cells, and $\Delta sir3$ cells as a control. RNAPII and TFIIIB are known to characterize PICs during gene activation (Hahn 2004; Kostrewa et al. 2009). As shown in Figure 1C, Ppr1 was enriched at the promoter of *URA3* at a similar level in the

ON and OFF states. In contrast, binding of TFIIIB and RNAPII was observed at the ON but not OFF telomere (Fig. 1D,E). Thus, based on these results from our medium-selected ON and OFF cells, heterochromatin is permissive to activator binding but not PIC assembly. We conclude that the epigenetic variation states of TPE are modulated at the PIC assembly step.

Histone methylation but not binding of heterochromatin proteins differentiates the ON and OFF telomeres

Differences in any of the steps of the heterochromatin assembly process could potentially explain how bistable ON and OFF chromatin states could exist at telomeres in wild-type yeast strains. To determine whether TPE can be explained by differences in the binding of key heterochromatin proteins, we measured the enrichment level of Rap1 and Sir3 at *URA3*-TEL07L in the medium-selected ON and OFF cells by ChIP. As shown in Figure 1F, binding of Rap1 to the ON and OFF telomeres was nearly identical. Similarly, and in contrast to previous models (Ng et al. 2003; Moazed 2011), we also observed that the level of Sir3 binding to nucleosomes along the subtelomeric

region in the ON and OFF cells was essentially the same (Fig. 1G). Importantly, our measurements took into account the fact that the number of nucleosomes was expectedly reduced at ON telomeres compared with those that were OFF (Supplemental Fig. S2; Pokholok et al. 2005). Nevertheless, our data support the idea that epigenetic variegation at telomeres cannot simply be explained by Rap1 binding or the extent of Sir3 binding to nucleosomes.

Since binding of Rap1 and Sir3 was similar between the ON and OFF telomeres, we next asked instead whether chromatin modifications antagonistic to silencing could be differentially enriched at these telomeres. To accomplish this, we performed ChIP at *URA3-TEL07L* in ON and OFF cells using antibodies specific to various chromatin modifications, including H4K16ac, H3K4me, H3K36me, and H3K79me. As expected from the efficient binding of Sir3, we found that H4K16, a key histone residue that regulates Sir3 spreading, was strongly hypoacetylated at both ON and OFF telomeres compared with $\Delta sir3$ (Fig. 1H; Supplemental Fig. S2). However, in contrast, we found that histone methylation was differentially enriched between the ON and OFF telomeres. Specifically, H3K79 monomethylation (H3K79me1), H3K79 dimethylation (H3K79me2), H3K4 trimethylation (H3K4me3), and H3K36me3 were enriched at the ON telomere (Fig. 2; Supplemental Fig. S2). We note that the enrichment levels of Htz1/H2AZ, H3K56ac, and H3K79me3, which are also capable of affecting gene silencing (Meneghini et al. 2003; Xu et al. 2007; Frederiks et al. 2008), were not obviously different between ON and OFF telomeres (Supplemental Fig. S2). The ChIP results for all of the above at the native TEL06R control locus are shown in Supplemental Figure S3. Therefore, our results argue that histone H3 methylation is enriched at ON telomeres and has the potential to disrupt gene silencing without affecting the amount of Sir3 binding to nucleosomes.

Sir proteins and RNAPII co-occupy chromatin in the ON state

As shown above, binding of the heterochromatin proteins Rap1 and Sir3 was similar between the ON and OFF telomeres. However, a ChIP assay measures the average level of protein binding or enrichment of a modification in a population of cells. Therefore, it was unclear whether the chromatin fragments with RNAPII binding that are responsible for gene activity were the same as those bound by heterochromatin proteins. To address this problem, we used sequential ChIP to determine whether RNAPII-bound telomere chromatin fragments were co-occupied by Rap1 or Sir3. The ON telomere fragments were first isolated by immunoprecipitation of Flag-tagged RNAPII using a Flag antibody, after which binding of Rap1 or Sir3 was measured by sequential ChIP (Fig. 3A). As shown in Figure 3B, RNAPII binding was low in wild-type *SIR3* but high in $\Delta sir3$ control cells, as expected. Control sequential ChIP reactions with an RNAPII antibody or no antibody confirmed that RNAPII-bound chromatin fragments were enriched during the initial RNAPII-Flag ChIP (Fig. 3C,D). Importantly, sequential ChIP of Rap1 and Sir3 showed that these two proteins were indeed bound to the ON telomere (Fig. 3E,F). Furthermore, consistent with our ChIP experiments above using medium selection, we found that H3K79me1 and H3K79me2 are also enriched at ON telomeres (Fig. 3G,H; Supplemental Fig. S4). We conclude that RNAPII binding in the ON state is compatible with Rap1 or Sir3 binding.

Fluorescence-activated cell sorting (FACS)-ChIP verification of the ON and OFF states

The sequential ChIP experiment described above showed that RNAPII and Rap1, Sir3, or H3K79me co-occupied the same chromatin fragments in the natural ON state of TPE. To further confirm this result and rule out the possibility that the medium-selection approach was

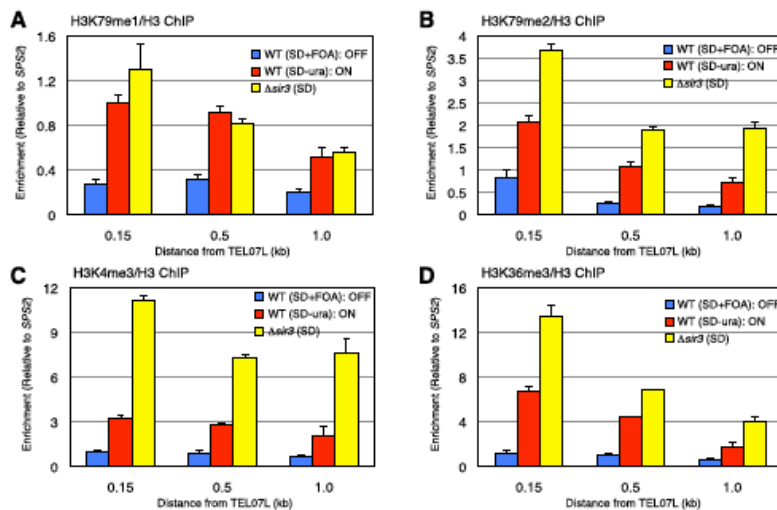


Figure 2. Histone methylation is enriched at ON telomeres. (A–D) ChIP of H3K79me1/H3 (A), H3K79me2/H3 (B), H3K4me3/H3 (C), and H3K36me3/H3 (D) at *URA3-TEL07L* depicted as in Figure 1B.

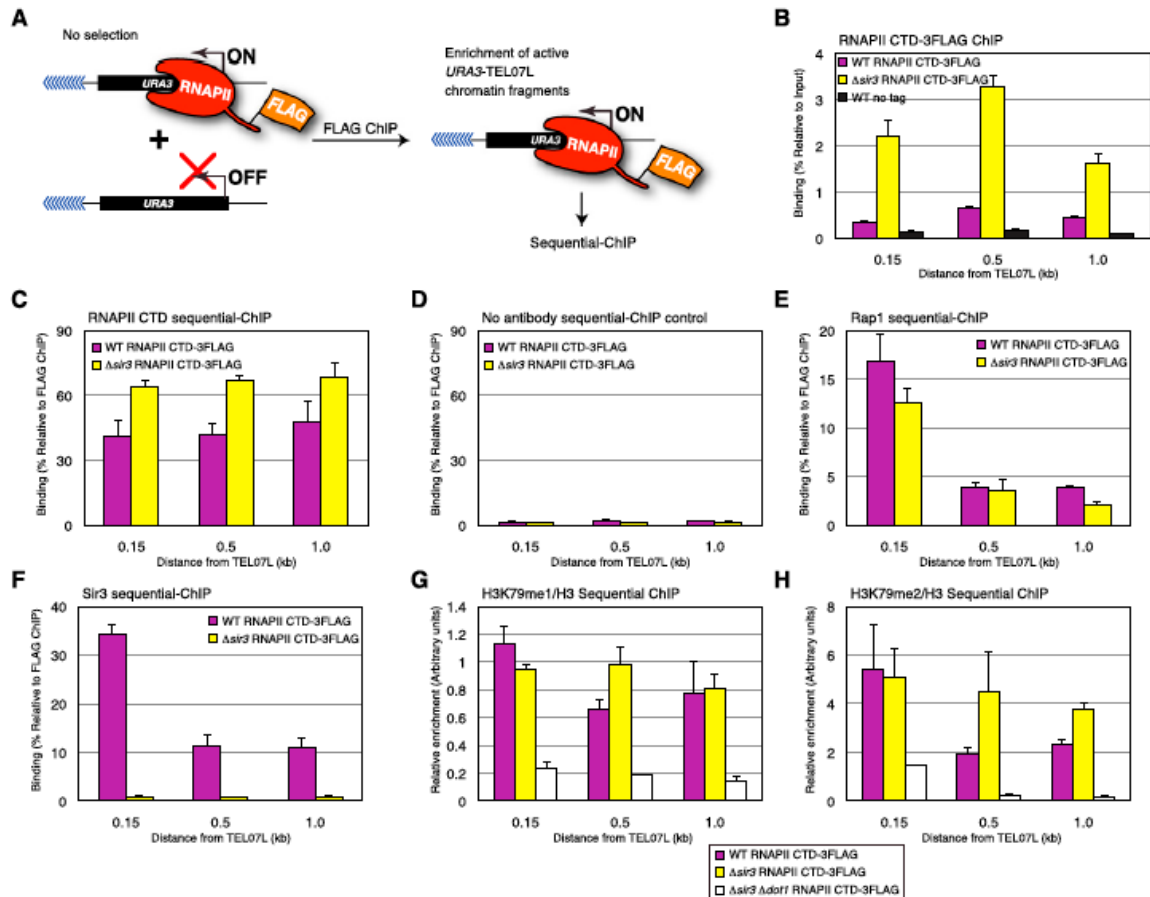


Figure 3. RNAPII-3Flag sequential ChIP assay confirms the co-occupancy of RNAPII and Rap1, Sir3, or H3K79me. (A) Schematic of the sequential ChIP approach to isolate ON telomeres. Rpb1, the subunit of the RNAPII complex containing the regulatory C-terminal domain (CTD), was C-terminally tagged with three tandem repeats of the Flag sequence and cultured in nonselective medium (YPD). ChIP was performed using an anti-Flag antibody to isolate chromatin fragments with RNAPII binding, including telomere fragments in the ON state. Probes were as in Figure 1A. (B) ChIP of RNAPII CTD-3Flag at *URA3-TEL07L* in wild-type (WT) *SIR3* RNAPII CTD-3Flag (purple bars) and $\Delta sir3$ RNAPII CTD-3Flag (yellow bars) cells grown in nonselective medium (YPD). A wild-type *SIR3* strain without a 3Flag tag (black bars) was used as a negative control. Data are presented as mean \pm SD. (C–F) Sequential ChIP of RNAPII (C), Rap1 (E), and Sir3 (F) at *URA3-TEL07L* depicted as in B. (D) A mock sequential ChIP without an antibody was performed as a negative control. (G,H) Sequential ChIP of H3K79me1/H3 (G) and H3K79me2/H3 (H) at *URA3-TEL07L*, depicted as in C–F with the addition of $\Delta sir3$ $\Delta dot1$ RNAPII CTD-3Flag (white bars), which was used as a control strain that lacks H3K79me.

causing an unexpected artifact, we wished to separate ON and OFF cells by FACS and compare the chromatin states of the ON and OFF telomeres using ChIP. To perform FACS-ChIP, we constructed a strain with a *URA3-GFP* fusion gene inserted at TEL07L (Fig. 4A). An octa-glycine (G8) linker was inserted between Ura3 and GFP so that GFP would not interfere with Ura3 function (Sabourin et al. 2007). To make the level of the GFP protein more accurately reflect the real-time expression state of the *URA3-GFP* gene, the half-life of Ura3-G8-GFP was reduced by attaching the Cln2 PEST domain (PD), a protein degradation sequence, to the C terminus of GFP (Xu et al. 2006). Last, to facilitate the visualization of Ura3-G8-GFP-PD, the fusion protein was concentrated in

the nucleus using a nuclear localization signal (NLS). The variegated gene expression pattern of *URA3-GFP* in this strain was confirmed by fluorescence microscopy in pre-FACS cells (Fig. 4B). For FACS, exponentially growing cells were fixed using formaldehyde, and GFP-positive and GFP-negative cells were separated and confirmed by microscopy and qRT-PCR (Fig. 4C,D). Approximately 1 million sorted cells were used for ChIP analysis per protein or histone modification tested. As shown in Figure 4E, Rap1 bound well at *URA3-GFP-TEL07L* in both ON and OFF cells. Importantly, we observed a significant amount of Sir3 binding in the ON cells as well as the OFF cells (Fig. 4F). The slight drop in the absolute level of Sir3 binding at the ON telomere was likely due to

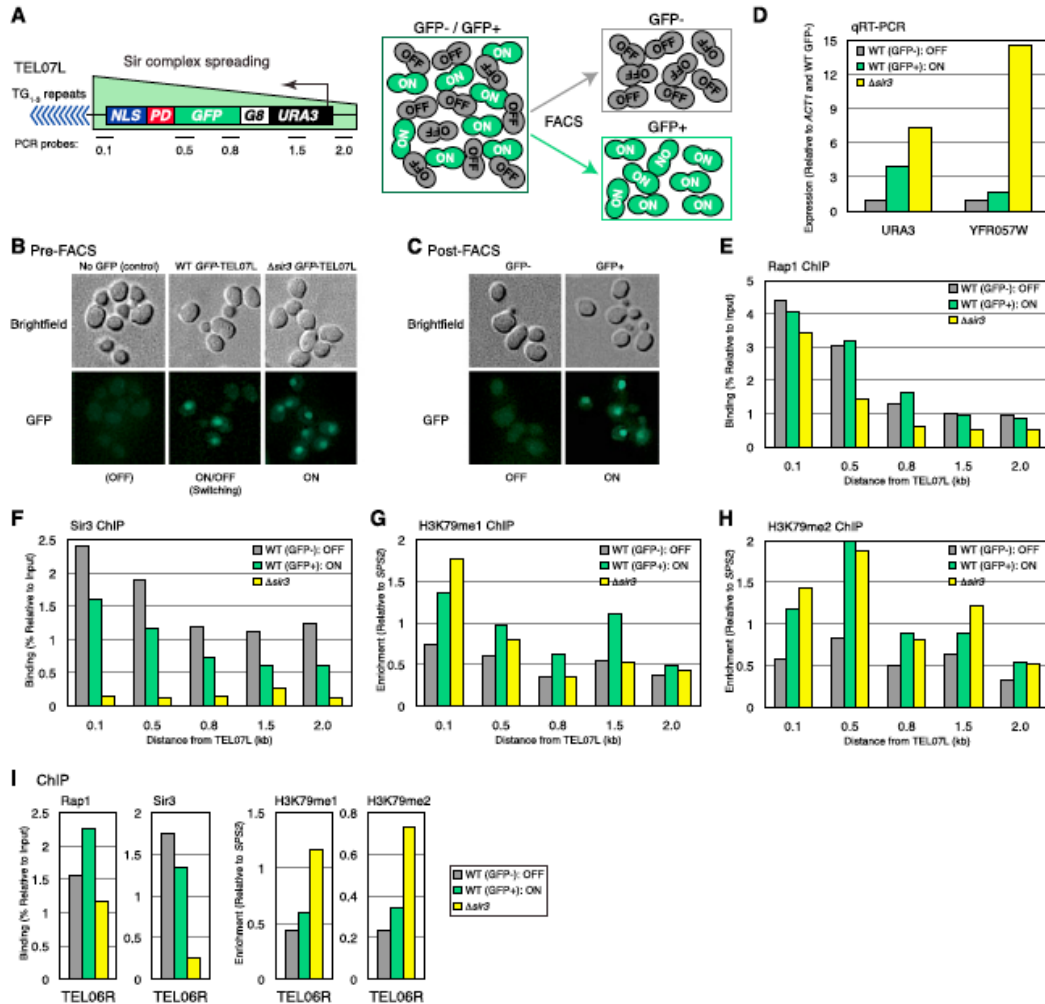


Figure 4. FACS-ChIP of *URA3-GFP-TEL07L* confirms that the ON and OFF states are differentiated by H3K79me. (A) Schematic of the FACS approach to isolate ON and OFF cells. *URA3* regulated under its native promoter was fused to a G8 linker followed by yeast-enhanced *GFP1*, a *CLN2* PD, and a NLS from SV40. Probes were ~0.1, 0.5, 0.8, 1.5, and 2.0 kb away from the telomeric repeats of *URA3-G8-GFP-PD-NLS-TEL07L*. (B,C) Representative bright-field and fluorescence images of wild-type (WT) *SIR3* and $\Delta sir3$ cells with *URA3-G8-GFP-PD-NLS-TEL07L* along with wild-type *SIR3* cells with native *TEL07L* lacking GFP (negative control) before FACS (B), and GFP⁻ and GFP⁺ wild-type *SIR3* *URA3-G8-GFP-PD-NLS-TEL07L* cells after FACS (C). (D) qRT-PCR of *URA3* at *TEL07L* and *YFR057W* at native *TEL06R* in wild-type *SIR3* GFP⁻ (gray bars) and GFP⁺ (green bars) cells and $\Delta sir3$ cells (yellow bars) grown in SD. Data are a representative result of three biological replicates. (E-H) ChIP of Rap1 (E), Sir3 (F), H3K79me1 (G), and H3K79me2 (H) at *URA3-G8-GFP-PD-NLS-TEL07L*, depicted as in D. (I) ChIP of Rap1, Sir3, H3K79me1, and H3K79me2 at native *TEL06R* using a probe ~0.5 kb away from the telomeric repeats, depicted as in D.

the expected decrease in nucleosome density of a transcriptionally active locus, similar to the ChIP results observed in the medium-selected cells (Supplemental Fig. S2). Finally, H3K79me1 and H3K79me2 were enriched at the ON telomere compared with OFF (Fig. 4G,H). As controls, the binding of Rap1 and Sir3 and the enrichment of H3K79me1 and H3K79me2 at native *TEL06R*, which lacks integrated *URA3*, are shown in Figure 4I. We found very little change in any of these components at native *TEL06R* in the *URA3* ON and OFF cells. Therefore, our FACS-ChIP data are consistent with

the medium selection ChIP results above showing that Rap1, Sir3, H3K79me1, and H3K79me2 are enriched at the ON telomere of *URA3-TEL07L*.

H3K79me disrupts gene silencing without affecting Sir complex binding in vitro

The methylation of histones has previously been implicated in disrupting gene silencing (van Leeuwen et al. 2002; Santos-Rosa et al. 2004; Altaf et al. 2007; Fingerman et al. 2007; Onishi et al. 2007; Tompa and Madhani 2007;

Martino et al. 2009; Verzijlbergen et al. 2009). However, since histone methylation, particularly H3K4me and H3K36me, generally correlates with transcription in yeast (Millar and Grunstein 2006), it was possible that the enrichment of some of these methylation marks was merely a consequence of, rather than the cause for, the ON state of TPE. Therefore, we sought to distinguish the function of these modifications and test directly whether they would be sufficient to disrupt Sir complex-mediated silencing using a yeast in vitro transcription (IVT) system (Fig. 5A,B).

In this system, we used a DNA template containing Gal4 DNA-binding sites and a TATA box (Fig. 5; Tantin et al. 1996). This template was previously shown to be highly responsive to activator GAL4-VP16 derivatives in a yeast nuclear extract (Ohashi et al. 1994). We assembled the template into chromatin using either unmodified histone octamers or octamers containing H3K4me3, H3K36me3, or H3K79me2. Methylated histones were generated using the methyl-lysine analog (MLA) technique (Simon et al. 2007) and validated by Western blot (Fig. 5C) and mass spectrometry (data not shown). GAL4-VP16

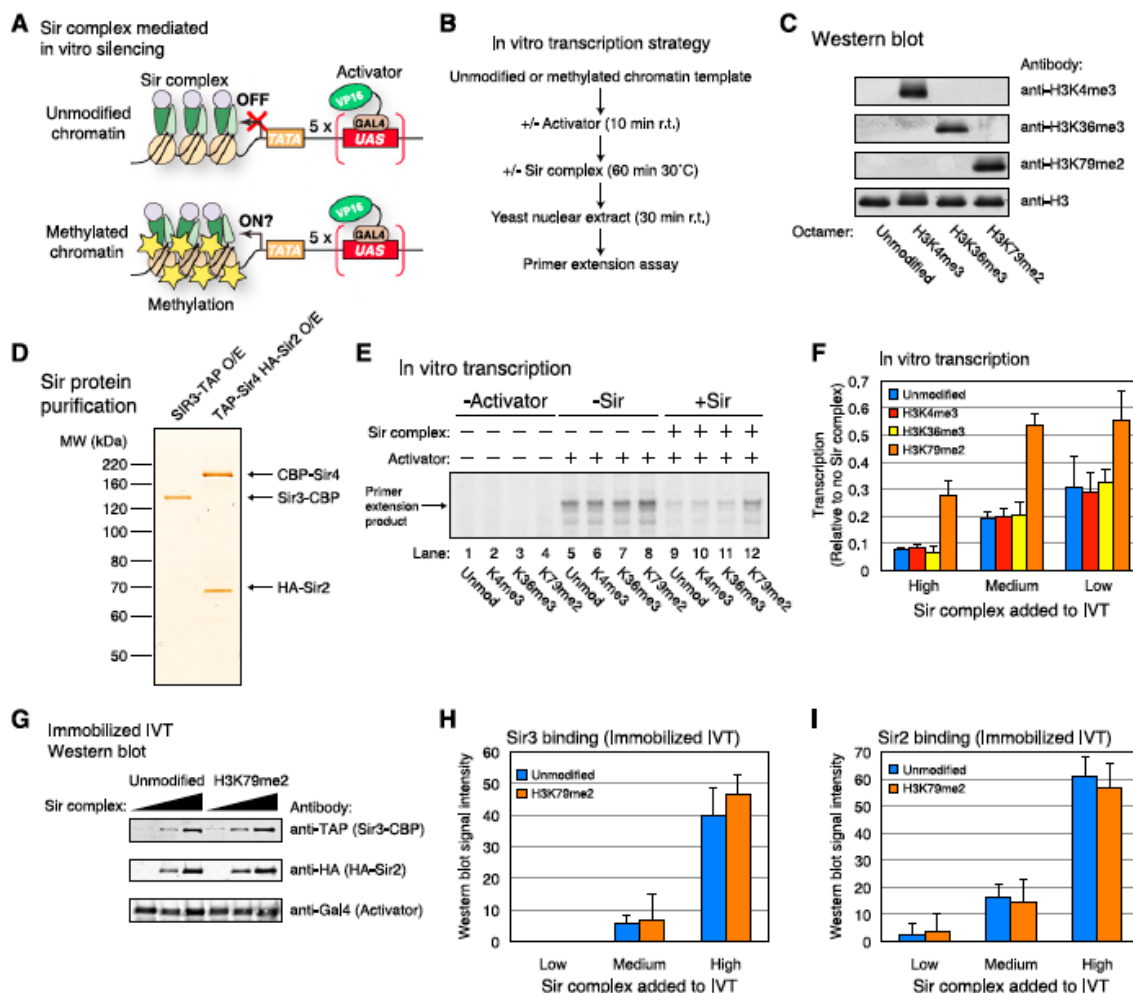


Figure 5. H3K79me disrupts gene silencing without affecting Sir complex binding in vitro. (A) Schematic of the chromatin template and protein components involved in the in vitro silencing assay. (B) Outline of the in vitro silencing experiment. (C) Western blot of the MLA nucleosomes used for chromatin assembly. Anti-H3K4me3, anti-H3K36me3, anti-H3K79me2, and anti-H3 antibodies were used. (D) Silver-staining gel of the Sir proteins purified from yeast cells overexpressing Sir3-TAP or TAP-Sir4/HA-Sir2. (E) Representative phosphor screen image of a primer extension assay from the IVT experiment outlined in B. The signal represents the ³²P end-labeled cDNA product generated by primer extension. (F) Quantification of phosphor screen images of the IVT experiments shown in E. Approximately 26 pmol of Sir3 and 8 pmol each of Sir2 and Sir4 were included in the reaction labeled “High.” Reactions labeled “Medium” and “Low” contained, respectively, one-half and one-fourth the amount of Sir proteins relative to “High.” Data are presented as mean ± SD. (G) Representative image of Sir protein binding from the immobilized IVT Western blot experiment. Anti-TAP, anti-HA, and anti-Gal4 antibodies were used. (H,I) Quantification of the immobilized IVT Western blot experiment shown in G. The binding levels of Sir3 (H) and Sir2 (I) are presented as mean ± SD.

was first prebound to the chromatinized templates, and purified Sir proteins (Sir2/Sir3/Sir4), sufficient for silencing *in vitro* (Johnson et al. 2009), were added to the reactions. Sir proteins (Sir3-TAP and TAP-Sir4/HA-Sir2) were purified using a yeast overexpression system described previously by Moazed and colleagues (Johnson et al. 2009) (Fig. 5D). Yeast nuclear extract was added to the reaction following the binding of Sir proteins to the chromatinized template along with nucleoside triphosphates (NTPs), and transcription was measured by primer extension. An outline of this *in vitro* silencing experiment is depicted in Figure 5B.

As shown in Figure 5E, transcription was strongly dependent on Activator (lanes 1–8) and was reduced by the addition of Sir proteins to the reaction (lanes 5–12). However, strikingly, when the chromatin template was dimethylated at H3K79, silencing was strongly reduced compared with the template with no modifications (Fig. 5E, lanes 9–12). This effect was specific to H3K79me₂, as neither H3K4me₃ nor H3K36me₃ was able to disrupt silencing (Fig. 5E, lanes 9–12). Transcription increased by approximately twofold to threefold on the H3K79me₂ chromatin template compared with the unmodified template in the presence of Sir proteins (Fig. 5F). Therefore, since H3K79me is found at subtelomeric chromatin selectively in the ON state and its presence on chromatin is sufficient to disrupt Sir protein-mediated silencing *in vitro*, we conclude that H3K79me plays a causal role in determining the natural epigenetic ON state.

We next sought to assess the amount of Sir protein binding to the unmodified and H3K79me₂ chromatin templates during IVT. To accomplish this, we performed an IVT reaction in a manner similar to that used above but with biotinylated unmodified and H3K79me₂ chromatin templates immobilized to streptavidin-coated magnetic beads (Lin and Carey 2012). The amount of Sir protein binding to the immobilized templates was determined by Western blot following IVT and washing (Fig. 5G). Critically, as quantified in Figure 5, H and I, binding of Sir3 and Sir2 did not differ between the unmodified and H3K79me₂ templates. Similarly, we did not observe a significant difference in the binding of the Sir complex to the unmodified and H3K79me₂ chromatin templates when the Sir complex–chromatin interaction was measured in the absence of Activator or yeast nuclear extract (Supplemental Fig. S5). We conclude that H3K79me₂ can disrupt gene silencing without noticeably affecting the amount of binding of the Sir complex to nucleosomes *in vitro*.

The discrepancy between our results and those of a previous study in which H3K79me had been shown to block Sir complex binding to a chromatin template *in vitro* (Martino et al. 2009) may be due to differences in the experimental techniques used. While the previous study had used electrophoretic mobility shift assays (EMSAs) to determine the Sir complex–chromatin interaction (Martino et al. 2009), here we used an immobilized chromatin template assay to directly measure Sir protein binding by Western blot and showed that the amount of Sir complex bound to chromatin was largely

not affected by H3K79me. In either case, methylation of H3K79 may disrupt the interaction between Sir3 and the region surrounding H3K79 (Altaf et al. 2007; Fingerman et al. 2007). We propose that this disruption alters the overall conformation of the Sir2/Sir3/Sir4–nucleosome complex and that this alteration in turn enables the epigenetic ON state.

Maintenance of H3K79me is dependent on transcription in the epigenetic ON state

As demonstrated above, the key difference between ON and OFF telomeres is the enrichment of H3K79me, which is capable of disrupting gene silencing. We next addressed how H3K79me is maintained epigenetically through multiple cell generations at the ON telomere. Since the H3K79 methyltransferase Dot1 is recruited to chromatin through transcription (Shahbazian et al. 2005; Millar and Grunstein 2006), we hypothesized that the maintenance of H3K79me in the ON state may be dependent on transcription. To test this possibility, we asked whether H3K79me at the ON telomere would be lost upon inhibition of transcription. We monitored the chromatin state of *ADE2*-TEL05R, whose ON state could be selected by growing cells in medium lacking adenine (SC–ade). As a control, we examined *YFR057W* at native TEL06R. Similar to the ON state of *URA3*-TEL07L, the *ADE2*-TEL05R ON state was accompanied by an increase in H3K79me (Supplemental Fig. S6). After selecting for *ADE2*-TEL05R ON by growing cells in SC–ade, we specifically repressed *ADE2* through negative feedback by adding excess adenine to the medium. This treatment causes the dissociation of the activator Pho2 from the promoter of *ADE2* (Fig. 6A; Pinson et al. 2009). The same method cannot be used for repression of *URA3*-TEL07L, since adding excess uracil to the medium would be toxic to the cells (Gadsden et al. 1993). As shown in Figure 6, B and C, by qRT–PCR and RNAPII ChIP, *ADE2* expression decreased rapidly to near-background level following adenine addition. In a corresponding manner, we found that H3K79me₁ is gradually lost every cell cycle and eventually drops to near-background level (Fig. 6D; Supplemental Fig. S6). These results imply that a self-reinforcing feedback loop in which H3K79me both results from and is causal for transcription maintains the epigenetic ON state of TPE.

Discussion

The mechanism of heterochromatin spreading and gene silencing at the telomeres of *Saccharomyces cerevisiae* has been characterized extensively (Rusche et al. 2003; Mondoux and Zakian 2006). However, how variegated gene expression occurs at telomeres has been unclear. To address this problem, we separated the natural ON and OFF cells from a population of yeast undergoing TPE and directly compared the chromatin structure of the natural ON state with that of the OFF state. This is unlike previous studies in which mixed ON and OFF telomeres were compared with the disrupted telomeres of *sir*

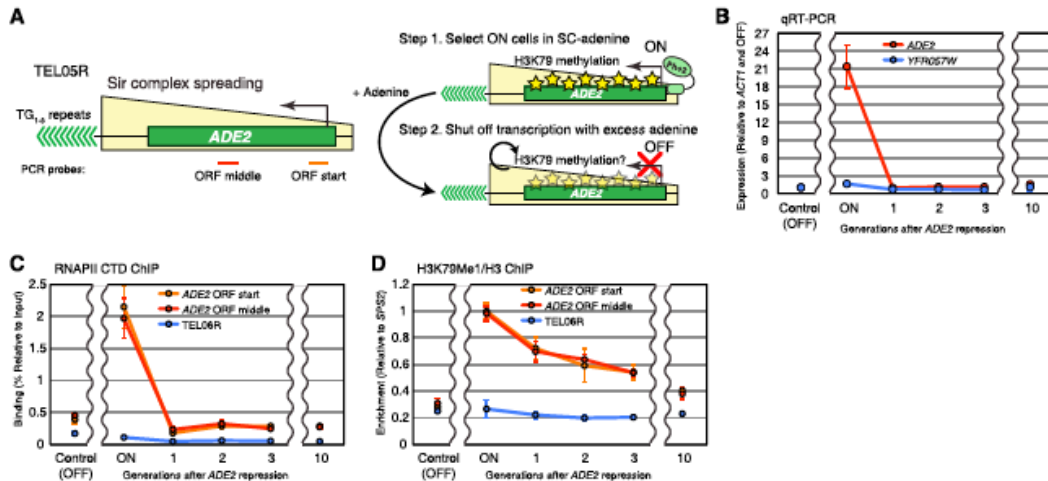


Figure 6. Maintenance of H3K79me at the ON telomere depends on transcription. (A) Schematic of the *ADE2* feedback repression experiment to monitor the level of histone methylation after inhibition of transcription. The *ADE2* ORF middle and ORF start probes are ~1.0 and 2.0 kb away, respectively, from the telomeric repeats of *ADE2*-TEL05R. (B) qRT-PCR of *ADE2* at TEL05R (red lines) and *YFR057W* at native TEL06R (blue lines) before and after the addition of adenine. A culture continuously grown in the presence of excess adenine (>30 generations) was used as an OFF control. Data are presented as mean \pm SD. (C, D) ChIP of RNAPII (C) and H3K79me1/H3 (D) at *ADE2*-TEL05R and native TEL06R using the cultures described in B. The *ADE2* ORF middle (red lines) and ORF start (orange lines) probes were as described in A. The native TEL06R (blue lines) probe is ~1.5 kb away from the telomeric repeats. Data are presented as mean \pm SD.

mutant strains, which made it impossible to characterize the natural ON state (Rusche et al. 2003). Our findings indicate that (1) the natural ON telomere is characterized by Sir complex binding to nucleosomes; (2) histone H4K16 is deacetylated at the ON telomere, which is consistent with the spreading of Sir3 through telomeric heterochromatin by its interaction with deacetylated H4K16; (3) H3K79 is methylated in the natural ON state and can disrupt silencing without affecting Sir complex binding *in vitro*; and (4) maintenance of H3K79me is dependent on a transcription-mediated positive feedback loop. Our results suggest that, since the ON telomere is characterized by Sir3 binding and H4K16 hypoacetylation, two factors that are normally associated with silencing, other factors must determine the ON state. We show that H3K79me is such a factor. This is in contrast to previous studies, which proposed that the variation in Sir complex binding to nucleosomes regulates TPE (Ng et al. 2003; Moazed 2011).

The deacetylation of H4K16, a major requirement of heterochromatin formation, in the ON state is of special interest. It argues that H4K16ac is not the determinant of epigenetic variegation. Thus, our study differentiates the function of two key histone modification marks at heterochromatin, where H4K16 deacetylation determines the distance of heterochromatin protein spreading from the telomere by virtue of its interaction with Sir3 (Johnson et al. 1990, 2009; Kimura et al. 2002; Suka et al. 2002; Liou et al. 2005; Onishi et al. 2007), and H3K79me regulates the actual ON/OFF expression state of a subtelomeric gene.

It had been proposed previously that H3K79me may disrupt the binding of the Sir complex to nucleosomes

based on pull-down assays that measured the binding of the Sir3 protein to a peptide containing the H3K79 region (Altaf et al. 2007; Fingerman et al. 2007). Subsequently, it had been shown that binding of the whole Sir complex to a trinucleosomal chromatin template is also affected by H3K79me using a gel shift assay (Martino et al. 2009). However, we showed *in vivo* by ChIP and *in vitro* using an immobilized template assay in the presence of yeast nuclear extract that the overall binding level of the Sir proteins to the nucleosome was not significantly disrupted by H3K79me. Therefore, we favor instead a model in which the methylation-dependent loss of the Sir3-H3K79 interaction leads to a conformational change in the structure of the Sir protein-nucleosome complex, which results in disrupted gene silencing.

H3K79me and its methyltransferase, Dot1, are conserved in many organisms, including fruit flies, mice, and humans (Nguyen and Zhang 2011). It has been shown that mutations in the fruit fly *DOT1* homolog *grappa* disrupts Polycomb group-mediated silencing as well as telomeric silencing in flies (Shanower et al. 2005). Similarly, knockout of the mouse *DOT1* homolog *Dot1L* leads to the loss of heterochromatin-associated marks such as H3K9me from centromeric and telomeric heterochromatin in mouse embryonic stem (ES) cells (Jones et al. 2008). Thus, H3K79me and Dot1 are relevant to gene silencing and heterochromatin formation in organisms other than the budding yeast.

In contrast, there are no homologs of Dot1 or detectable levels of H3K79me in the fission yeast *Schizosaccharomyces pombe* (Sinha et al. 2010). Thus, while gene expression at the heterochromatin of *S. pombe* is also known to be

regulated epigenetically, the mechanism inevitably cannot involve H3K79me. Allshire and colleagues (Ekwall et al. 1997) have shown that transient treatment of *S. pombe* cells with an HDAC inhibitor leads to a heritable hyperacetylated chromatin state accompanied by the loss of gene silencing at centromeric heterochromatin. Likewise, Grewal and colleagues (Nakayama et al. 2000) have shown that expression of a gene at the partially compromised centromeric heterochromatin of *S. pombe* is associated with hyperacetylation and lack of heterochromatin protein Swi6/HP1 binding. The epigenetic inheritance of gene expression in these studies could be explained by a positive feedback loop involving histone acetylation and lack of heterochromatin-binding proteins. This is in stark contrast to our findings at the telomeric heterochromatin of *S. cerevisiae*, which show that neither H4K16ac nor binding of heterochromatin proteins is a key regulator of gene variegation.

Instead, a positive feedback loop mediated by transcription and H3K79me is at the heart of our model regarding the mechanism of epigenetic variegation at *S. cerevisiae* telomeres, as described below (Fig. 7). In this model, the ON state is characterized by H3K79me. The maintenance of H3K79me is dependent on transcription, which had previously been shown to recruit the histone H3 Lys79 methyltransferase Dot1 (Shahbazian et al. 2005). H3K79me in turn disrupts the local interaction between Sir3 and the H3 core region surrounding Lys79 (Altaf et al. 2007; Fingermaier et al. 2007). However, in contrast to previous models, the Sir complex as a whole can still spread along the subtelomere through its interaction with deacetylated H4K16. In this structure, the methylation of H3K79 enables PIC assembly and transcription, possibly by inducing a conformational change in the Sir protein-nucleosome complex, thus promoting a positive feedback loop. The possible absence of an H3K79 histone demethylase (Liang et al. 2007) may further enhance the stability of this continuous ON state. In contrast, the absence of transcription in the OFF state precludes Dot1 recruitment and ensures H3K79 hypomethylation. It had previously been shown that Sir3 binding to nucleosomes can prevent Dot1 from methylating chromatin (Altaf et al. 2007; Fingermaier et al. 2007). Therefore, the lack of Dot1

recruitment and the prevention of Dot1 access to the H3K79 residue help establish a stable OFF state.

How is it then possible for a gene in one expression state to escape these feedback loops and convert to the other state? One possibility may be that changes in the length of telomeres (elongation/shortening) lead to the interconversion of epigenetic expression states. Previous studies from Lustig and colleagues (Kyriou et al. 1993; Park and Lustig 2000) have shown that elongated telomeres are associated with stronger subtelomeric gene silencing. Since the length of telomeres naturally fluctuates within a cell (Shore and Bianchi 2009), some telomeres may become abnormally shortened, and this may lead to a compromised heterochromatin structure susceptible to transcription. In contrast, abnormal lengthening may cause a structural change at an ON telomere that can overcome the anti-silencing effect of H3K79me and dampen gene expression until methylation is passively lost. In any case, whether the natural variation in telomere length is sufficient to induce epigenetic switching is still unknown. Changes in H3K79me are shown here to regulate the maintenance of the variegated ON/OFF expression states at telomeric heterochromatin. However, the rare transient upstream events that initiate switching between the ON and OFF states remain to be observed and determined.

Materials and methods

Yeast strains, plasmids, and oligonucleotide probes

Yeast strains, plasmids, and oligonucleotide probes used in this study are listed in the Supplemental Material. Plasmid and PCR product-based genetic manipulations were performed using standard yeast transformation techniques (Gietz and Woods 2002). Full details are provided in the Supplemental Material.

Protein purification

Xenopus laevis histones and histone mutants (H3, H3C110AK4C, H3C110AK36C, H3C110AK79C, H4, H2A, and H2B) were purified as described previously (Luger et al. 1997). GAL4-VP16 was purified as described previously (Tantin et al. 1996). Sir proteins were purified as described previously (Tanny et al. 2004; Johnson et al. 2009) with some modifications to the protocol. Full details are provided in the Supplemental Material.

MLA histone preparation

H3K4me3, H3K36me3, and H3K79me2 MLA histones were generated from H3C110AK4C, H3C110AK36C, and H3C110AK79C histone mutants, respectively, as described previously (Simon et al. 2007).

qRT-PCR

RNA was extracted using the hot acid phenol extraction method (Bookout et al. 2006). The extracted RNA samples were treated with DNase I (Qiagen), purified, and reverse-transcribed using random primers and M-MLV reverse transcriptase (Invitrogen). qPCR was performed and analyzed using the $\Delta\Delta C_t$ method (Bookout et al. 2006). Full details are provided in the Supplemental Material.

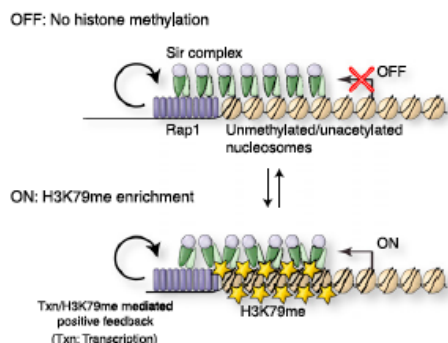


Figure 7. Model to explain the variegated gene expression pattern of TPE. See the text for details.

Western blot

Western blot assays were performed using the ODYSSEY infrared imaging system (LI-COR) following the manufacturer's protocol. Full details are provided in the Supplemental Material.

ChIP

Standard ChIP assays were performed as described previously (Hecht et al. 1996; Suka et al. 2001) with minor modifications to the protocol. Full details are provided in the Supplemental Material.

Sequential ChIP

Sequential ChIP was performed as described elsewhere (Kao et al. 2004) with minor modifications to the protocol. Briefly, chromatin lysate was immunoprecipitated overnight with anti-Flag M2 agarose beads (Sigma-Aldrich). The agarose beads were washed, and the chromatin fragments were eluted off the beads with 3x Flag peptide (Sigma-Aldrich). Part of the eluate was saved and used as the input control DNA for the second (sequential) ChIP. Sequential ChIP assays were performed using the same protocol as standard ChIP. Full details are provided in the Supplemental Material.

FACS-ChIP

FACS was performed using BD FACSAria II (BD Biosciences) according to the manufacturer's manual. Full details are provided in the Supplemental Material.

IVT/silencing

IVT was performed as described previously (Lin and Carey 2012) with minor modifications to the protocol. The DNA template containing five Gal4 DNA-binding sites and an adenovirus E4 promoter (GSE4T) (Tantin et al. 1996) was assembled into chromatin by salt dilution as described previously (Steger et al. 1997). Following prebinding of GAL4-VP16 to the template, Sir proteins were added to the IVT reaction. Yeast nuclear extract, prepared as described previously (Rani et al. 2004), was added to the reaction, and primer extension was performed to measure the amount of transcription. Full details are provided in the Supplemental Material.

Immobilized chromatin template

The immobilized chromatin template assays were performed essentially as described previously (Lin and Carey 2012) with some modifications to the protocol. Buffer conditions and DNA/protein components were as described above for the IVT/silencing experiments except that GAL4-VP4, a variant of GAL4-VP16 containing four tandem repeats of the activation domain, was used (Ohashi et al. 1994). We confirmed that the results of the IVT/silencing experiments described above were reproducible when GAL4-VP4 was substituted for GAL4-VP16 in the reaction (data not shown). Briefly, biotinylated chromatin templates were immobilized on M280 streptavidin beads, and IVT reactions were incubated by rotation. The beads were washed twice with reaction buffer and eluted with Laemmli buffer. Western blot was performed as described above and quantified using ImageQuant TL software.

Acknowledgments

We thank the present and past members of the laboratories of M.G., M.C. (especially Lynn Lehmann for GAL4-VP16, Justin Lin

for H3K4me3 octamer, and Jason Gehrke), and Siavash Kurdastani (especially Maria Vogelauer) for providing materials, valuable suggestions, and constructive criticisms during the course of this work. We also thank Daniel Gottschling, James Broach, Danesh Moazed, and Ivan Sadowski for plasmids, strains, and antibodies; Aaron Johnson for sharing his TAP-Sir4/HA-Sir2 purification protocol; Rachele Crosbie for sharing her fluorescence microscope; and Jamie Marshall for microscopy advice. Flow cytometry was performed in the UCLA Jonsson Comprehensive Cancer Center (JCCC) and Center for AIDS Research Flow Cytometry Core Facility, which is supported by National Institutes of Health awards CA-16042 and AI-28697 and by the JCCC, the UCLA AIDS Institute, the David Geffen School of Medicine at UCLA, and the UCLA Chancellor's Office. T.K. was supported by a fellowship from the Nakajima Foundation. B.G.K. was supported by Ruth L. Kirschstein National Research Service Award GM007185. This work was supported by National Institutes of Health grants GM23674, GM42421 (to M.G.), GM074701, and GM085002 (to M.C.).

References

- Altaf M, Utley RT, Lacoste N, Tan S, Briggs SD, Cote J. 2007. Interplay of chromatin modifiers on a short basic patch of histone H4 tail defines the boundary of telomeric heterochromatin. *Mol Cell* **28**: 1002–1014.
- Armache KJ, Garlick JD, Canzio D, Narlikar GJ, Kingston RE. 2011. Structural basis of silencing: Sir3 BAH domain in complex with a nucleosome at 3.0 Å resolution. *Science* **334**: 977–982.
- Boeke JD, Trueheart J, Natsoulis G, Fink GR. 1987. 5-Fluoroorotic acid as a selective agent in yeast molecular genetics. *Methods Enzymol* **154**: 164–175.
- Bookout AL, Cummins CL, Mangelsdorf DJ, Pesola JM, Kramer MF. 2006. High-throughput real-time quantitative reverse transcription PCR. *Curr Protoc Mol Biol* **73**: 15.8.1–15.8.28.
- Buchman AR, Kimmerly WJ, Rine J, Kornberg RD. 1988. Two DNA-binding factors recognize specific sequences at silencers, upstream activating sequences, autonomously replicating sequences, and telomeres in *Saccharomyces cerevisiae*. *Mol Cell Biol* **8**: 210–225.
- Chen L, Widom J. 2005. Mechanism of transcriptional silencing in yeast. *Cell* **120**: 37–48.
- Ehrentraut S, Hassler M, Oppikofer M, Kueng S, Weber JM, Mueller JW, Gasser SM, Ladurner AG, Ehrenhofer-Murray AE. 2011. Structural basis for the role of the Sir3 AAA⁺ domain in silencing: Interaction with Sir4 and unmethylated histone H3K79. *Genes Dev* **25**: 1835–1846.
- Ekwall K, Olsson T, Turner BM, Cranston G, Allshire RC. 1997. Transient inhibition of histone deacetylation alters the structural and functional imprint at fission yeast centromeres. *Cell* **91**: 1021–1032.
- Fingerman IM, Li HC, Briggs SD. 2007. A charge-based interaction between histone H4 and Dot1 is required for H3K79 methylation and telomere silencing: Identification of a new *trans*-histone pathway. *Genes Dev* **21**: 2018–2029.
- Frederiks F, Tzouros M, Oudgenoeg G, van Welsem T, Fornerod M, Krijgsveld J, van Leeuwen F. 2008. Nonprocessive methylation by Dot1 leads to functional redundancy of histone H3K79 methylation states. *Nat Struct Mol Biol* **15**: 550–557.
- Gadsden MH, McIntosh EM, Game JC, Wilson PJ, Haynes RH. 1993. dUTP pyrophosphatase is an essential enzyme in *Saccharomyces cerevisiae*. *EMBO J* **12**: 4425–4431.
- Gao L, Gross DS. 2008. Sir2 silences gene transcription by targeting the transition between RNA polymerase II initiation and elongation. *Mol Cell Biol* **28**: 3979–3994.

- Gietz RD, Woods RA. 2002. Transformation of yeast by lithium acetate/single-stranded carrier DNA/polyethylene glycol method. *Methods Enzymol* **350**: 87–96.
- Girton JR, Johansen KM. 2008. Chromatin structure and the regulation of gene expression: The lessons of PEV in *Drosophila*. *Adv Genet* **61**: 1–43.
- Gottschling DE, Aparicio OM, Billington BL, Zakian VA. 1990. Position effect at *S. cerevisiae* telomeres: Reversible repression of Pol II transcription. *Cell* **63**: 751–762.
- Hahn S. 2004. Structure and mechanism of the RNA polymerase II transcription machinery. *Nat Struct Mol Biol* **11**: 394–403.
- Hecht A, Strahl-Bolsinger S, Grunstein M. 1996. Spreading of transcriptional repressor SIR3 from telomeric heterochromatin. *Nature* **383**: 92–96.
- Hoppe GJ, Tanny JC, Rudner AD, Gerber SA, Danaie S, Gygi SP, Moazed D. 2002. Steps in assembly of silent chromatin in yeast: Sir3-independent binding of a Sir2/Sir4 complex to silencers and role for Sir2-dependent deacetylation. *Mol Cell Biol* **22**: 4167–4180.
- Imai S, Armstrong CM, Kaeberlein M, Guarente L. 2000. Transcriptional silencing and longevity protein Sir2 is an NAD-dependent histone deacetylase. *Nature* **403**: 795–800.
- Johnson LM, Kayne PS, Kahn ES, Grunstein M. 1990. Genetic evidence for an interaction between SIR3 and histone H4 in the repression of the silent mating loci in *Saccharomyces cerevisiae*. *Proc Natl Acad Sci* **87**: 6286–6290.
- Johnson A, Li G, Sikorski TW, Buratowski S, Woodcock CL, Moazed D. 2009. Reconstitution of heterochromatin-dependent transcriptional gene silencing. *Mol Cell* **35**: 769–781.
- Jones B, Su H, Bhat A, Lei H, Bajko J, Hevi S, Baltus G, Kadam S, Zhai H, Valdez R, et al. 2008. The histone H3K79 methyltransferase Dot1L is essential for mammalian development and heterochromatin structure. *PLoS Genet* **4**: e1000190. doi: 10.1371/journal.pgen.1000190.
- Kao CF, Hillyer C, Tsukuda T, Henry K, Berger S, Osley MA. 2004. Rad6 plays a role in transcriptional activation through ubiquitylation of histone H2B. *Genes Dev* **18**: 184–195.
- Katan-Khaykovich Y, Struhl K. 2005. Heterochromatin formation involves changes in histone modifications over multiple cell generations. *EMBO J* **24**: 2138–2149.
- Kimura A, Umehara T, Horikoshi M. 2002. Chromosomal gradient of histone acetylation established by Sas2p and Sir2p functions as a shield against gene silencing. *Nat Genet* **32**: 370–377.
- Kirchmaier AL, Rine J. 2006. Cell cycle requirements in assembling silent chromatin in *Saccharomyces cerevisiae*. *Mol Cell Biol* **26**: 852–862.
- Klein F, Laroche T, Cardenas ME, Hofmann JF, Schweizer D, Gasser SM. 1992. Localization of RAP1 and topoisomerase II in nuclei and meiotic chromosomes of yeast. *J Biol Chem* **267**: 935–948.
- Kostrewa D, Zeller ME, Armache KJ, Seizl M, Leike K, Thomm M, Cramer P. 2009. RNA polymerase II-TFIIB structure and mechanism of transcription initiation. *Nature* **462**: 323–330.
- Kyrion G, Liu K, Liu C, Lustig AJ. 1993. RAP1 and telomere structure regulate telomere position effects in *Saccharomyces cerevisiae*. *Genes Dev* **7**: 1146–1159.
- Landry J, Slama JT, Sternglanz R. 2000. Role of NAD⁺ in the deacetylase activity of the SIR2-like proteins. *Biochem Biophys Res Commun* **278**: 685–690.
- Li B, Lustig AJ. 1996. A novel mechanism for telomere size control in *Saccharomyces cerevisiae*. *Genes Dev* **10**: 1310–1326.
- Liang G, Klose RJ, Gardner KE, Zhang Y. 2007. Yeast Jhd2p is a histone H3 Lys4 trimethyl demethylase. *Nat Struct Mol Biol* **14**: 243–245.
- Lin JJ, Carey M. 2012. In vitro transcription and immobilized template analysis of preinitiation complexes. *Curr Protoc Mol Biol* **97**: 12.14.1–12.14.19.
- Liou GG, Tanny JC, Kruger RG, Walz T, Moazed D. 2005. Assembly of the SIR complex and its regulation by O-acetyl-ADP-ribose, a product of NAD-dependent histone deacetylation. *Cell* **121**: 515–527.
- Luger K, Rechsteiner TJ, Flaus AJ, Wayne MM, Richmond TJ. 1997. Characterization of nucleosome core particles containing histone proteins made in bacteria. *J Mol Biol* **272**: 301–311.
- Luo K, Vega-Palas MA, Grunstein M. 2002. Rap1–Sir4 binding independent of other Sir, yKu, or histone interactions initiates the assembly of telomeric heterochromatin in yeast. *Genes Dev* **16**: 1528–1539.
- Madhani HD. 2007. *From a to α: Yeast as a model for cellular differentiation*. Cold Spring Harbor Laboratory Press, Cold Spring Harbor, NY.
- Martino F, Kueng S, Robinson P, Tsai-Pflugfelder M, van Leeuwen F, Ziegler M, Cubizolles F, Cockell MM, Rhodes D, Gasser SM. 2009. Reconstitution of yeast silent chromatin: Multiple contact sites and O-AADPR binding load SIR complexes onto nucleosomes in vitro. *Mol Cell* **33**: 323–334.
- Meneghini MD, Wu M, Madhani HD. 2003. Conserved histone variant H2A.Z protects euchromatin from the ectopic spread of silent heterochromatin. *Cell* **112**: 725–736.
- Millar CB, Grunstein M. 2006. Genome-wide patterns of histone modifications in yeast. *Nat Rev Mol Cell Biol* **7**: 657–666.
- Mishra K, Shore D. 1999. Yeast Ku protein plays a direct role in telomeric silencing and counteracts inhibition by rif proteins. *Curr Biol* **9**: 1123–1126.
- Moazed D. 2011. Mechanisms for the inheritance of chromatin States. *Cell* **146**: 510–518.
- Moazed D, Kistler A, Axelrod A, Rine J, Johnson AD. 1997. Silent information regulator protein complexes in *Saccharomyces cerevisiae*: A SIR2/SIR4 complex and evidence for a regulatory domain in SIR4 that inhibits its interaction with SIR3. *Proc Natl Acad Sci* **94**: 2186–2191.
- Mondoux MA, Zakian VA. 2006. Telomere position effect: Silencing near the end. In *Telomeres*, Cold Spring Harbor Monograph Series 45 (ed. T de Lange et al.), pp. 261–316. Cold Spring Harbor Laboratory Press, Cold Spring Harbor, NY.
- Moretti P, Freeman K, Coodly L, Shore D. 1994. Evidence that a complex of SIR proteins interacts with the silencer and telomere-binding protein RAP1. *Genes Dev* **8**: 2257–2269.
- Nakayama J, Klar AJ, Grewal SI. 2000. A chromodomain protein, Swi6, performs imprinting functions in fission yeast during mitosis and meiosis. *Cell* **101**: 307–317.
- Ng HH, Feng Q, Wang H, Erdjument-Bromage H, Tempst P, Zhang Y, Struhl K. 2002. Lysine methylation within the globular domain of histone H3 by Dot1 is important for telomeric silencing and Sir protein association. *Genes Dev* **16**: 1518–1527.
- Ng HH, Ciccone DN, Morshead KB, Oettinger MA, Struhl K. 2003. Lysine-79 of histone H3 is hypomethylated at silenced loci in yeast and mammalian cells: A potential mechanism for position-effect variegation. *Proc Natl Acad Sci* **100**: 1820–1825.
- Nguyen AT, Zhang Y. 2011. The diverse functions of Dot1 and H3K79 methylation. *Genes Dev* **25**: 1345–1358.
- Ohashi Y, Brickman JM, Furman E, Middleton B, Carey M. 1994. Modulating the potency of an activator in a yeast in vitro transcription system. *Mol Cell Biol* **14**: 2731–2739.

- Onishi M, Liou GG, Buchberger JR, Walz T, Moazed D. 2007. Role of the conserved Sir3-BAH domain in nucleosome binding and silent chromatin assembly. *Mol Cell* **28**: 1015–1028.
- Osborne EA, Dudoit S, Rine J. 2009. The establishment of gene silencing at single-cell resolution. *Nat Genet* **41**: 800–806.
- Park Y, Lustig AJ. 2000. Telomere structure regulates the heritability of repressed subtelomeric chromatin in *Saccharomyces cerevisiae*. *Genetics* **154**: 587–598.
- Pinson B, Vaur S, Sagot I, Coulpier F, Lemoine S, Daignan-Fornier B. 2009. Metabolic intermediates selectively stimulate transcription factor interaction and modulate phosphate and purine pathways. *Genes Dev* **23**: 1399–1407.
- Pokholok DK, Harbison CT, Levine S, Cole M, Hannett NM, Lee TI, Bell GW, Walker K, Rolfe PA, Herbolsheimer E, et al. 2005. Genome-wide map of nucleosome acetylation and methylation in yeast. *Cell* **122**: 517–527.
- Ptashne M. 2002. *Genes & signals*. CSHL Press, Cold Spring Harbor, NY.
- Rani PG, Ranish JA, Hahn S. 2004. RNA polymerase II (Pol II)-TFIIIF and Pol II-mediator complexes: The major stable Pol II complexes and their activity in transcription initiation and reinitiation. *Mol Cell Biol* **24**: 1709–1720.
- Riggs AD, Martienssen RA, Russo VEA. 1996. Introduction. In *Epigenetic mechanisms of gene regulation*, Cold Spring Harbor Monograph Series 32 [ed. VEA Russo et al.], pp. 1–4. Cold Spring Harbor Laboratory Press, Cold Spring Harbor, NY.
- Rossmann MP, Luo W, Tsaponina O, Chabes A, Stillman B. 2011. A common telomeric gene silencing assay is affected by nucleotide metabolism. *Mol Cell* **42**: 127–136.
- Rusche LN, Kirchmaier AL, Rine J. 2003. The establishment, inheritance, and function of silenced chromatin in *Saccharomyces cerevisiae*. *Annu Rev Biochem* **72**: 481–516.
- Sabourin M, Tuzon CT, Fisher TS, Zakian VA. 2007. A flexible protein linker improves the function of epitope-tagged proteins in *Saccharomyces cerevisiae*. *Yeast* **24**: 39–45.
- Santos-Rosa H, Bannister AJ, Dehe PM, Geli V, Kouzarides T. 2004. Methylation of H3 lysine 4 at euchromatin promotes Sir3p association with heterochromatin. *J Biol Chem* **279**: 47506–47512.
- Sekinger EA, Gross DS. 2001. Silenced chromatin is permissive to activator binding and PIC recruitment. *Cell* **105**: 403–414.
- Shahbazian MD, Zhang K, Grunstein M. 2005. Histone H2B ubiquitylation controls processive methylation but not monomethylation by Dot1 and Set1. *Mol Cell* **19**: 271–277.
- Shanower GA, Muller M, Blanton JL, Honti V, Gyurkovics H, Schedl P. 2005. Characterization of the grappa gene, the *Drosophila* histone H3 lysine 79 methyltransferase. *Genetics* **169**: 173–184.
- Shia WJ, Li B, Workman JL. 2006. SAS-mediated acetylation of histone H4 Lys 16 is required for H2A.Z incorporation at subtelomeric regions in *Saccharomyces cerevisiae*. *Genes Dev* **20**: 2507–2512.
- Shore D, Bianchi A. 2009. Telomere length regulation: Coupling DNA end processing to feedback regulation of telomerase. *EMBO J* **28**: 2309–2322.
- Simon MD, Chu F, Racki LR, de la Cruz CC, Burlingame AL, Panning B, Narlikar GJ, Shokat KM. 2007. The site-specific installation of methyl-lysine analogs into recombinant histones. *Cell* **128**: 1003–1012.
- Singer MS, Kahana A, Wolf AJ, Meisinger LL, Peterson SE, Goggin C, Mahowald M, Gottschling DE. 1998. Identification of high-copy disruptors of telomeric silencing in *Saccharomyces cerevisiae*. *Genetics* **150**: 613–632.
- Sinha I, Buchanan L, Ronnerblad M, Bonilla C, Durand-Dubief M, Shevchenko A, Grunstein M, Stewart AF, Ekwall K. 2010. Genome-wide mapping of histone modifications and mass spectrometry reveal H4 acetylation bias and H3K36 methylation at gene promoters in fission yeast. *Epigenomics* **2**: 377–393.
- Smith JS, Brachmann CB, Celic I, Kenna MA, Muhammad S, Starai VJ, Avalos JL, Escalante-Semerena JC, Grubmeyer C, Wolberger C, et al. 2000. A phylogenetically conserved NAD⁺-dependent protein deacetylase activity in the Sir2 protein family. *Proc Natl Acad Sci* **97**: 6658–6663.
- Sperling AS, Grunstein M. 2009. Histone H3 N-terminus regulates higher order structure of yeast heterochromatin. *Proc Natl Acad Sci* **106**: 13153–13159.
- Steger DJ, Owen-Hughes T, John S, Workman JL. 1997. Analysis of transcription factor-mediated remodeling of nucleosomal arrays in a purified system. *Methods* **12**: 276–285.
- Strahl-Bolsinger S, Hecht A, Luo K, Grunstein M. 1997. SIR2 and SIR4 interactions differ in core and extended telomeric heterochromatin in yeast. *Genes Dev* **11**: 83–93.
- Suka N, Suka Y, Carmen AA, Wu J, Grunstein M. 2001. Highly specific antibodies determine histone acetylation site usage in yeast heterochromatin and euchromatin. *Mol Cell* **8**: 473–479.
- Suka N, Luo K, Grunstein M. 2002. Sir2p and Sas2p opposingly regulate acetylation of yeast histone H4 lysine 16 and spreading of heterochromatin. *Nat Genet* **32**: 378–383.
- Takahashi YH, Schulze JM, Jackson J, Hentrich T, Seidel C, Jaspersen SL, Kobor MS, Shilatifard A. 2011. Dot1 and histone H3K79 methylation in natural telomeric and HM silencing. *Mol Cell* **42**: 118–126.
- Tanny JC, Kirkpatrick DS, Gerber SA, Gygi SP, Moazed D. 2004. Budding yeast silencing complexes and regulation of Sir2 activity by protein-protein interactions. *Mol Cell Biol* **24**: 6931–6946.
- Tantin D, Chi T, Hori R, Pyo S, Carey M. 1996. Biochemical mechanism of transcriptional activation by GAL4-VP16. *Methods Enzymol* **274**: 133–149.
- Tompa R, Madhani HD. 2007. Histone H3 lysine 36 methylation antagonizes silencing in *Saccharomyces cerevisiae* independently of the Rpd3S histone deacetylase complex. *Genetics* **175**: 585–593.
- van Leeuwen F, Gafken PR, Gottschling DE. 2002. Dot1p modulates silencing in yeast by methylation of the nucleosome core. *Cell* **109**: 745–756.
- Verzijlbergen KF, Faber AW, Stulemeijer IJ, van Leeuwen F. 2009. Multiple histone modifications in euchromatin promote heterochromatin formation by redundant mechanisms in *Saccharomyces cerevisiae*. *BMC Mol Biol* **10**: 76. doi: 10.1186/1471-2199-10-76.
- Xu EY, Zawadzki KA, Broach JR. 2006. Single-cell observations reveal intermediate transcriptional silencing states. *Mol Cell* **23**: 219–229.
- Xu F, Zhang Q, Zhang K, Xie W, Grunstein M. 2007. Sir2 deacetylates histone H3 lysine 56 to regulate telomeric heterochromatin structure in yeast. *Mol Cell* **27**: 890–900.
- Yang B, Britton J, Kirchmaier AL. 2008. Insights into the impact of histone acetylation and methylation on Sir protein recruitment, spreading, and silencing in *Saccharomyces cerevisiae*. *J Mol Biol* **381**: 826–844.

Supplemental Material

Inventory of Supplemental Material

Supplemental Materials and methods

Supplemental Tables

Table S1. Yeast strains used in this study

Table S2. Plasmids used for strain construction

Table S3. Oligonucleotide probes used in this study

Supplemental Figures

Figure S1. Variegated gene expression at *ADE2-TEL05R*. Related to Fig. 1,2.

Figure S2. ON and OFF chromatin states at *URA3-TEL07L*. Related to Fig. 1,2.

Figure S3. ChIP of control telomere native *TEL06R* harboring the endogenous *YFR057W* gene. Related to Fig. 1,2.

Figure S4. RNAPII-3FLAG sequential-ChIP assay. Related to Fig. 3.

Figure S5. Sir complex binding to the unmodified and H3K79me2 immobilized chromatin templates. Related to Fig. 5.

Figure S6. ON chromatin state and inheritance of H3K79me at *ADE2-TEL05R*. Related to Fig. 6.

Supplemental References

Supplemental Materials and methods

Yeast strains

Yeast strains used in this study are listed in Table S1. TKY4565 was constructed from UCC4562 (*MATa ade2-101 his3-200 leu2-1 lys2-801 trp1Δ1 ura3-52 adh4::URA3-TEL07L ADE2-TEL05R*, a kind gift from Daniel Gottschling (Singer et al. 1998)) as follows. *ura3-52* was deleted from UCC4562 and replaced with the *LEU2* gene from pRS405 (see Plasmids) by one-step PCR transformation to create TKY4562u. The defective promoter of the *GAL3* gene (due to the *trp1Δ1* mutation) was restored in TKY4562u by integration of the *HpaI* digestion product of pTK006 (see Plasmids), containing the natMX4 marker, by homologous recombination to create TKY4562uG. *ade2-101* was deleted from TKY4562uG and replaced with the *HIS3* gene by integration of the *NruI* digestion product of pTK009 (see Plasmids) by homologous recombination to create TKY4565. TKY4565R was constructed from TKY4565 using p3FLAG-KanMX (see Plasmids), containing 3FLAG and the *kanMX4* marker, by one-step PCR transformation. TKY4741-GFP3 was constructed from BY4741 (see Table S1) by

integration of the *Sall/EcoRI* double digestion product of pTK023 (see Plasmids), containing the *URA3* gene, by homologous recombination. TKY751 was constructed from TKY4565 using pFA6a-13myc-kanMX (see Plasmids), containing 13Myc and the *kanMX4* marker, by one-step PCR transformation. TKY754 was constructed from TKY4565 using pFA6a-3HA-kanMX (see Plasmids), containing 3HA and the *kanMX4* marker, by one-step PCR transformation. TKY4565S was constructed from TKY4565, TKY4565RS from TKY4565R, TKY4741-GFP3S from TKY4741-GFP3, TKY751S from TKY751, TKY754S from TKY754 using pAG32 (see Plasmids), containing the *hphMX4* marker, by one-step PCR transformation. TKY4565RS-D was constructed from TKY4565RS using pFA6a-TRP1 (see Plasmids), containing the *TRP1* marker, by one-step PCR transformation. Each strain construction step was verified by PCR and/or Western blot and/or Southern blot and/or fluorescence microscopy, accordingly.

Plasmids

Plasmids used for strain construction are listed in Table S2. PfuUltra II fusion HS DNA polymerase (Stratagene) was used according to the manufacturer's protocol for all PCR reactions related to plasmid construction. pTK006 was constructed from pAG25 (*natMX4 AmpR*) (Goldstein and McCusker 1999) as follows. The promoter region of the *TRP1* gene (393 bp of DNA immediately upstream of the ORF) was PCR amplified from the genomic DNA of YDS2 (*MATa ade2-1 can1-100 his3-11 leu2-3,112 trp1-1 ura3-1*) and inserted into the *PvuII/BglIII* digested pAG25 vector to create pTK005 (*P_{TRP1} natMX4 AmpR*) using the In-Fusion PCR Cloning kit (Clontech) following the manufacturer's instructions. The terminator region of *TRP1* (822 bp of DNA immediately downstream of the *TRP1* ORF), including most of the *GAL3* promoter region, was PCR amplified from the genomic DNA of YDS2 and inserted into the *SacI/SpeI* digested pTK005 to create pTK006 using In-Fusion. pTK009 was constructed from pFA6a-His3MX6 (*His3MX6 AmpR*) (Longtine et al. 1998) as follows. The terminator region of the *ADE2* gene (643 bp of DNA immediately downstream of the stop codon) was PCR amplified from the genomic DNA of YPH250 and inserted into the *PmeI/EcoRV* digested pFA6a-His3MX6 vector to create pTK008 (*His3MX6 T_{ADE2} AmpR*) using In-Fusion. The promoter region of *ADE2* (1196 bp of DNA upstream of the ORF beginning at position -168) was PCR amplified from the genomic DNA of YPH250 and inserted into the *BamHI/BglIII* digested pTK008 to create pTK009 using In-Fusion. pTK023 was constructed from pEX372 (*P_{URA3-yEGFP1-PD_{CLN2}-NLS_{SV40}}*) (Xu et al. 2006) and pADHUCA-IV (*adh4-URA3-TG AmpR*) (Gottschling et al. 1990) as follows. *P_{URA3-yEGFP1-PD_{CLN2}}* fused to a stop codon, PCR amplified from pEX372, and the terminator region of *URA3*, PCR amplified from pADHUCA-IV, were simultaneously inserted into *HindIII/BamHI* digested pADHUCA-IV to create pTK020 (*ADH4- P_{URA3-yEGFP1-PD_{CLN2}-T_{URA3}-TG}*) using In-Fusion. The *URA3* coding region fused to an octa-glycine linker was PCR amplified from pADHUCA-IV and inserted into *BspEI* digested pTK020 to create pTK021 (*ADH4- P_{URA3-G8-yEGFP1-PD_{CLN2}-T_{URA3}-TG}*), using In-Fusion. *PD_{CLN2} (partial)-NLS_{SV40}-T_{URA3}* was PCR amplified and inserted into *SacI/BamHI* digested pTK021 to create pTK023 using In-Fusion. Plasmid sequences are available upon request.

Oligonucleotide probes

Oligonucleotide probes used in this study are listed in Table S3. Probes used for multiple purposes are included redundantly under different probe names for convenience.

Protein purification

Xenopus laevis histones and histone mutants (H3, H3C110AK4C, H3C110AK36C, H3C110AK79C, H4, H2A, and H2B) were purified as described previously (Luger et al. 1997). Gal4-VP16 was purified as described previously (Tantin et al. 1996). Sir proteins were purified as described previously (Tanny et al. 2004; Johnson et al. 2009) with some modifications to the protocol. Briefly, for HA-Sir2/TAP-Sir4 purification, SF10 (*MATa lys2-801 leu2Δ1 trp1 ura3-52 pep4Δ::HIS3 prb1Δ1.6R can1*, a kind gift from Danesh Moazed (Tanny et al. 2004)) was transformed with plasmids pDM641 (*P_{GALI}-3HA-SIR2 CEN/LEU2 AmpR*) and pDM654 (*P_{GALI}-TAP-SIR4 CEN/URA3 AmpR*) (both kind gifts from Danesh Moazed (Johnson et al. 2009)). Fresh transformants were scraped from a plate and inoculated into 10 ml of SR-leu-ura (starting OD₆₀₀ was ~0.5). The culture was grown overnight until saturation, diluted into 100 ml of SR-leu-ura and incubated overnight until the OD₆₀₀ reached ~5. This was further diluted into 1.2 l of SR-leu-ura and grown to OD₆₀₀ of ~4. This culture was split into 300 ml each and added to 2.7 l each of SG-leu-ura medium (2% galactose final concentration, pre-warmed to 30°C). This culture was allowed to induce Sir2 and Sir4 for 5 hours. Induction methods for Sir3-TAP purification using DMY2364 (*MATa lys2-801 leu2Δ1 trp1 ura3-52 pep4Δ::HIS3 prb1Δ1.6R can1* pDM598 (*P_{GALI}-SIR3-TAP CEN/LEU2 AmpR*), a kind gift from Danesh Moazed) were as described previously (Tanny et al. 2004). Cells were then collected and washed once with ice cold sterile water and frozen in liquid nitrogen and stored at -80°C. Frozen cells were thawed in an equal volume of 2 x lysis buffer (100 mM HEPES pH 7.6, 600 mM KCl, 4 mM EDTA pH 8.0, 2 mM EGTA pH 8.0, 100 mM NaF, 0.2 mM Na₃VO₄, 0.2% NP-40, 40 mM β-ME, 2 mM PMSF, and Roche Complete Protease Inhibitor EDTA-free) at room temperature, then lysed with glass beads (12 x 20 sec pulses with 1 min 40 sec rest between pulses) using a 300 ml bead-beating chamber (filled with 1 x lysis buffer) at 4°C. The extract was collected and centrifuged at 30,000 G for 25 min. The supernatant (split into ~50 ml each) was incubated with ~1 ml each of IgG Sepharose 6 Fast Flow beads (GE healthcare, washed and re-suspended in 1 x lysis buffer). After a 3 hr incubation, the beads were collected and washed three times with 10 ml each of IgG wash buffer (10 mM Tris-HCl pH 8.0, 300 mM KCl, 0.1% NP-40, 1 mM DTT, 1 mM PMSF, and Roche Complete Protease Inhibitor EDTA-free), then once with 10 ml of TEV cleavage buffer (10 mM Tris-HCl pH 8.0, 300 mM KCl, 0.1% NP-40, 0.5 mM EDTA, 5% glycerol, 1 mM DTT, 1 mM PMSF, and Roche Complete Protease Inhibitor EDTA-free). The beads were then incubated with 1 ml TEV cleavage buffer containing 20 μl TEV protease overnight. For HA-Sir2/TAP-Sir4 purification, the eluate was dialyzed against Sir2/Sir4 dialysis buffer (100 mM potassium acetate pH 7.6, 20 mM HEPES pH 7.6, 1 mM EDTA, and 10% glycerol) using a Slide-A-Lyzer dialysis cassette (Pierce) according to the manufacturer's manual.

qRT-PCR

RNA was extracted from exponentially growing cells using the hot acid phenol extraction method (Bookout et al. 2006). For RNA extraction from formaldehyde fixed cells, incubation in phenol was done at 95°C instead of 65°C. Contaminating DNA was digested with DNase I (QIAGEN) and purified using the QIAGEN RNeasy mini column according to the manufacturer's instructions. Random primers (New England Biolabs) were hybridized to the RNA and RT was performed to produce cDNA using M-MLV reverse transcriptase (Invitrogen) in the presence of RNasin Plus RNase inhibitor (Promega) following the manufacturer's protocol. qPCR of the cDNA was performed on an Applied Biosystems 7500 Real-Time PCR system using the Maxima SYBR Green qPCR Master Mix (Fermentas) according to the manufacturer's instructions. The $\Delta\Delta C_t$ method was used to calculate relative gene expression levels (Bookout et al. 2006).

Western blot

Western blot assays were performed using the ODYSSEY infrared imaging system (LICOR) following the manufacturer's protocol. Samples were separated on an SDS-PAGE gel and transferred to a nitrocellulose membrane using the iBlot Dry Blotting System (Life Technologies) following the manufacturer's protocol. The following dilutions were used for primary antibody incubation: 1:1000 H3K4me3 (Active Motif/39159), 1:500 H3K36me3 (Abcam/ab9050), 1:2000 H3K79me2 (in house/532), 1:5000 H3 (Active Motif/39163), 1:1000 TAP (Open Biosystems/CAB1001), and 1:1000 HA (Roche/12CA5).

Silver staining

Silver staining was performed as follows. SDS-PAGE gels were fixed for 15 min on a shaker in a solution containing 40% water, 10% acetic acid, and 50% methanol. The solution was discarded and the gel was incubated for 7 min in 30% methanol, then washed with water for 5 min three times. The gel was sensitized for 2.5 min with 20% sodium thiosulphate solution and rinsed with water three times. The gel was then incubated 15 min with 0.2% silver nitrate and rinsed with water three times. Finally, the gel was developed in developing solution containing sodium carbonate, sodium thiosulphate, and formaldehyde. Once the bands appeared, development was stopped with 6% acetic acid.

ChIP

Standard ChIP assays were performed as described previously (Hecht et al. 1996; Suka et al. 2001) with minor modifications to the protocol. 50 μ l of lysate were used per ChIP

assay with the following amounts of antibodies: 3 μ l Myc (Roche/9E10), 0.5 μ l HA (Upstate/12CA5), 2 μ l RNAPII (Covance/8WG16), 1 μ l Rap1 (in house/477), 1 μ l Sir3 (in house/347), 4 μ l H4K16ac (in house/268), 2 μ l H3K79me1 (Abcam/ab2886 or Active Motif/39145), 2 μ l H3K79me2 (in house/532), 5 μ l H3K79me3 (in house/644), 3 μ l H3K4me3 (Active Motif/39159), 4 μ l H3K36me3 (Abcam/ab9050) and 5 μ l Htz1 (in house/660). DNA was extracted from the immunoprecipitated chromatin using the fast ChIP method (Nelson et al. 2006). For the H3 ChIP, 100 μ l of chromatin was diluted with 800 μ l of 140 mM lysis buffer (Hecht et al. 1996) and incubated overnight along with 2 μ l of anti-H3 antibody (Millipore/A3S or Active Motif/39163) and 50 μ l of 50% protein-A sepharose beads. Chromatin from the H3 ChIP assay was heat denatured at 95°C for 25 min and purified using the QIAquick PCR Purification Kit (QIAGEN).

Sequential-ChIP

Sequential-ChIP was performed as described elsewhere (Kao et al. 2004) with minor modifications to the protocol. Briefly, 200 μ l of chromatin lysate in sequential-ChIP buffer (50 mM HEPES/KOH pH7.5, 140 mM NaCl, 1mM EDTA, 1% Triton X-100, 0.1% Na-deoxycholate) were immunoprecipitated overnight at 4°C with 100 μ l of 50% ANTI-FLAG M2 agarose beads (Sigma-Aldrich) equilibrated with sequential-ChIP buffer (first ChIP). The agarose beads were washed four times for 5 min each with sequential-ChIP buffer at 4°C. The chromatin fragments were eluted off the beads overnight with 100 μ l sequential-ChIP buffer containing 200 μ g/ml 3 x FLAG peptide (Sigma-Aldrich) at 4°C. 10 μ l of eluate was saved and used as the input control DNA for the second (sequential) ChIP. 5 μ l of 100 mg/ml BSA (usb), 4.5 μ l of 500 μ g/ml λ phage DNA (New England Biolabs), 0.5 μ l of 10 mg/ml E. coli tRNA (Roche) were added to the remaining 90 μ l of eluate from the first ChIP and used for sequential-ChIP.

Sequential-ChIP assays were performed using the following amounts of antibodies: 4 μ l RNAPII (Covance/8WG16), 2 μ l Rap1 (in house/477), 2 μ l Sir3 (in house/347), 2 μ l H3 (Active Motif/39163) 1 μ l H3K79me1 (Active Motif/39145) and 1 μ l H3K79me2 (in house/532). Washing conditions for the sequential-ChIP assays were the same as that of the standard ChIP assay described above. Chromatin was eluted by incubating the beads twice for 10 min with 50 μ l of ChIP elution buffer (50 mM Tris/Cl pH 8.0, 10 mM EDTA, 1% SDS) at room temperature. The eluate was incubated at 95°C for 25 min to reverse the crosslinking of chromatin, treated with proteinase K for 30 min, and DNA was purified using the QIAquick PCR Purification Kit (QIAGEN). qPCR was performed as described above.

FACS-ChIP

FACS was performed using BD FACSAria II (BD Biosciences) according to the manufacturer's manual. Samples were prepared for FACS as follows. Cells were first grown in SC medium overnight, then diluted and grown overnight again until the OD₆₀₀ reached ~0.7. Cells were then diluted again into 50 ml of SC medium and grown from OD₆₀₀ of ~0.1 to ~0.4 and fixed with formaldehyde (1% final concentration) for 15 min.

Cells were quenched with glycine (125 mM final concentration) for 5 min, washed twice with PBS, and re-suspended in 500 μ l PBS. 3 μ l of RNasin Plus RNase inhibitor was added to the sample and the cells were sonicated using the Bioruptor sonication device (Diagenode) at medium level for 30 sec. The cell concentration was then adjusted to $\sim 2 \times 10^7$ cells/ml using PBS in a 15 ml conical tube and cells were sorted by FACS based on fluorescence intensity (FITC channel).

Microscopy

Microscopy was performed using an Axioplan 2 microscope (Zeiss) according to the manufacturer's manual. Samples were prepared as described above (see FACS-ChIP). Slides were prepared as follows. Cells were spotted onto cover slips coated with 2 mg/ml concanavalin A type IV (Sigma-Aldrich) / 0.1% poly-L-lysine solution (Sigma-Aldrich). Cells were allowed to settle by incubation for 1 hr at 4°C. Excess liquid was aspirated and the samples were dried in a fume hood for ~ 3 min. VECTASHIELD mounting medium (Vector Laboratories) was spotted onto the samples and the cover slip was placed on a microscope slide and sealed with nail polish. Images were taken using DIC and FITC settings with a 40 x objective.

URA3 ON/OFF telomere medium-selection

When a yeast strain with *URA3* at TEL07L is cultured in SD-ura, only *URA3* ON cells can grow. On the other hand, when the strain is cultured in the presence of the drug 5-fluoroorotic acid (5-FOA), which is toxic to cells with Ura3 activity (Boeke et al. 1987), only *URA3* OFF cells can grow. To isolate the *URA3* ON cells, the *URA3*-TEL07L strain was incubated for 3 days on SD-ura agar medium, pre-cultured overnight to stationary phase, diluted, and cultured exponentially in SD-ura for two cell generations. The *URA3* OFF cells were isolated in a similar manner by incubating the *URA3*-TEL07L strain for three days on SD + 1g/L 5-FOA agar medium, pre-culturing overnight to stationary phase, diluting, and culturing exponentially in SD + 10 mg/L 5-FOA for two cell generations.

ADE2 feedback repression

To isolate the *ADE2* ON cells, the *ADE2*-TEL07L strain was incubated for three days on SC-ade agar medium, pre-cultured overnight to stationary phase, diluted, and cultured exponentially in SC-ade for two cell generations. *ADE2* feedback repression was performed by collecting the ON cells by centrifugation and replacing SC-ade with synthetic complete medium containing 160 mg/L adenine (SC+160 mg/L ade). The control *ADE2* OFF cells were isolated using the same procedures described in the *ADE2* ON cell-isolation protocol above, except that synthetic complete medium containing 40 mg/L adenine (SC+40 mg/L ade) was used instead of SC-ade.

ADE2 color visualization

Color visualization of *ADE2* expression was done as described elsewhere (van Leeuwen and Gottschling 2002) by incubating the cells on medium with reduced adenine (SC low ade) for three days at 30°C followed by incubation at 4°C for one week.

In vitro transcription/silencing

IVT was performed as described previously (Lin and Carey 2012) with minor modifications to the protocol. The DNA template containing five Gal4 DNA binding sites and an adenovirus E4 promoter (Tantin et al. 1996) was generated by PCR. Histones and methyl-lysine analog histones were assembled into octamers as described previously (Luger et al. 1997). The G5E4T DNA template and histone octamers were assembled into chromatin by salt dilution as described previously (Steger et al. 1997). Following the 10 min pre-binding of Gal4-VP16 to the G5E4T chromatin template at room temperature, Sir proteins (~26 pmol of Sir3 and ~8 pmol each of Sir2 and Sir4) were added to the IVT reaction for 1 hr at 30°C. The Sir3 protein, purified as described above (see Protein Purification), was diluted 1:10 in Sir2/Sir4 dialysis buffer (100 mM potassium acetate pH 7.6, 20 mM HEPES pH 7.6, 1 mM EDTA, and 10% glycerol) before use in the silencing reaction. Yeast nuclear extract, prepared as described previously (Rani et al. 2004), was added to the reaction for 30 min at room temperature. Primer extension was performed to measure the amount of transcription. All reactions were balanced so that the concentrations of all components in the reaction other than Gal4-VP16 or the Sir proteins were identical.

Supplemental Tables

Table S1. *Yeast strains used in this study*

Strain	Genotype	Source
BY4741	<i>MATa his3Δ1 leu2Δ0 met15Δ0 ura3Δ0</i>	Jef Boeke (Brachmann et al. 1998).
TKY4565	<i>MATa his3-200 leu2-1 lys2-801 ade2Δ::His3MX6 ura3Δ::LEU2 trp1Δ::natMX4 adh4::URA3-TEL07L ADE2-TEL05R</i>	This study.
TKY4565R	<i>MATa his3-200 leu2-1 lys2-801 ade2Δ::His3MX6 ura3Δ::LEU2 trp1Δ::natMX4 adh4::URA3-TEL07L ADE2-TEL05R RPB1-3FLAG::kanMX6</i>	This study.
TKY4565RS	<i>MATa his3-200 leu2-1 lys2-801 ade2Δ::His3MX6 ura3Δ::LEU2 trp1Δ::natMX4 adh4::URA3-TEL07L ADE2-TEL05R RPB1-3FLAG::kanMX6 sir3Δ::hphMX4</i>	This study.

TKY4565RS-D	<i>MATa his3-200 leu2-1 lys2-801 ade2Δ::His3MX6 ura3Δ::LEU2 trp1Δ::natMX4 adh4::URA3-TEL07L ADE2-TEL05R RPB1-3FLAG::kanMX6 sir3Δ::hphMX4 dot1Δ::TRP1</i>	This study.
TKY4565S	<i>MATa his3-200 leu2-1 lys2-801 ade2Δ::His3MX6 ura3Δ::LEU2 trp1Δ::natMX4 adh4::URA3-TEL07L ADE2-TEL05R sir3Δ::hphMX4</i>	This study.
TKY4741-GFP3	<i>MATa his3Δ1 leu2Δ0 met15Δ0 ura3Δ0 adh4::P_{URA3}-URA3-G8-yEGFP1-PD_{CLN2}-NLS_{SV40}-TEL07L</i>	This study.
TKY4741-GFP3S	<i>MATa his3Δ1 leu2Δ0 met15Δ0 ura3Δ0 adh4::P_{URA3}-URA3-G8-yEGFP1-PD_{CLN2}-NLS_{SV40}-TEL07L sir3Δ::hphMX4</i>	This study.
TKY751	<i>MATa his3-200 leu2-1 lys2-801 ade2Δ::His3MX6 ura3Δ::LEU2 trp1Δ::natMX4 adh4::URA3-TEL07L ADE2-TEL05R PPR1-13myc::KanMX6</i>	This study.
TKY751S	<i>MATa his3-200 leu2-1 lys2-801 ade2Δ::His3MX6 ura3Δ::LEU2 trp1Δ::natMX4 adh4::URA3-TEL07L ADE2-TEL05R PPR1-13myc::KanMX6 sir3Δ::hphMX4</i>	This study.
TKY754	<i>MATa his3-200 leu2-1 lys2-801 ade2Δ::His3MX6 ura3Δ::LEU2 trp1Δ::natMX4 adh4::URA3-TEL07L ADE2-TEL05R SUA7-3HA::KanMX6</i>	This study.
TKY754S	<i>MATa his3-200 leu2-1 lys2-801 ade2Δ::His3MX6 ura3Δ::LEU2 trp1Δ::natMX4 adh4::URA3-TEL07L ADE2-TEL05R SUA7-3HA::KanMX6 sir3Δ::hphMX4</i>	This study.
YPH250	<i>MATa ade2-101 his3-200 leu2-1 lys2-801 trp1Δ1 ura3-52</i>	Philip Hieter (Sikorski and Hieter 1989).

Table S2. Plasmids used for strain construction

Plasmid	Description	Source
p3FLAG-KanMX	<i>3FLAG-kanMX4 AmpR</i>	Toshio Tsukiyama (Gelbart et al. 2001).
pAG32	<i>hphMX4 AmpR</i>	John McCusker (Goldstein and McCusker 1999).
pFA6a-13Myc-kanMX6	<i>13Myc-T_{ADHI} kanMX6 AmpR</i>	Mark Longtine (Longtine et al. 1998).
pFA6a-3HA-kanMX6	<i>3HA-T_{ADHI} kanMX6 AmpR</i>	Mark Longtine (Longtine et al. 1998).
pFA6a-TRP1	<i>TRP1 AmpR</i>	Mark Longtine (Longtine et al. 1998).
pRS405	<i>LEU2 AmpR</i>	Stratagene.

pTK006	P_{TRP1} <i>natMX4</i> P_{GAL3} <i>AmpR</i>	This study.
pTK009	P_{ADE2} <i>His3MX6</i> T_{ADE2} <i>AmpR</i>	This study.
pTK023	<i>ADH4</i> - P_{URA3^-} - <i>URA3-G8-yEGFP1-CLN2_{PD}-NLS_{SV40}-T_{URA3^-}</i> <i>TG AmpR</i>	This study.

Table S3. Oligonucleotide probes used in this study

Probe	Sequence	Purpose
ADE2-middle-F/ADE2-TEL05R-1.0-F	AGCAATGGTCAAACCATTGGTTGG	ChIP
ADE2-middle-R/ADE2-TEL05R-1.0-R	GCTGACATCCTATGTGGAGTTCTA	ChIP
ADE2-start-F/ADE2-TEL05R-2.0-F	CTCTTGATATCGAAAACTAGCTG	ChIP
ADE2-start-R/ADE2-TEL05R-2.0-R	GTCTCACTGGCTTGTCCACAGGA	ChIP
ADE2-TEL05R-0.1-F	AAAGCGTCATTTCGATTCCAGTGAC	ChIP
ADE2-TEL05R-0.1-R	CTCTCACATCTACCTCTACTCT	ChIP
SPS2-F	GGATAGCATGTTGAACCAGTTG	ChIP
SPS2-R	CGGTCCACCATTAGGTTCAACTGC	ChIP
TEL06R-0.2-F	ACGTTTAGCTGAGTTTAACGGTG	ChIP
TEL06R-0.2-R	CATGACCAGTCCCTCATTTCATC	ChIP
TEL06R-0.5-F	GCGTAACAAAGCCATAATGCCTCC	ChIP
TEL06R-0.5-R	CTCGTTAGGATCACGTTTCAATCC	ChIP
TEL06R-1.5-F	TGGTTAGTTATTGGGGATCATCATGC	ChIP
TEL06R-1.5-R	GTACAGTCCAGAAATCGCTCCTTTA	ChIP
URA3-GFP-TEL07L-0.1-F	CGCGCTGTA CTCCACCAAAGAAG	ChIP
URA3-GFP-TEL07L-0.1-R	TCTGGGATCCGTCGAGGGTAATAA	ChIP
URA3-GFP-TEL07L-0.5-F	ATACTCCAATTGGTGATGGTCCAG	ChIP
URA3-GFP-TEL07L-0.5-R	CAATTCATCCATACCATGGG	ChIP
URA3-GFP-TEL07L-0.8-F	CATGGCCAACCTTAGTCACTACTT	ChIP

URA3-GFP-TEL07L-0.8-R	CTGGTCTTGTAGTTACCGTCATCT	ChIP
URA3-GFP-TEL07L-1.5-F	ATTGTTAGCGGTTTGAAGCAGGCG	ChIP
URA3-GFP-TEL07L-1.5-R	CTTCGCAATGTCAACAGTACCCT	ChIP
URA3-GFP-TEL07L-2.0-F	AAGCCATACCTGCCAAGTATTCTG	ChIP
URA3-GFP-TEL07L-2.0-R	TACCAATCTAAGTCTGTGCTCC	ChIP
URA3-TEL07L-0.15-F	TAGAACCGTGGATGATGTGGTCTC	ChIP
URA3-TEL07L-0.15-R	CTCTCACATCTACCTCTACTCT	ChIP
URA3-TEL07L-0.5-F	ATTGTTAGCGGTTTGAAGCAGGCG	ChIP
URA3-TEL07L-0.5-R	CTTCGCAATGTCAACAGTACCCT	ChIP
URA3-TEL07L-1.0-F	CGTAACACATATCAGTTCTGGCCT	ChIP
URA3-TEL07L-1.0-R	TGTTCTGTGCAGTTGGGTTAAG	ChIP
E4-primer	AGCGGCAGCCATAACAGTCAGCCTTACCAG	Primer extension
ACT1-F	TCCATCCAAGCCGTTTTGTCCTTG	qRT-PCR
ACT1-R	TCTCTACCGGCCAAATCGATTCTC	qRT-PCR
ADE2-F	CTCTTGATATCGAAAACTAGCTG	qRT-PCR
ADE2-R	GTCTCACTGGCTTGTCCACAGGA	qRT-PCR
URA3-F	TAAGGAACGTGCTGCTACTCATCC	qRT-PCR
URA3-R	CTGTGCCCTCCATGGAAAAATCAG	qRT-PCR
YFR057W-F	CTAGTGTCTATAGTAAGTGCTCGG	qRT-PCR

Supplemental References

- Boeke JD, Trueheart J, Natsoulis G, Fink GR. 1987. 5-Fluoroorotic acid as a selective agent in yeast molecular genetics. *Methods Enzymol* **154**: 164-175.
- Bookout AL, Cummins CL, Mangelsdorf DJ, Pesola JM, Kramer MF. 2006. High-Throughput Real-Time Quantitative Reverse Transcription PCR. in *Current Protocols in Molecular Biology* (eds. FM Ausubel, R Brent, RE Kingston, DD Moore, JG Seidman, JA Smith, K Struhl). Wiley, Hoboken, NJ.
- Brachmann CB, Davies A, Cost GJ, Caputo E, Li J, Hieter P, Boeke JD. 1998. Designer deletion strains derived from *Saccharomyces cerevisiae* S288C: a useful set of strains and plasmids for PCR-mediated gene disruption and other applications. *Yeast* **14**: 115-132.
- Gelbart ME, Rechsteiner T, Richmond TJ, Tsukiyama T. 2001. Interactions of Isw2 chromatin remodeling complex with nucleosomal arrays: analyses using recombinant yeast histones and immobilized templates. *Mol Cell Biol* **21**: 2098-2106.
- Goldstein AL, McCusker JH. 1999. Three new dominant drug resistance cassettes for gene disruption in *Saccharomyces cerevisiae*. *Yeast* **15**: 1541-1553.
- Gottschling DE, Aparicio OM, Billington BL, Zakian VA. 1990. Position effect at *S. cerevisiae* telomeres: reversible repression of Pol II transcription. *Cell* **63**: 751-762.
- Hecht A, Strahl-Bolsinger S, Grunstein M. 1996. Spreading of transcriptional repressor SIR3 from telomeric heterochromatin. *Nature* **383**: 92-96.
- Johnson A, Li G, Sikorski TW, Buratowski S, Woodcock CL, Moazed D. 2009. Reconstitution of heterochromatin-dependent transcriptional gene silencing. *Mol Cell* **35**: 769-781.
- Kao CF, Hillyer C, Tsukuda T, Henry K, Berger S, Osley MA. 2004. Rad6 plays a role in transcriptional activation through ubiquitylation of histone H2B. *Genes Dev* **18**: 184-195.
- Lin JJ, Carey M. 2012. In vitro transcription and immobilized template analysis of preinitiation complexes. in *Current Protocols in Molecular Biology* (eds. FM Ausubel, R Brent, RE Kingston, DD Moore, JG Seidman, JA Smith, K Struhl). Wiley, Hoboken, NJ.
- Longtine MS, McKenzie A, Demarini DJ, Shah NG, Wach A, Brachat A, Philippsen P, Pringle JR. 1998. Additional modules for versatile and economical PCR-based gene deletion and modification in *Saccharomyces cerevisiae*. *Yeast* **14**: 953-961.
- Luger K, Rechsteiner TJ, Flaus AJ, Waye MM, Richmond TJ. 1997. Characterization of nucleosome core particles containing histone proteins made in bacteria. *J Mol Biol* **272**: 301-311.
- Nelson JD, Denisenko O, Sova P, Bomsztyk K. 2006. Fast chromatin immunoprecipitation assay. *Nucleic Acids Res* **34**: e2.
- Rani PG, Ranish JA, Hahn S. 2004. RNA polymerase II (Pol II)-TFIIF and Pol II-mediator complexes: the major stable Pol II complexes and their activity in transcription initiation and reinitiation. *Mol Cell Biol* **24**: 1709-1720.
- Sikorski RS, Hieter P. 1989. A system of shuttle vectors and yeast host strains designed for efficient manipulation of DNA in *Saccharomyces cerevisiae*. *Genetics* **122**: 19-27.

- Singer MS, Kahana A, Wolf AJ, Meisinger LL, Peterson SE, Goggin C, Mahowald M, Gottschling DE. 1998. Identification of high-copy disruptors of telomeric silencing in *Saccharomyces cerevisiae*. *Genetics* **150**: 613-632.
- Steger DJ, Owen-Hughes T, John S, Workman JL. 1997. Analysis of transcription factor-mediated remodeling of nucleosomal arrays in a purified system. *Methods* **12**: 276-285.
- Suka N, Suka Y, Carmen AA, Wu J, Grunstein M. 2001. Highly specific antibodies determine histone acetylation site usage in yeast heterochromatin and euchromatin. *Mol Cell* **8**: 473-479.
- Tanny JC, Kirkpatrick DS, Gerber SA, Gygi SP, Moazed D. 2004. Budding yeast silencing complexes and regulation of Sir2 activity by protein-protein interactions. *Mol Cell Biol* **24**: 6931-6946.
- Tantin D, Chi T, Hori R, Pyo S, Carey M. 1996. Biochemical mechanism of transcriptional activation by GAL4-VP16. *Methods Enzymol* **274**: 133-149.
- van Leeuwen F, Gottschling DE. 2002. Assays for gene silencing in yeast. *Methods Enzymol* **350**: 165-186.
- Xu EY, Zawadzki KA, Broach JR. 2006. Single-cell observations reveal intermediate transcriptional silencing states. *Mol Cell* **23**: 219-229.

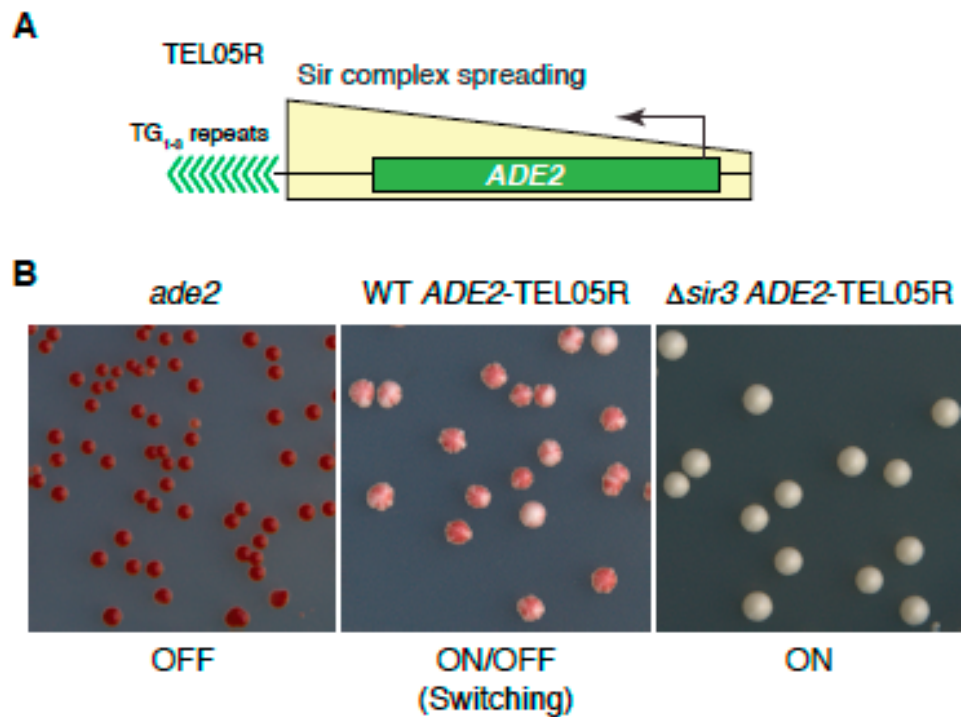


Figure S1. Variegated gene expression at *ADE2*-TEL05R. (A) Schematic of the *ADE2*-TEL05R telomere. **(B)** Visualization of *ADE2* gene expression. Yeast cells that do not express *ADE2* appear red (*ade2*), while those that constitutively express *ADE2* appear white (Δ *sir3* *ADE2*-TEL05R). WT *ADE2*-TEL05R cells switch epigenetically between *ADE2* ON and OFF (exemplified by the white and red patches within each colony).

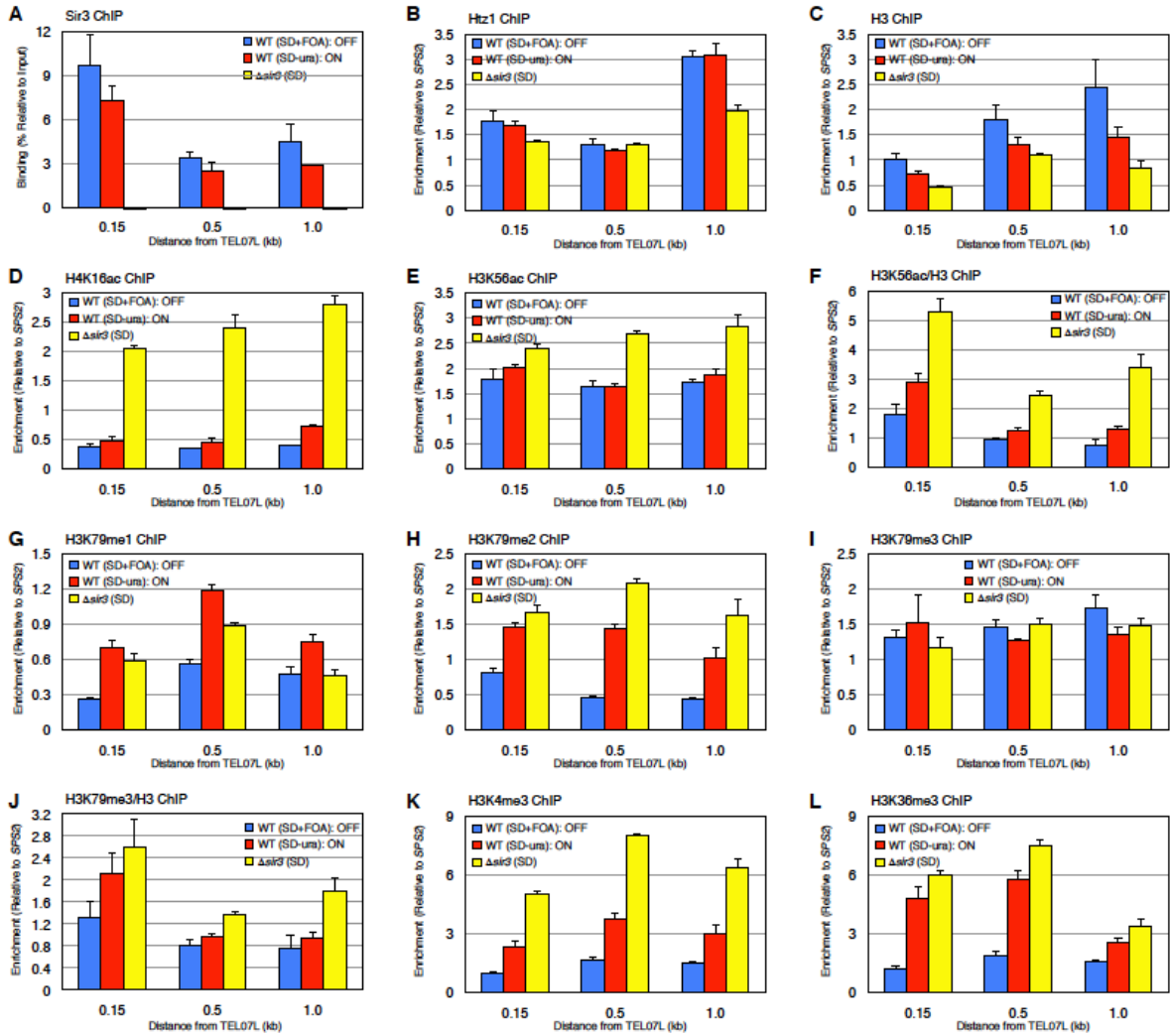
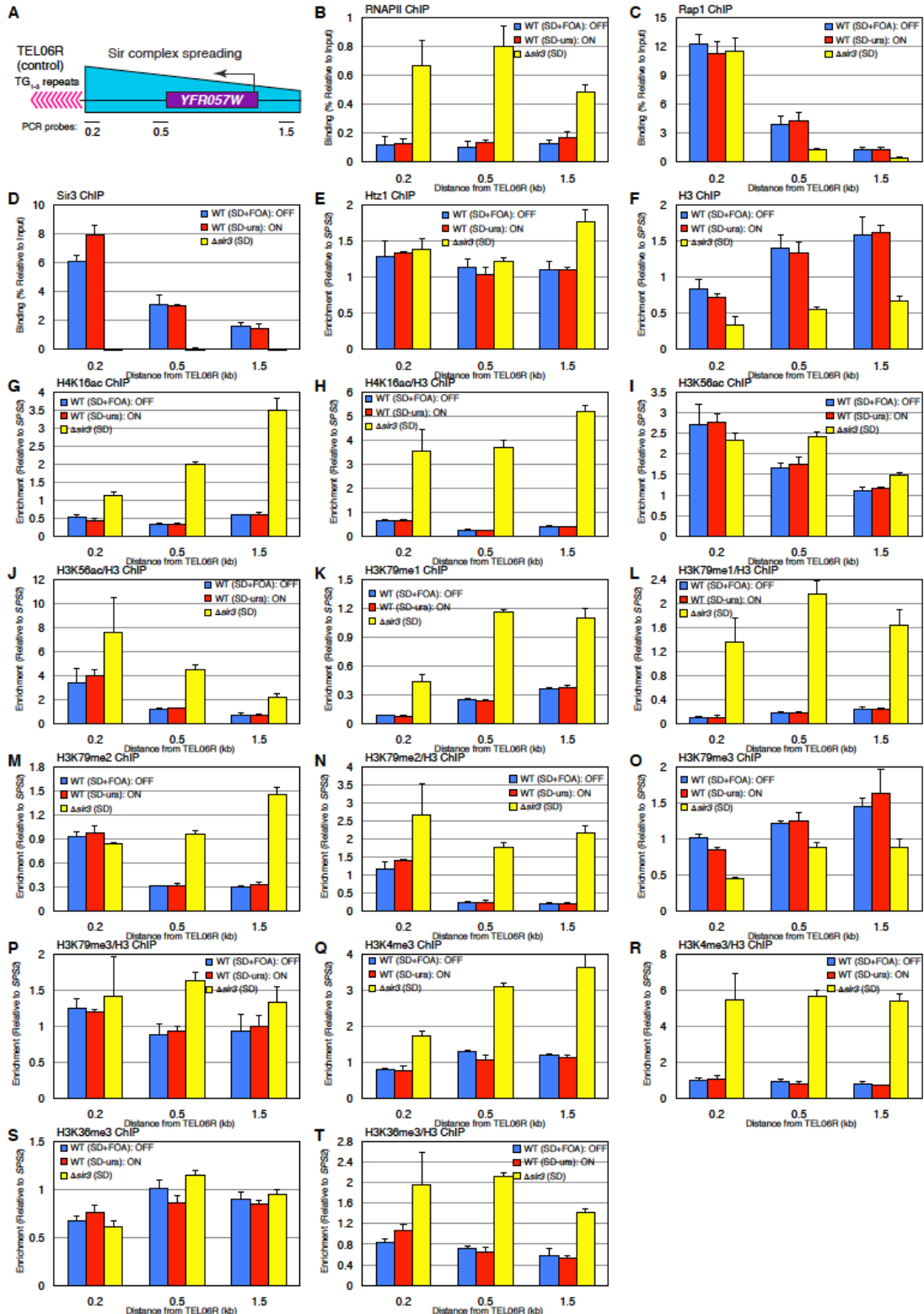


Figure S2. ON and OFF chromatin states at *URA3-TEL07L*. (A-L) ChIP of Sir3 (A), Htz1 (B), H3 (C), H4K16ac (D), H3K56ac (E), H3K56ac/H3 (F), H3K79me1 (G), H3K79me2 (H), H3K79me3 (I), H3K79me3/H3 (J), H3K4me3 (K), and H3K36me3 (L) at *URA3-TEL07L* depicted as in Fig. 1E-H. See Fig. 1A for probes and schematic of *URA3-TEL07L*.



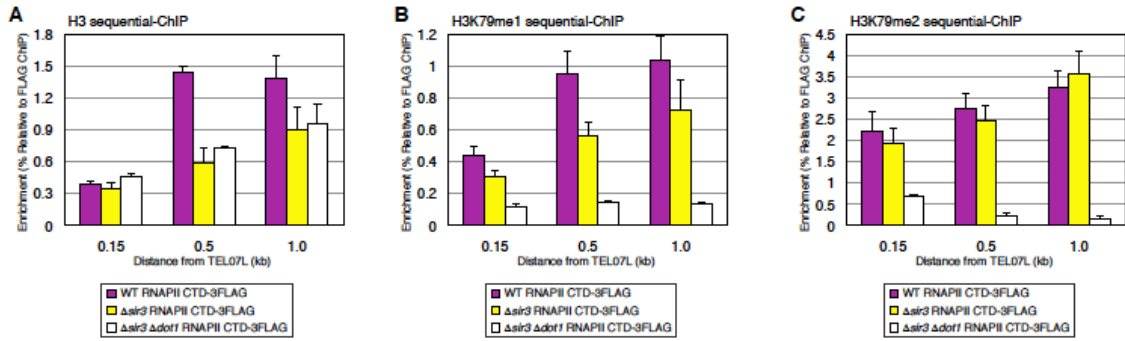


Figure S4. RNAPII-3FLAG sequential-ChIP assay. (A-C) Sequential-ChIP of H3 (A), H3K79me1 (B), and H3K79me2 (C) at *URA3-TEL07L* depicted as in Fig. 3G,H. See Fig. 1A for probes and schematic of *URA3-TEL07L*.

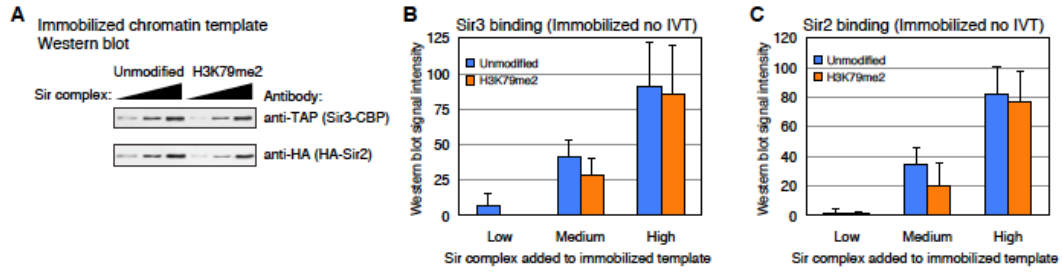


Figure S5. Sir complex binding to the unmodified and H3K79me2 immobilized chromatin templates. (A) Representative image of Sir protein binding from the immobilized chromatin template Western blot experiment. (B,C) Quantification of the immobilized chromatin template Western blot experiment shown in (A). Binding level of Sir3 (B) and Sir2 (C) are presented as mean \pm SD.

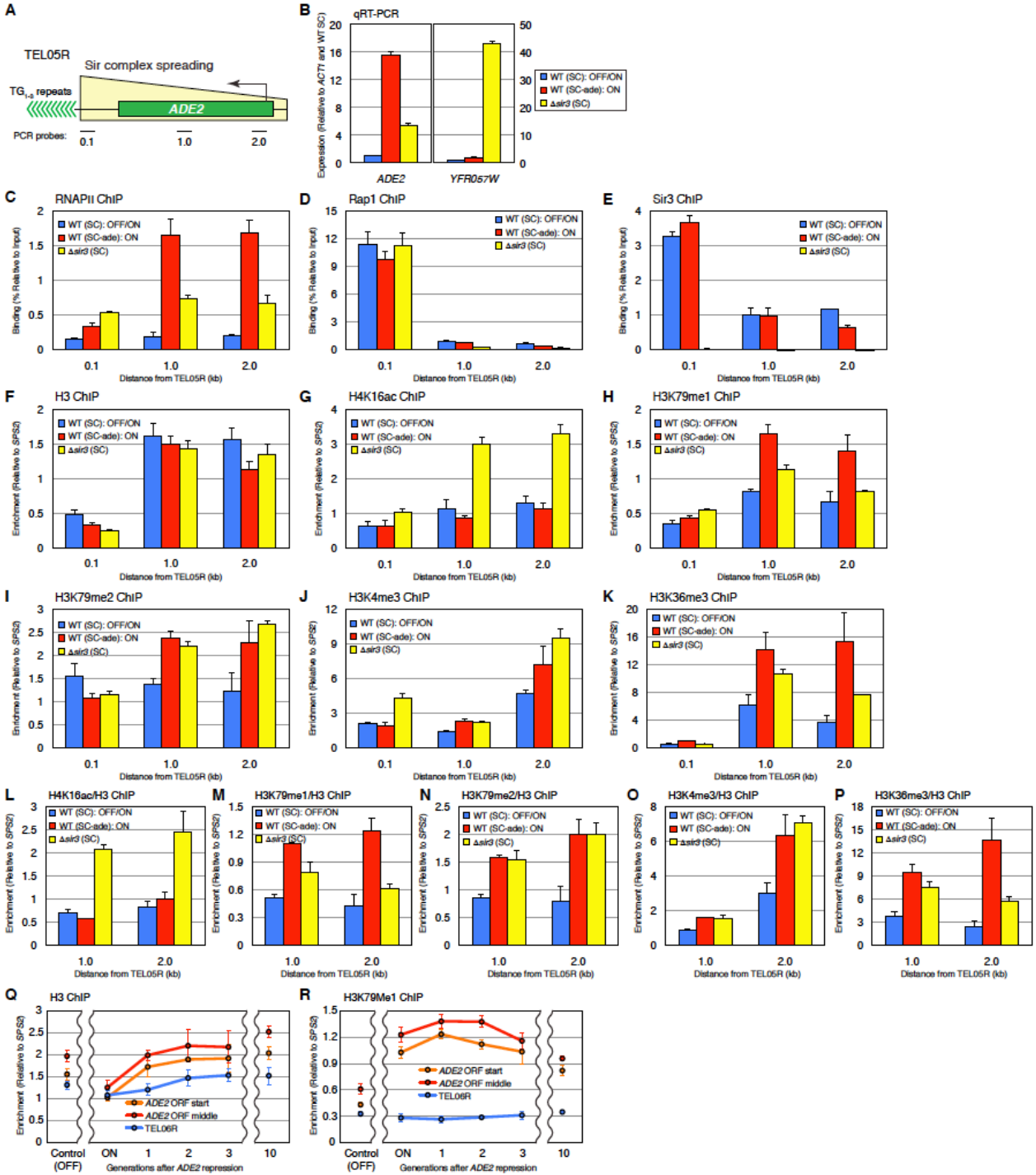


Figure S6. ON chromatin state and inheritance of H3K79me at *ADE2*-TEL05R. (A) Schematic of *ADE2*-TEL05R. Probes were approximately 0.1, 1.0, and 2.0 kb away from the telomeric repeats of *ADE2*-TEL05R. (B) qRT-PCR of *ADE2* at TEL05R and *YFR057W* at native TEL06R in WT *SIR3* cells grown in non-selective media (SC, blue bars), in media lacking adenine (SC-ade) to select for *ADE2* ON (red bars), or $\Delta sir3$ cells grown in SC (yellow bars). Data are presented as mean \pm SD. (C-P) ChIP of RNAPII (C), Rap1 (D), Sir3 (E), H3 (F), H4K16ac (G), H3K79me1 (H), H3K79me2 (I), H3K4me3 (J), H3K36me3 (K), H4K16ac/H3 (L), H3K79me1/H3 (M), H3K79me2/H3 (N), H3K4me3/H3 (O), and H3K36me3/H3 (P), at *ADE2*-TEL05R depicted as in (B). (Q,R) ChIP of H3 (Q) and H3K79me1 (R) at *ADE2*-TEL05R and native TEL06R depicted as in Fig. 6C,D. See Fig. 6A and Supplemental Fig. S2A for probes and schematic of *ADE2*-TEL05R and native TEL06R respectively.

Contribution

The work presented in this chapter was Tasuku Kitada's primary dissertation research. I contributed by helping him set up the in vitro system used for the biochemical portion of the project. I assisted in generating reagents and provided the data for Figures 4G, H and I.

Chapter 5

Identification of the Ino80 Complex as a regulator of silent chromatin

Introduction

The genomes of eukaryotes are organized into two general categories of chromatin: euchromatin and heterochromatin. Euchromatin contains active regions of the genome and is characterized by an open and accessible structure. Heterochromatin, on the other hand, contains inactive regions and has a compact structure. The proteins that make up heterochromatin vary among organisms but similar strategies for the initiation and spreading of heterochromatin are shared. In this respect, *S. cerevisiae* serves as an important model organism for the study of heterochromatin.

In *S. cerevisiae*, gene silencing in heterochromatin is dependent on the Silent Information Regulator (Sir) proteins. The Sir proteins were originally identified in genetic screens for activation of the silent mating loci HML and HMR, but they also function at the telomere [1, 2]. Sir2, Sir3, and Sir4 form the key structural components of heterochromatin. Binding of the Sirs is directed by silencer elements encoded in the genome. HML and HMR are flanked by silencer elements termed E and I, for 'essential' and 'important' functions in silencing the loci (Fig 1A and B) and the telomere contains TG₁₋₃ repeats (Fig 1C). The Sir proteins assemble on silencer elements based on interactions with the sequence specific binding factors (Rap1, Orc1, and Abf1) and each other [3]. Spreading occurs via the deacetylation of H4K16 on adjacent nucleosomes by the NAD-dependent histone deacetylase (HDAC) activity of Sir2 [4-6]. Deacetylation of H4K16 by Sir2 creates binding site for Sir3 [7, 8], which then recruits more Sir4 and Sir2 [9]. Cycles of Sir2 deacetylation followed binding of Sir3, Sir4 and more Sir2 continue until the spreading is stopped by Sas2-mediated H4K16 acetylation [10, 11]. A recent crystal structure of the Sir3 BAH domain in complex with a nucleosome was solved. This structure shows a negatively charged binding pocket specific for unmodified H4K16 [12], thus providing a structural basis for how acetylation of H4K16 prevents Sir3 function.

While much is known about the Sir proteins, it is unknown if other important proteins in heterochromatin can be identified. In vivo genetic screens have been proven invaluable, but they may have limitations. For instance, proteins with essential functions that produce severe or lethal phenotypes when mutated would be difficult to identify. To overcome this, we employed a proteomic approach to identify proteins that interact with heterochromatin. This screen revealed several proteins specifically enriched on heterochromatin, including the ATP-dependent chromatin remodeling complex Ino80 (Ino80C). We confirmed that the presence of the Sir proteins enhances Ino80C binding in vitro and in vivo. A targeted genetic screen of Ino80C subunits revealed that the Arp5 and Ies6 subunits are required for silencing of HML. While loss of these proteins disrupts silencing, it does not have an appreciable effect on the binding of the Sir proteins to the region. This suggests that the presence of the Sir proteins and Ino80C are both necessary for the silencing of HML.

Results

Proteomic analysis of *S. cerevisiae* heterochromatin

To identify new components of *S. cerevisiae* silent chromatin we hypothesized that reconstituted heterochromatin would pull down proteins important in silencing from nuclear extract. In our experimental setup we used unmodified reconstituted chromatin plus and minus purified Sir2, Sir3, and Sir4 as baits to pull down proteins from yeast nuclear extract and identify them by mass spectrometry.

First, Sir proteins were expressed and purified to near homogeneity from *S. cerevisiae* (Fig 2A). We then reconstituted chromatin using biotinylated DNA templates and recombinant histones. Templates were immobilized on streptavidin beads and incubated with the Sir proteins to form heterochromatin. In our previous work, we showed this heterochromatin functions to silence transcription in vitro and recapitulates sensitivity to H3K79 methylation [13].

The immobilized chromatin templates were incubated with yeast nuclear extract, washed, eluted, and analyzed by MuDPIT (Fig2B). We identified several protein and protein complexes that were enriched in presence of Sir proteins (Fig2C, compare unmodified to unmodified + SIR). Ino80C was among the most enriched complexes in our data set. Other top hits included Rap1, Nhp6, Mot1, and NC2. Rap1 was expected because of its known interaction with the Sir proteins. To our knowledge, Ino80C has not previously been shown to be directed to silent chromatin or interact with the Sirs.

Ino80C interacts with heterochromatin in a purified system

Direct interactions with heterochromatin cannot be inferred from our pull down assay because we utilized nuclear extract. The possibility exists that there are other proteins that bridge the interaction of enriched proteins with heterochromatin. To address this, we purified Ino80C from *S. cerevisiae* using a TAP-tagged strain (Fig 3A). A titration of the purified complex was incubated with immobilized chromatin in the presence or absence of the Sir proteins. We found that binding of Ino80C to the chromatin template was greatly enhanced by the presence of the Sirs (Fig 3B). This supports the conclusion that the Ino80C directly interacts with heterochromatin.

The Arp5 and les6 subunits of Ino80C are required to maintain silencing at HML

After confirming the interaction between Ino80C and heterochromatin in vitro, we sought to discern whether there was a functional role for the complex in silent chromatin. To do this we screened Ino80C subunit deletions for expression of two native genes repressed by silent chromatin. We chose the subtelomeric gene YFR057W and the HML gene alpha1 to allow us to screen for defects at both telomeric and hidden mating loci heterochromatin (refer to Fig 1C and 1A for schematics). The results of our screen revealed that deletions in Ino80C subunits les6

and Arp5 caused a silencing defect at HML, but not near the telomere (Fig 4A). The silencing defect at HML was also detected in fresh mutant spores dissected from an IES6/*ies6* heterozygous diploid (Fig 4B).

Ino80 is recruited to heterochromatin in vivo

We showed that Ino80C interacts with heterochromatin in the context of yeast nuclear extract and in a purified system. However, is it important to answer the question of whether or not heterochromatin can direct Ino80C binding in vivo. To address this we measured the enrichment of Ino80 at HML and the telomere in SIR3 and Δ *sir3* cells by ChIP. Deletion of Sir3 stops the spreading of heterochromatin at both the hidden mating loci and telomere [3]. The results in Figure 5 show that both across the HML region, and at the telomere, Ino80 binding is reduced in Δ *sir3* cells. In contrast, Act1, a gene not regulated by the Sir proteins, has is no significant change in Ino80 binding.

Sir3 is present at HML in cells lacking Ino80C subunits Arp5 and les6

One explanation for our results is that Ino80C helps maintain Sir proteins across HML. We hypothesized that remodeling activity of the enzyme may be required to exclude barriers to heterochromatin or to optimally space nucleosomes for Sir protein spreading. To test this, we measured the enrichment of Sir3 in the two strains harboring a silencing defect and compared them to wild type cells. Figure 6 shows that the binding of Sir3 does not substantially change across HML upon deletion of Arp5 or *les6*. Therefore, this data contradicts models where the absence of Sir proteins would explain the silencing defect observed in these strains.

Discussion

Mechanisms of heterochromatin spreading and gene silencing by the Sir proteins in *S. cerevisiae* have been extensively researched. However, there has not been a proteomic

analysis of yeast silent chromatin. We employed this approach in order to identify unknown proteins that might have been missed in previous genetic screens. We identified several proteins that were enriched from the nuclear extract on heterochromatin. We confirmed that one of these proteins, Ino80C, has a direct interaction with heterochromatin.

This interaction raised the possibility that there may be an undiscovered function for the complex in maintaining silent chromatin. We screened Ino80C subunit mutants for silencing defects and discovered that Arp5 and Ies6 were required to maintain the silent state at HML. We further showed that the binding of Ino80 to HML and the telomere is dependent on Sir3, which indicates that the Sir proteins are recruiting Ino80 *in vivo*.

Interestingly, deletion of Arp5 and Ies6 did not disrupt Sir3 binding to HML. This suggests that the silencing defect is independent of the Sir proteins. Previous studies have shown that deletions of Spt10 and Spt21, mutations in H3K56, and the presence of H3K79 methylation can disrupt silencing without major effects on Sir protein binding [13-15]. Collectively these studies show that the Sir proteins are necessary, but not sufficient for gene silencing *in vivo*. It has been proposed that the increased *dam* methylase accessibility observed in some of these studies indicates that the desilencing effect may be caused by changes in higher order structure [14, 15].

Questions remain about the mechanism by which the Ino80C functions in silencing at HML. Ino80C has been shown to space nucleosomes in regular arrays [16] and to remove the histone variant H2AZ [17]. These activities raise the possibility the complex is required to create the proper chromatin environment for Sir protein-dependent silencing to occur. Further studies with *dam* methylase would shed light on whether we are observing a phenomenon similar to previous studies. The lack of a silencing defect at YFR057W indicates that this not a universal

effect at all heterochromatin. The function of the Ino80C may be specific to HML or it may be present at other genes near the telomere that were not investigated. This would be an important line of research in future studies.

Materials and Methods

Protein purification, chromatin assembly, and preparation of yeast nuclear extract

X. laevis histones were expressed in *E. coli* and purified as previously described [18]. The preparation of yeast nuclear extract and purification Sir3 and Sir2-Sir4 were performed as previously described [13]. TAP-purification of Ino80C was performed following standard TAP purification protocols [19] using a TAP-tagged *les1* strain. Chromatin assembly of the biotinylated G5E4T template [20] was performed as in [13].

Immobilized template assays

The immobilized template assays were performed as previously described [13] with the some modifications. In the proteomic screen, immobilized chromatin (500 ng) was incubated with or without Sir proteins for 10 min at 22 °C rotating in a 235 ul volume. After incubation, 1 mg of yeast nuclear extract (15 ul) was added to the reactions for 45 min. Beads were washed twice with reaction buffer and proteins were eluted using 50 mM Tris pH 8 and 6 M urea buffer. For both conditions, 10 reactions of this scale were pooled. Proteins were then TCA precipitated, digested with trypsin, and analyzed by MuDPIT. In the purified system, purified TAP-*les1* was titrated into 25 ul reactions with 20 ng of chromatin in the presence of absence of the Sir proteins. The reactions were incubated at 22 °C for 30 min while rotating. The beads were washed twice with reaction buffer, eluted with Laemmli buffer, and analyzed by western blot.

Yeast strains and Primers

The yeast strains used in this study can be found in Table 1. The primer sequences used are shown in Table 2.

qRT-PCR

RNA was extracted from log phase growing cells using hot acid phenol [21]. The RNA was isolated by ethanol precipitation and contaminating DNA was removed by digestion with amplification grade DNase I (Invitrogen). Digestion was performed as recommended by the manufacturer except reactions contained 1 ug RNA, 1 U enzyme, and were incubated for 15 min at 37 °C. cDNAs were generated using the Invitrogen SuperScript® III First-Strand Synthesis SuperMix and following the manufacturer's instructions. qPCR was performed on a Stratagene MX3000P system using a homemade SYBR Green master mix [22] with Rox (Invitrogen) and FastStart Taq Polymerase (Roche). Relative gene expression levels were determined using the Pfaffl method [23] with ACT1 serving as an internal control.

ChIP

ChIP assays were performed as described previously [13] with some modifications. After lysis of the cells, the soluble and insoluble fractions were separated by centrifugation at 4 °C. The insoluble fraction containing the chromatin was washed once in 500 mM lysis buffer and resuspended in 140 mM lysis buffer. The chromatin was sheared by sonication at 4 °C with Misonix Ultra Liquid Sonicator using the cup horn probe (80% intensity, 30 s on 30 s off) for a total on 30 min on time. DNA fragments obtained were approximately 250 bp in size. The sheared chromatin was spun down and the supernatant used for immunoprecipitations. Magnetic beads were used instead of sepharose. Decrosslinking was performed by overnight incubation at 65 °C. DNA was purified using the QIAquick PCR Purification Kit (QIAGEN). qPCR was performed on a Stratagene MX3000P system using the same homemade mix as with qRT-PCR. Enrichment levels were normalized to SPS2 for Figure 5 or ACT1 for Figure 6. An

untagged control for Figure 5 and a Sir3 deletion strain for Figure 6 were used to determine the background signals of the antibodies, which were then subtracted before making the bar graphs.

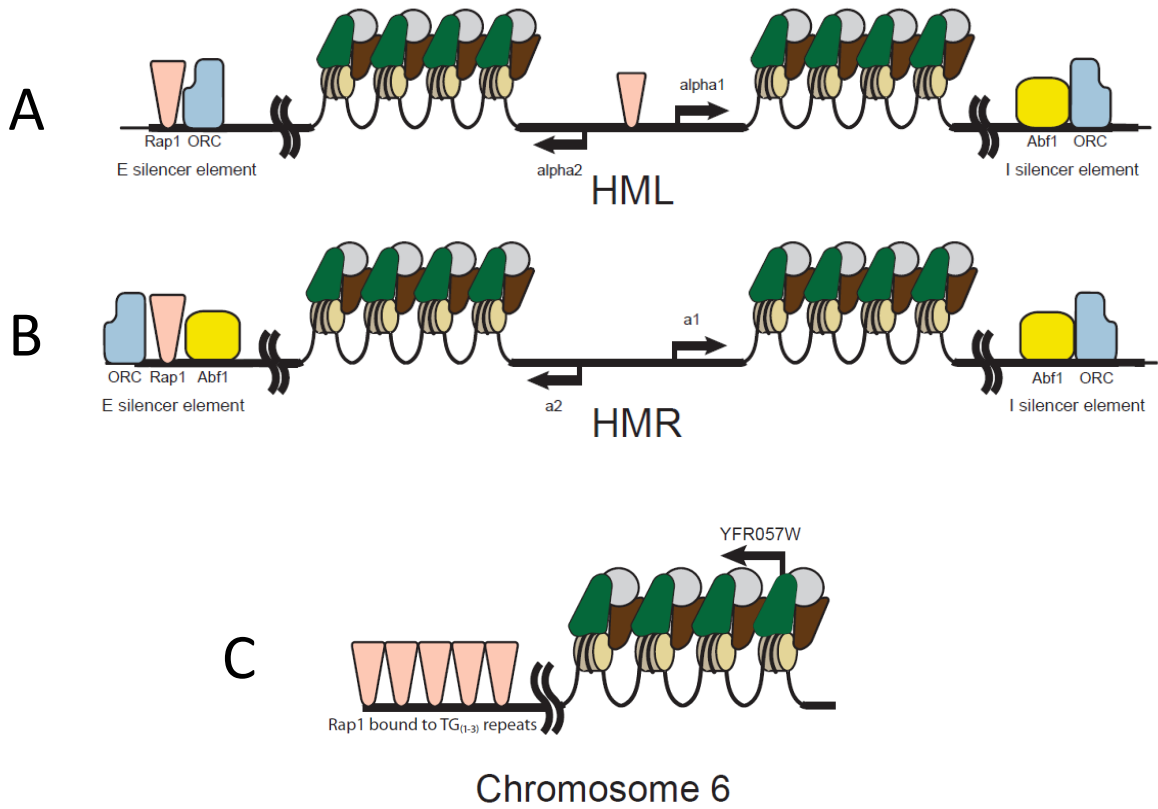


Figure 1. Organization of the hidden mating loci and a subtelomeric gene. (A) HML, (B) HMR, and (C) YFR057W.

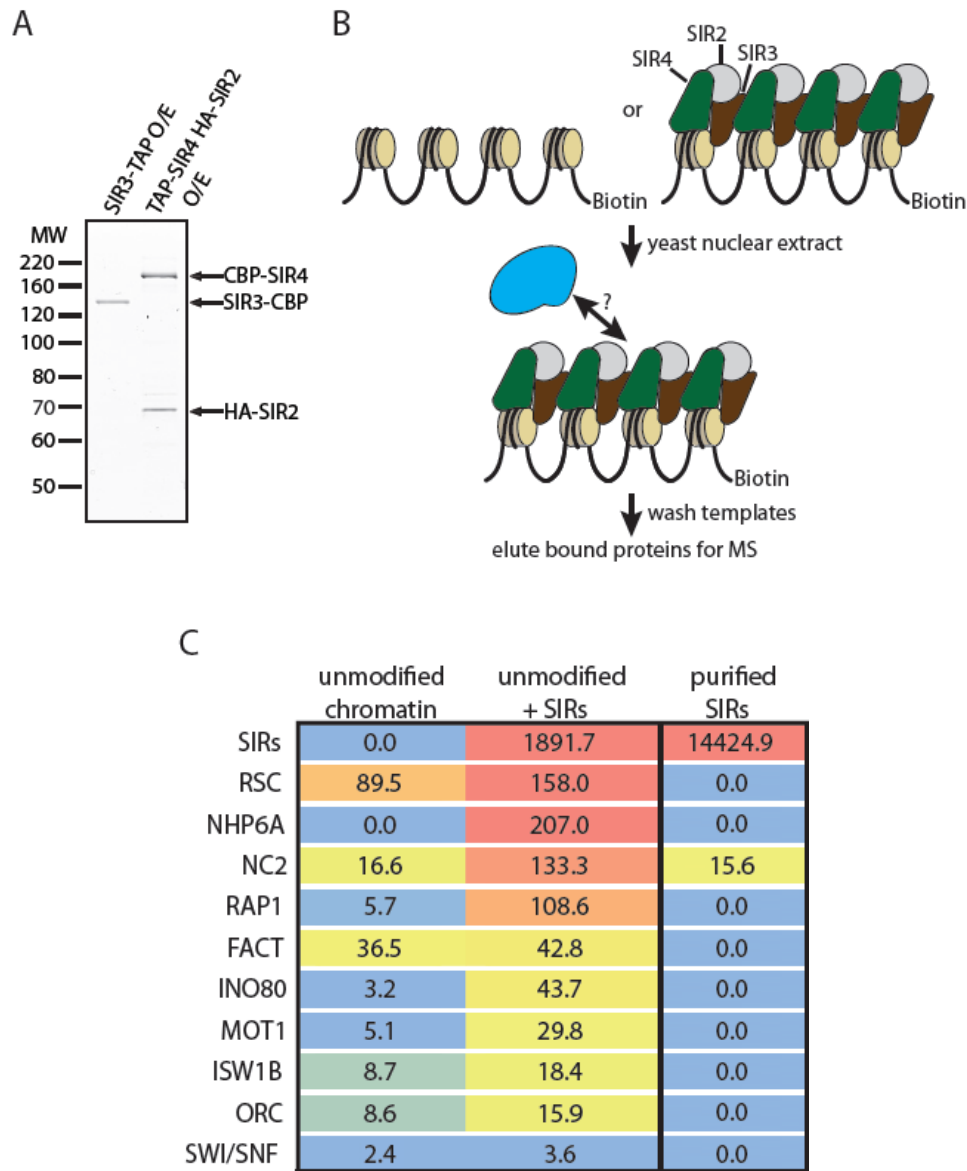


Figure 2. Proteomic pull down assay for heterochromatin. (A) Sir3 and Sir2-4 were over expressed and purified using a tandem affinity purification strategy. A silver stain of the final products is shown. (B) Schematic representing the workflow for the proteomic pull-down assay. (C) Results of proteomic assay. The first two columns show the results from the pull down assay and the third column is a control with the purified Sir proteins and no chromatin or nuclear extract. This chart shows the average NSAF₅ of various protein complexes detected.

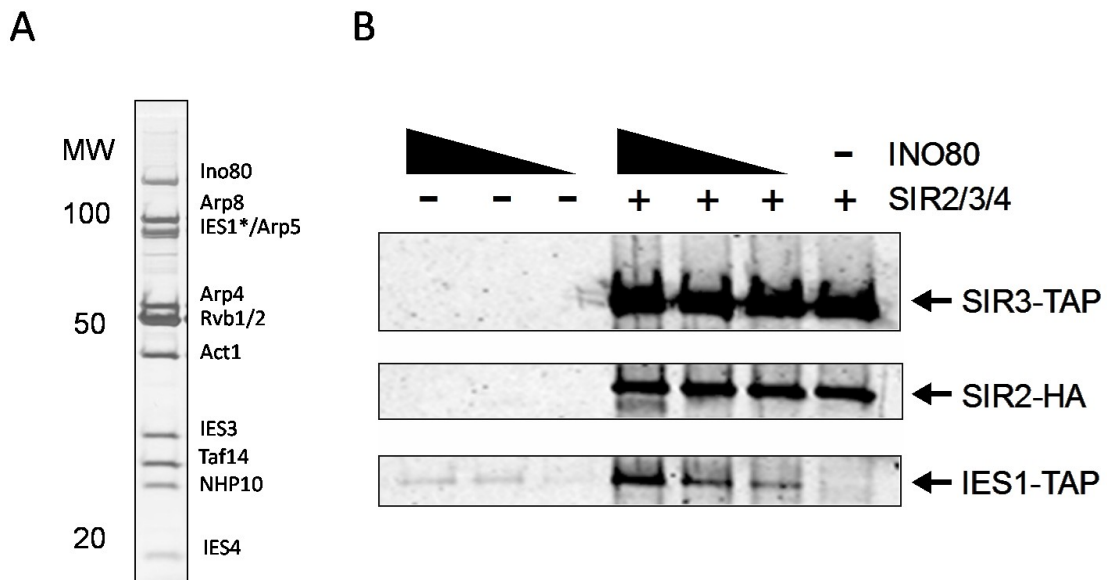


Figure 3. Ino80C interacts with heterochromatin in a purified system. (A) A silver stain of TAP-purified Ino80C is shown. The asterisk (*) indicates the tagged subunit, Ies1. (B) Immobilized template with Sir proteins and Ino80C. Ino80C was titrated into reactions containing immobilized chromatin plus and minus Sir proteins. Western blots for Sir3, Sir2, and Ies1 (Ino80C) are shown.

	YFR057W	alpha1
<i>ies1</i>	1.1 ± 0.32	1.6 ± 0.38
<i>ies2</i>	0.99 ± 0.22	2.1 ± 0.47
<i>ies3</i>	0.78 ± 0.21	0.95 ± 0.23
<i>ies4</i>	4.5 ± 0.40	2.1 ± 0.73
<i>ies5</i>	3.3 ± 0.41*	1.4 ± 0.41*
<i>ies6</i>	3.6 ± 0.40	240 ± 71
<i>arp5</i>	3.0 ± 0.41	210 ± 53
<i>arp8</i>	2.0 ± 0.36	1.4 ± 0.91
<i>nhp10</i>	2.3 ± 0.26	1.5 ± 0.17
<i>sir3</i>	91 ± 7.6	47 ± 8

Fold expression over WT

	SPS2	alpha1
IES6-a	1.0 ± 0.28	1.0 ± 0.32
<i>ies6-a</i>	2.0 ± 0.69	38 ± 15
IES6-α	3.2 ± 0.95	1.2 ± 0.22
<i>ies6-α</i>	5.6 ± 2.1	2.8 ± 0.78

Fold expression over WT

Figure 4. Gene expression analysis in Ino80C subunit deletion strains. (A) RNA was isolated from the indicated deletion strains and normalized to Act1. The fold expression over a WT control is shown. The data is an average plus and minus SEM from three biological replicates unless indicated with an asterisk (*), in which case it is from two biological replicates. (B) Same as (A) but with fresh spores generated from a heterozygous IES6/*ies6* strain. SPS2, a gene not regulated by Sir proteins, is shown.

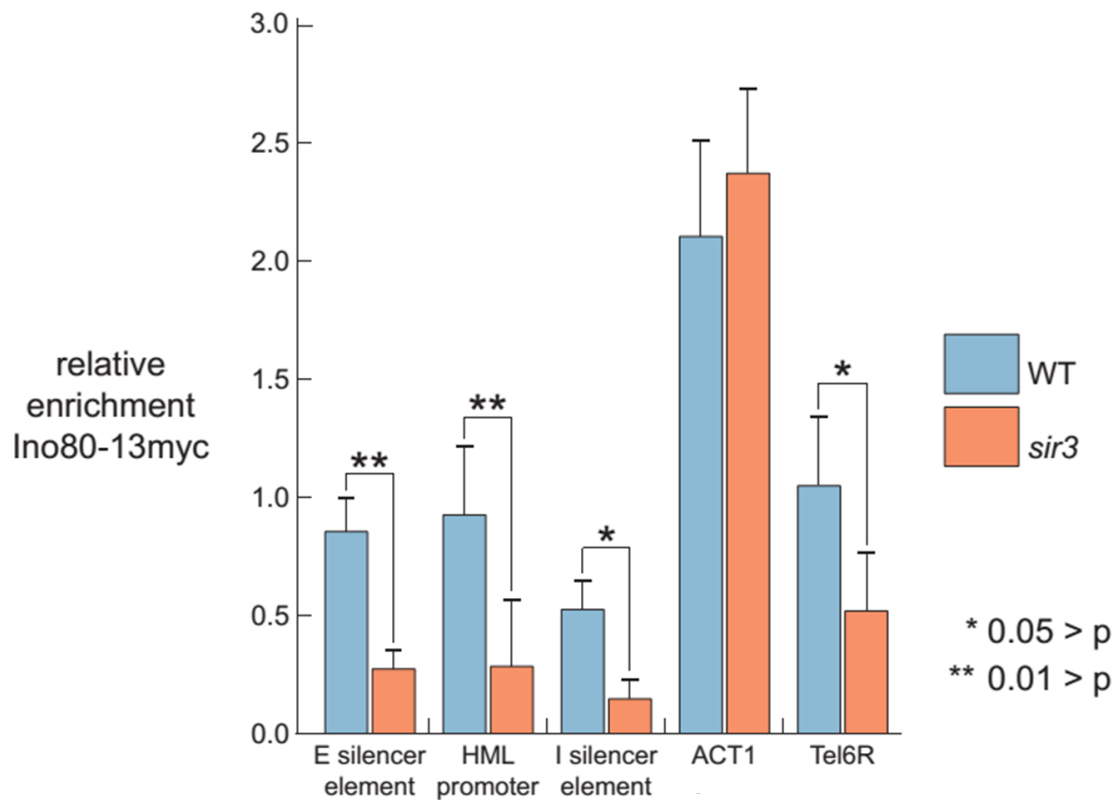


Figure 5. Heterochromatin enhances Ino80 binding in vivo. ChIP experiment showing the relative enrichment of Ino80 in WT and $\Delta sir3$ strains. In the strain lacking Sir3, Ino80 binding is reduced across HML and at the telomere, but not at Act1. Bar graphs show an average enrichment from six independent replicates. Error bars display the SEM. The p-values were calculated using a two-tailed Student's t-test after verifying that the data fit a normal distribution.

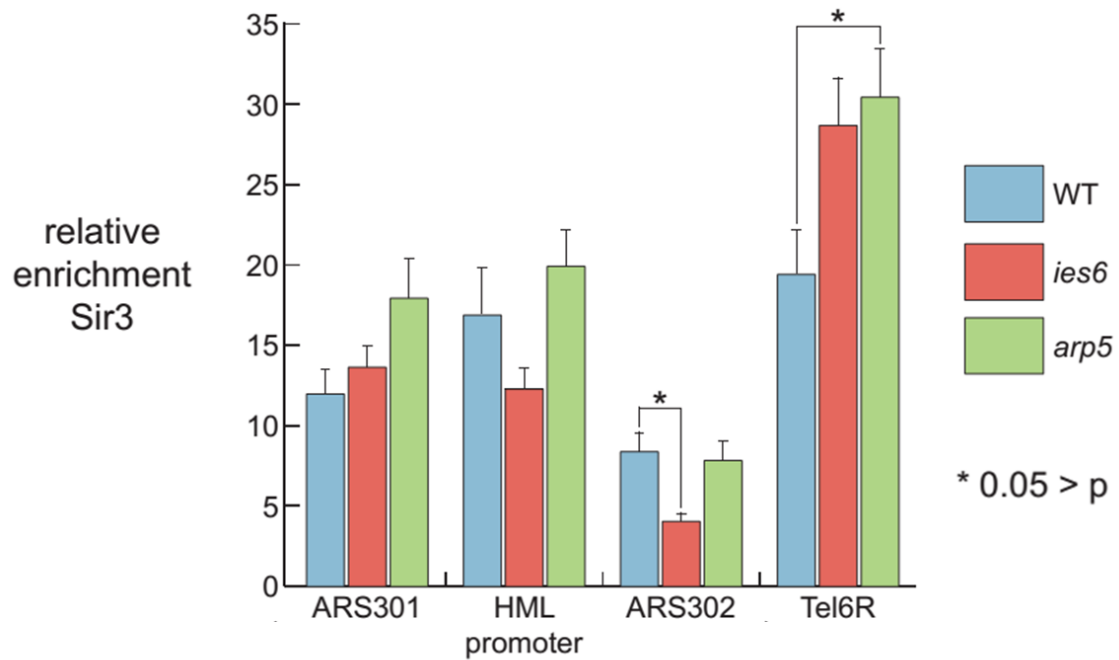


Figure 6. Sir3 binding at HML and the telomere is not reduced in $\Delta arp5$ and $\Delta ies6$ strains. ChIP experiment showing the relative enrichment of Sir3 in WT, $\Delta arp5$ and $\Delta ies6$ strains. Bar graphs show an average enrichment from six independent replicates. Error bars display the SEM. The p-values were calculated using a two-tailed Student's t-test after verifying that the data fit a normal distribution.

Strain	Genotype	Source
BY4741	MATa his3Δ1 leu2Δ0 met15Δ0 ura3Δ0	Grunstein Lab
BY4742	MATα his3Δ1 leu2Δ0 lys2Δ0 ura3Δ0	Grunstein Lab
<i>ies1</i>	MATa his3Δ1 leu2Δ0 met15Δ0 ura3Δ0 ies1::Kan	Open Biosystems
<i>ies2</i>	MATa his3Δ1 leu2Δ0 met15Δ0 ura3Δ1 ies2::Kan	Open Biosystems
<i>ies3</i>	MATa his3Δ1 leu2Δ0 met15Δ0 ura3Δ2 ies3::Kan	Open Biosystems
<i>ies4</i>	MATa his3Δ1 leu2Δ0 met15Δ0 ura3Δ3 ies4::Kan	Open Biosystems
<i>ies5</i>	MATa his3Δ1 leu2Δ0 met15Δ0 ura3Δ4 ies5::Kan	Open Biosystems
<i>ies6</i>	MATa his3Δ1 leu2Δ0 met15Δ0 ura3Δ5 ies6::Kan	Open Biosystems
<i>arp5</i>	MATa his3Δ1 leu2Δ0 met15Δ0 ura3Δ7 arp5::Kan	Open Biosystems
<i>arp8</i>	MATa his3Δ1 leu2Δ0 met15Δ0 ura3Δ8 arp8::Kan	Open Biosystems
<i>nhp10</i>	MATa his3Δ1 leu2Δ0 met15Δ0 ura3Δ9 nhp10::Kan	Open Biosystems
Ino80-myc	MATa his3Δ1 leu2Δ0 met15Δ0 ura3Δ10 Ino80- 13myc::Kan	This study
Ino80-myc, <i>sir3</i>	MATa his3Δ1 leu2Δ0 met15Δ0 ura3Δ11 Ino80- 13myc::Kan sir3::Hph	This study
<i>sir3</i>	MATa his3Δ1 leu2Δ0 met15Δ0 ura3Δ12 sir3::Hph	This study
<i>JDY853</i>	MATa/α IES6/ies6::Kan his3Δ1/his3Δ1 leu2Δ0/leu2Δ0 lys2Δ0/LYS2 met15Δ0 ura3Δ0/ura3Δ0	Jessica Downs Lab
IES6-a	MATa IES6 spore from JDY853	This study
<i>ies6-a</i>	MATa ies6::Kan spore from JDY853	This study
IES6-alpha	MATα IES6 spore from JDY853	This study
<i>ies6-alpha</i>	MATα ies6::Kan spore from JDY853	This study

Table 1. Yeast Strains.

Primer	Sequence	Notes
ARS301-F	TAAAGTTTTTCGGCACGGACT	"E" ChIP
ARS301-R	GCCCCGAAATCGATAATAA	"E" ChIP
ARS302-F	GTAAGTGGGGTTCTGGGTGA	"I" ChIP
ARS302-R	CACCTCCGGCGAAAATATAA	"I" ChIP
HMLalpha1_ORF-F	GAGGCCAAGCTGCTTCAATA	ChIP/RT
HMLalpha1_ORF-R	TCGAGAGGAAGGAACAGGAA	ChIP/RT
HMLalpha2_ORF-F	CCTTTTAAATCCACAAATCACAGA	ChIP/RT
HMLalpha2_ORF-R	TACGGTTTTTGTGGCCCTA	ChIP/RT
HMLalpha2_PRO-F	TGAAAGCAGGCTTCGAAGTAA	HMLalpha promoter ChIP
HMLalpha2_PRO-R	TGCTTCCCAATGTAGAAAAGTACA	HMLalpha promoter ChIP
HMR16a	GGATGATATTTGTAGTATGGCGG	HMR a1 gene RT
HMR16b	GATTTTCCCTTTGGGCTCTTCTC	HMR a1 gene RT
ACT1-F	TCCATCCAAGCCGTTTTGTCTTG	ChIP/RT
ACT1-R	TCTTACCGCCAAATCGATTCTC	ChIP/RT
SPS2-F	ACTGTCCCGTCATTGATGCGTCTC	ChIP/RT
SPS2-R	CATTAGTTCAACTGCAGCGGATG	ChIP/RT
YFR057W-F	ATATGCACTAGTTGCACTAGGCG	ChIP/RT
YFR057W-R	GGCTTTGTTACGCTTGCACTTGA	ChIP/RT
TEL6R F1	GCGTAACAAAGCCATAATGCCTCC	ChIP
TEL6R R1	CTCGTTAGGATCACGTTCGAATCC	ChIP

Table 2. Primers

Contribution

The work presented in this chapter is my portion of collaboration with Tasuku Kitada, Nancy Tran and Jason Gehrke. Nancy generated the proteomic data in Figure 2C, Jason analyzed it and generated the chart, Tasuku purified the Sir proteins in Figure 2A and help generate strains I used in ChIP and RT-PCR experiments.

References

1. Rine, J. and I. Herskowitz, *Four genes responsible for a position effect on expression from HML and HMR in Saccharomyces cerevisiae*. Genetics, 1987. **116**(1): p. 9-22.
2. Hecht, A., S. Strahl-Bolsinger, and M. Grunstein, *Spreading of transcriptional repressor SIR3 from telomeric heterochromatin*. Nature, 1996. **383**(6595): p. 92-6.
3. Rusche, L.N., A.L. Kirchmaier, and J. Rine, *The establishment, inheritance, and function of silenced chromatin in Saccharomyces cerevisiae*. Annu Rev Biochem, 2003. **72**: p. 481-516.
4. Imai, S., et al., *Transcriptional silencing and longevity protein Sir2 is an NAD-dependent histone deacetylase*. Nature, 2000. **403**(6771): p. 795-800.
5. Landry, J., J.T. Slama, and R. Sternglanz, *Role of NAD(+) in the deacetylase activity of the SIR2-like proteins*. Biochem Biophys Res Commun, 2000. **278**(3): p. 685-90.
6. Smith, J.S., et al., *A phylogenetically conserved NAD⁺-dependent protein deacetylase activity in the Sir2 protein family*. Proc Natl Acad Sci U S A, 2000. **97**(12): p. 6658-63.
7. Johnson, L.M., et al., *Genetic evidence for an interaction between SIR3 and histone H4 in the repression of the silent mating loci in Saccharomyces cerevisiae*. Proc Natl Acad Sci U S A, 1990. **87**(16): p. 6286-90.
8. Liou, G.G., et al., *Assembly of the SIR complex and its regulation by O-acetyl-ADP-ribose, a product of NAD-dependent histone deacetylation*. Cell, 2005. **121**(4): p. 515-27.
9. Hoppe, G.J., et al., *Steps in assembly of silent chromatin in yeast: Sir3-independent binding of a Sir2/Sir4 complex to silencers and role for Sir2-dependent deacetylation*. Mol Cell Biol, 2002. **22**(12): p. 4167-80.
10. Kimura, A., T. Umehara, and M. Horikoshi, *Chromosomal gradient of histone acetylation established by Sas2p and Sir2p functions as a shield against gene silencing*. Nat Genet, 2002. **32**(3): p. 370-7.
11. Suka, N., K. Luo, and M. Grunstein, *Sir2p and Sas2p opposingly regulate acetylation of yeast histone H4 lysine16 and spreading of heterochromatin*. Nat Genet, 2002. **32**(3): p. 378-83.
12. Armache, K.J., et al., *Structural basis of silencing: Sir3 BAH domain in complex with a nucleosome at 3.0 Å resolution*. Science, 2011. **334**(6058): p. 977-82.
13. Kitada, T., et al., *Mechanism for epigenetic variegation of gene expression at yeast telomeric heterochromatin*. Genes Dev, 2012. **26**(21): p. 2443-55.
14. Chang, J.S. and F. Winston, *Spt10 and Spt21 are required for transcriptional silencing in Saccharomyces cerevisiae*. Eukaryot Cell, 2011. **10**(1): p. 118-29.

15. Xu, F., et al., *Sir2 deacetylates histone H3 lysine 56 to regulate telomeric heterochromatin structure in yeast*. *Mol Cell*, 2007. **27**(6): p. 890-900.
16. Udugama, M., A. Sabri, and B. Bartholomew, *The INO80 ATP-dependent chromatin remodeling complex is a nucleosome spacing factor*. *Mol Cell Biol*, 2011. **31**(4): p. 662-73.
17. Papamichos-Chronakis, M., et al., *Global regulation of H2A.Z localization by the INO80 chromatin-remodeling enzyme is essential for genome integrity*. *Cell*, 2011. **144**(2): p. 200-13.
18. Luger, K., et al., *Characterization of nucleosome core particles containing histone proteins made in bacteria*. *J Mol Biol*, 1997. **272**(3): p. 301-11.
19. Li, B., et al., *The Set2 histone methyltransferase functions through the phosphorylated carboxyl-terminal domain of RNA polymerase II*. *J Biol Chem*, 2003. **278**(11): p. 8897-903.
20. Tantin, D., et al., *Biochemical mechanism of transcriptional activation by GAL4-VP16*. *Methods Enzymol*, 1996. **274**: p. 133-49.
21. Bookout, A.L., et al., *High-throughput real-time quantitative reverse transcription PCR*. *Curr Protoc Mol Biol*, 2006. **Chapter 15**: p. Unit 15 8.
22. Pellissier, F., et al., *Lab assembly of a low-cost, robust SYBR green buffer system for quantitative real-time polymerase chain reaction*. *Anal Biochem*, 2006. **350**(2): p. 310-2.
23. Pfaffl, M.W., *A new mathematical model for relative quantification in real-time RT-PCR*. *Nucleic Acids Res*, 2001. **29**(9): p. e45.